Issue 97, 2020

WSL Berichte

ISSN 2296-3456

Full-scale Testing of Rockfall Nets in Real Terrain

Results of tests at Chant Sura: 13th September and 4th October, 2019

Miguel A. Sanchez
Andrin Caviezel

August 27, 2020

WSL-Institut für Schnee- und Lawinenforschung SLF

Eidg. Forschungsanstalt für Wald, Schnee und Landschaft WSL
CH-8903 Birmensdorf

Issue 97, 2020
WSL Berichte
ISSN 2296-3456

Full-scale Testing of Rockfall Nets in Real Terrain

Results of tests at Chant Sura: 13th September and 4th October, 2019

Miguel A. Sanchez
Andrin Caviezel

August 27, 2020

WSL-Institut für Schnee- und Lawinenforschung SLF

Eidg. Forschungsanstalt für Wald, Schnee und Landschaft WSL
CH-8903 Birmensdorf

Responsible for the publication of this series
Prof. Dr. Konrad Steffen, Direktor WSL

Responsible for this issue
Prof. Dr. Jürg Schweizer, Head of research unit Snow Avalanches and Prevention

Managing Editor: Sandra Gurzeler, Teamleiterin Publikationen, WSL

Citation
Sanchez, M.A.; Caviezel, A., 2020: Results of tests at Chant Sura: 13th September and 4th October, 2019. WSL Ber. 97. 81 p.

ISSN 2296-3448 (Print)
ISSN 2296-3456 (Online)

Photos cover
1. Deposition of a cubic 2670 kg block on the release platform. Photo by Guillaume Meyrat, SLF.
2./3. Descending blocks. Photo by Geobrugg AG.
4. Cubic 2670 kg block caught by the rockfall fence. Photo by Miguel Sanchez, SLF
5. Deteriorated test block after several runs. Photo by Geobrugg AG.

Partner

Research for People and the Environment: The Swiss Federal Institute for Forest Snow and Landscape Research WSL monitors and studies forest, landscape, biodiversity, natural hazards and snow and ice. WSL is a research institute of the Swiss Confederation and part of the ETH Domain. The WSL Institute for Snow and Avalanche Research SLF is part of the WSL since 1989.

Summary

Rockfall impacts with a flexible barrier include both translational and rotational kinetic energy. Traditionally rotational energy is not included in barrier design. Furthermore, the dissipation of translational kinetic energy has been considered only in idealized conditions, such as free-fall experiments.

To study how rockfall barriers absorb rotational and translational energies in realistic conditions we performed a series of full-scale rockfall tests in natural terrain. The test were performed on the 13th of September and 4th of October, 2019, at the WSL rockfall test site located at Chant Sura, near Davos. Exhaustive block tracking as well as internal measurement devices in the barrier provides fundamental data to describe the physical processes detailing rock motion and its impact interaction against protection solutions.

The presented methodologies pave the way to a comprehensive understanding of rock-ground and rock-net interaction, a key requirement to improve the design of flexible barriers that account for the role of rock shape, spin and eccentric impacts in rockfall protection.

Rockfall Research
RAMMS Rapid Mass Movements
WSL Institute for Snow and Avalanche Research, SLF

Flüelastrasse 11
7260 Davos Dorf, Switzerland
miguel.sanchez@slf.ch, andrin.caviezel@slf.ch
http://ramms.slf.ch

Zusammenfassung

Einschläge von Steinen auf flexible Barrieren beinhalten sowohl translatorische als auch rotatorische kinetische Energie. Traditionell wird die Rotationsenergie bei der Konstruktion von Barrieren nicht berücksichtigt. Darüber hinaus wurde die Dissipation der translatorischen kinetischen Energie meisten nur unter idealisierten Bedingungen, wie z.B. bei Freifallexperimenten, berücksichtigt.

Um zu untersuchen, wie Steinschlag-Barrieren Rotations- und Translationsenergie unter realistischen Bedingungen absorbieren, haben wir eine Reihe von Steinschlagversuchen im natürlichen Gelände in großem Maßstab durchgeführt. Die Tests wurden am 13. September und 4. Oktober 2019 auf dem WSL-Steinschlagversuchsgelände in Chant Sura bei Davos durchgeführt. Eine umfassende Blockverfolgung sowie interne Messvorrichtungen in der Barriere liefern grundlegende Daten zur Beschreibung der physikalischen Prozesse, die die Bewegung des Blocks und ihre Wechselwirkung mit den Schutzlösungen beschreiben.

Die vorgestellten Methoden ebnen den Weg zu einem umfassenden Verständnis der Wechselwirkung zwischen Fels und Boden sowie zwischen Fels und Netz, eine Schlüsselvoraussetzung für die Konstruktion effizienter Steinschlagschutzbarrieren, der Entwicklung numerischer Modelle und der Berücksichtigung realistischeren Einwirkungen, die die Rolle von Felsform, Drehung und exzentrischen Einwirkungen beim Schutz vor Steinschlag berücksichtigen.

Rockfall Research
RAMMS Rapid Mass Movements
WSL Institute for Snow and Avalanche Research, SLF

Flüelastrasse 11
7260 Davos Dorf, Switzerland
miguel.sanchez@slf.ch, andrin.caviezel@slf.ch
http://ramms.slf.ch

Contents

List of Figures

List of Tables

1. Introduction

Rockfall research and testing of flexible rockfall barrier have a well established tradition at the Swiss Federal Institute for Forest, Snow and Landscape Research WSL. Being the first test center for rockfall protection barriers with its own test facility recognized by the European Union by 2010, numerous tests have been conducted at the Lochezen quary in collaboration with Geobrugg AG in order to validate and improve performance of various protection systems. Since 2015, the WSL Institute for Snow and Avalanche research SLF increased its activities with respect to rockfall research with focus on kinematic characteristics in unobstructed terrain. Main goal is the determination of the relevant parameters of interest such as kinetic energy and jump heights in order to improve hazard mapping, early warning and protective measures. Single block, induced rockfall experiments equipped with measuring probes have been conducted on several test slopes. This allows us to gather information about their trajectory, rotation and impact.

The Chant Sura test site, located near the Flüelapass, Eastern Swiss Alps, has been used for various test series of unobstructed rockfall experiments performed by the SLF since 2017. Artificial rocks, made of steel-reinforced concrete were lifted by helicopter to a specific starting location and repeatedly released. In an initial series of experiments, all the rocks had the same cubic shape but different mass to investigate the effect of mass on movement behaviour. The lightest mass was only 44 kg, the heaviest reached 2670 kg. In 2017-2018, wheel-shaped rocks were included to determine the effect of shape [2] on run-out behaviour. By 2019, 181 real-scale rockfall tests had been conducted, obtaining valuable data sets [1] for the calibration of the rockfall modelling program RAMMS::ROCKFALL.

In September 2019, a flexible rockfall barrier was installed at the Chant Sura test site. The location of the barrier was selected using the results of the previous tests. Here, we report the first barrier tests carried out during September/October 2019. This report summarizes the data of this Chant Sura barrier tests and first conclusions are drawn.

Figure 1.1.: Impressions rockfall experiments. Left: Ground-block interaction. Middle: Rock impacts on a flexible barrier (Pictures: Geobrugg AG). Right: investigating trees as a natural mitigation measure against rockfalls.

Before the experiments are conducted, artificial rocks of a suitable shape and size are manufactured and equipped with sensors [6, 3]. The sensors that are currently available are capable of measuring translational accelerations of up to 400 g (g = gravitational acceleration) and rotational speeds of up to 11 revolutions per second (4000 ^{o}/s). Conventional video recordings pinpoint the rock's trajectory from initiation to runout along the mountain slope. The jump heights and jump lengths are thereby determined. Coupled with the measured accelerations (ground impact forces) and the rotational speed of the rock, a rather complete picture of the rockfall process is obtained. In the latest series of experiments, the flexible barrier is likewise instrumented with load sensors to measure rope forces. Each rock impact into the barrier is recorded with high-speed video cameras to gain insight on the mechanics of how barriers catch rocks in real conditions.

The Chant Sura slope (46.74625 N, 9.96720 E) is a prototypical alpine slope consisting of a steep acceleration zone gradually easing off into a flat runout. Figure 1.2 depicts a counter slope view of the site taken on the day of the GeoSummit test, 4 October 2019, with the spectator buses standing on the partially closed pass road across the runout scree field. The installed rockfall barrier is hardly discernible within the autumn colored surroundings. Figure 1.3a displays an UAS generated orthophoto overlaid with the deposition points of the unobstructed non-barrier tests and visualizes the spatial variance of trajectory endpoints. Figure 1.3b shows the slope angle with the barrier position indicated at the beginning of the runout zone. The spatial distribution of the deposition points, slope consideration, installation feasibility and optimized cost-value ratio lead to the planning of a six field flexible barrier on the indicated position in Figure 1.3a.

Figure 1.2.: Counter slope view of experimental site

Figure 1.4 presents an aerial photograph with the barrier shortly after installation. The scarring patterns on the relatively soft alpine meadow from preceding experiments are clearly visible. The scarring plays an important role with respect to energy losses throughout the block trajectory before an impact on the barrier. Figure 1.5 shows a camera view from the bottom (behind the scree field). Here, we differentiate between acceleration zone and cliff where the rock gains translational and rotational speed, and the transition zone characterized by the scarred soil layer.

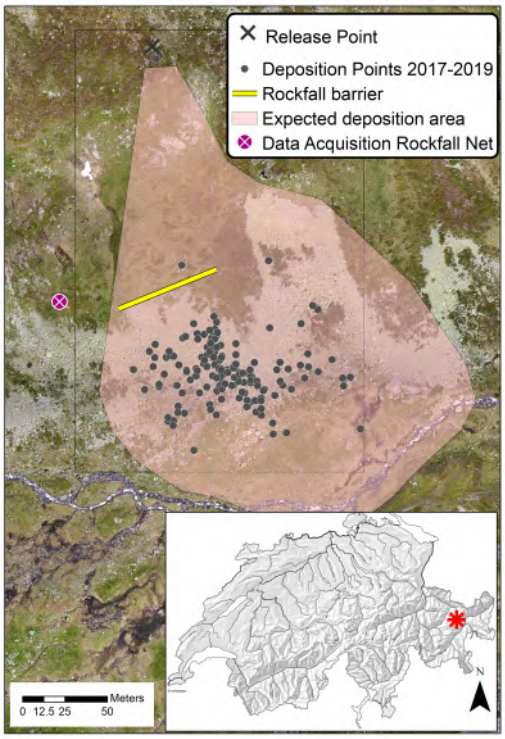

(a) UAS generated orthophoto. Magenta circle indicates data acquisition point for barrier instrumentation. Inset shows the geographic location within Switzerland.

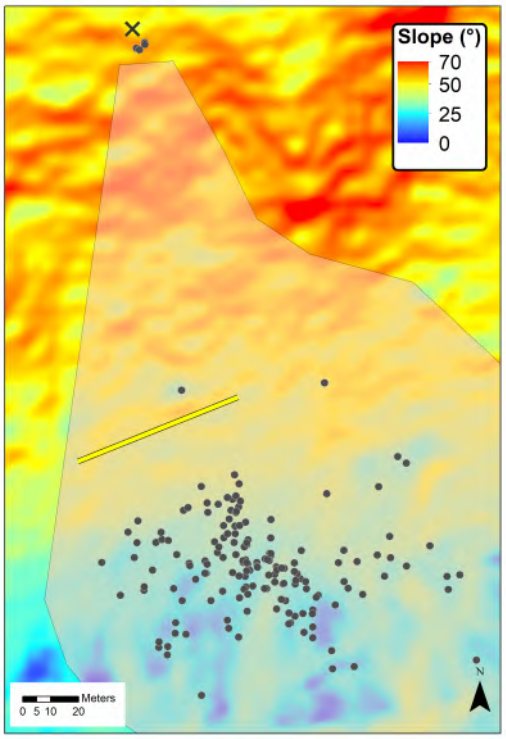

(b) Close-up of marked slope extent - black rectangle in a) - with slope angles of the test site. Barrier placement at the beginning of the runout zone is marked.

Figure 1.3.: The Chant Sura test site. Both panels feature the deposition points of the unobstructed rockfall experiments used as guideline for barrier placement (yellow line).

The aim of the barrier tests is to record the entire trajectory of a rock as it descends the slope and impacts into the rockfall barrier. Preceding experimental campaigns lead to the toolbox needed to track and reconstruct the complete rockfall trajectory with all relevant parameters of interest such as kinetic energy, rotational velocities, impact forces, jump heights and lengths. A systematic test series provides more accurate and comprehensive data than individual case studies. The data obtained will be used as a basis for improving the design of flexible barriers, for barrier simulation programs and for testing upgrades to the RAMMS::ROCKFALL simulation software [4, 5].

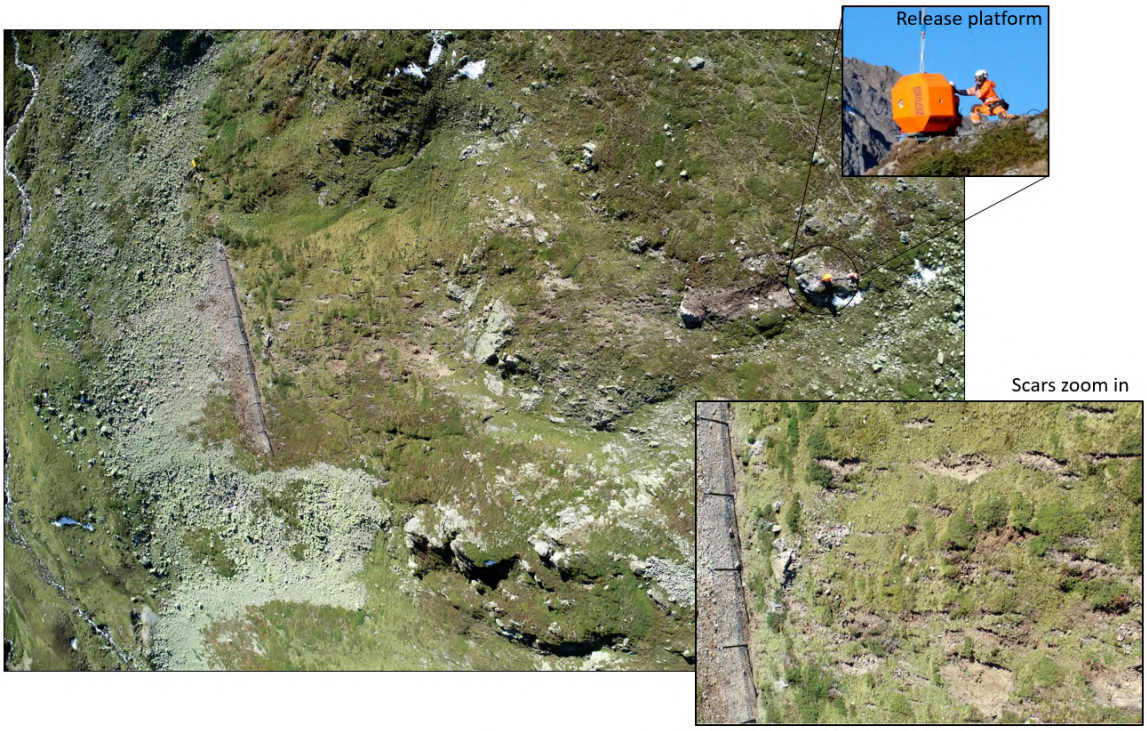

Figure 1.4.: Aerial view of the test site with alpine meadow interspersed with rocks. Inset show the release platform and the scarring in front of the flexible barrier.

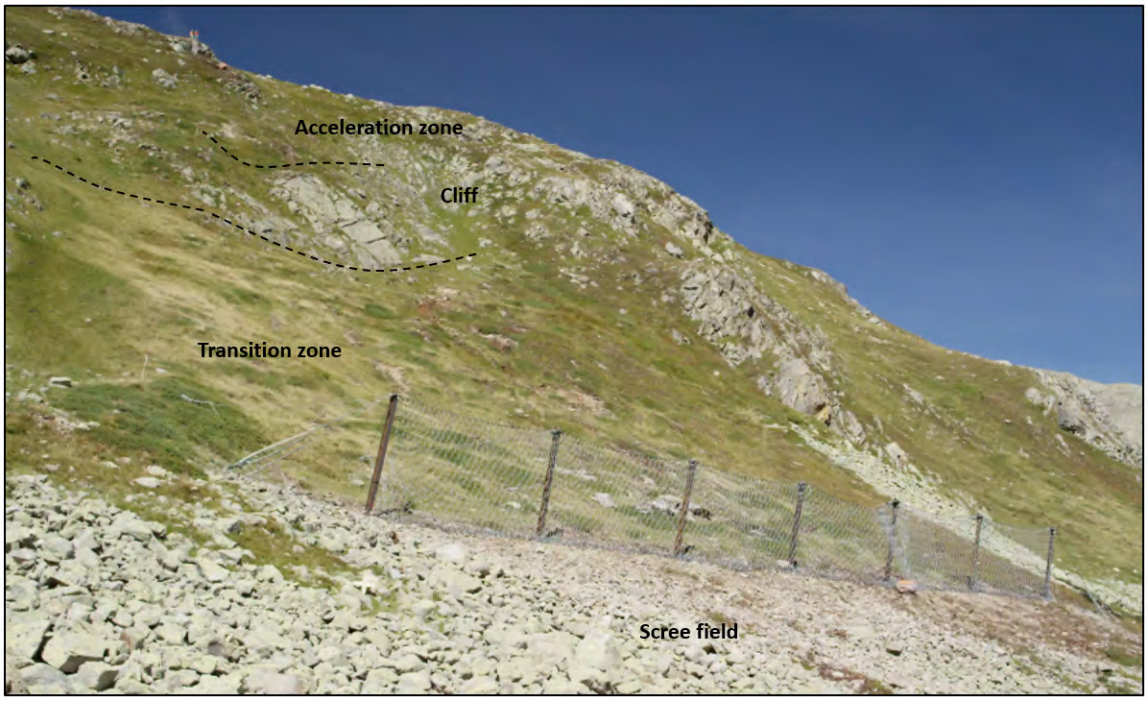

Figure 1.5.: Test site with: Acceleration zone; the cliff where hard impacts with little energy loss occur; the transition zone where the soft compactable soil leads to more energy dissipation upon impact; the installed flexible barrier; and the former scree field runout.

2. Methodology

2.1. Test site

The experimental site is located on the Flüelapass, 12 km southeast of Davos, Switzerland (6.74625 N, 9.96720 E). The release point is located at an elevation of 2380 m a.s.l., yielding a projected travelling distance of 145 m until reaching the installed rockfall barrier. The slope has been used during the last three years for rockfall tests in unobstructed conditions, which played a key role for positioning of the barrier.

2.2. Experimental setup

The deployed external and in-situ measurement devices are equivalent to the previous experimental campaigns carried out at the same slope during preceding years [1]. They comprise a pre- and 19 post-experimental UAS surveys in order to generate latest high-resolution digital terrain surface models with a grid resolution of 5 cm and the possibility of a-posteriori scar mapping via the difference map.

The tests were recorded with several cameras situated above (top), behind (runout) and lateral to the net as well as on the counter-slope. The videogrammetry specifications are as follows:

Table 2.1.: Videogrammetry hardware specifications

Location	Purpose	Resolution	frame rate
Top	overview	1920 x 1080 pix	30 fps
Top	high speed net	1280 x 1024 pix	50 fps
Lateral	high speed net	1920 x 1080 pix	100 fps
Lateral	close-up net	3840 x 2160 pix	50 fps
Runout	overview	1920 x 1080 pix	25 fps
Runout	overview high res	4096 x 2160 pix	25 fps
Counter-slope	high-speed overview	3840 x 2160 pix	50 fps

Three-axial in-situ sensors mounted in the rocks measure rotations and accelerations during its descent. The deployed videogrammetry setup allows for complete trajectory reconstruction if needed. Information about kinetic energies, jump height and lengths on the trajectory level will be available. These tests also aim to determine the accuracy for these reconstructed parameters with respect to the barrier impact itself.

2.2.1. Test rocks

StoneNode v1.2 sensors mounted in the rock's centre of mass record gyroscopic motions up to 4000 °/s and accelerations up to 400 g with a data acquisition rate of 1 kHz. Recording times of several hours allows the tracking of all runs with the use of a single sensor [6, 3]. Test rocks are the equant, cubic EOTA_{111} and wheel shaped, platy EOTA_{221} variants of the perfectly symmetric norm rock of the European Organization for Technical Assessment used in standardized rock fence testing procedures in official European Technical Approval Guidelines (EAD 340059-00-0106, 2018).

Testing flexible barriers with standardized rocks (overall dimensions of the blocks in Figure 2.1) in rock rolling tests provides further insight into real case impact scenarios and the new data sets can be cross-checked with drop tests to analyse similarities and differences.

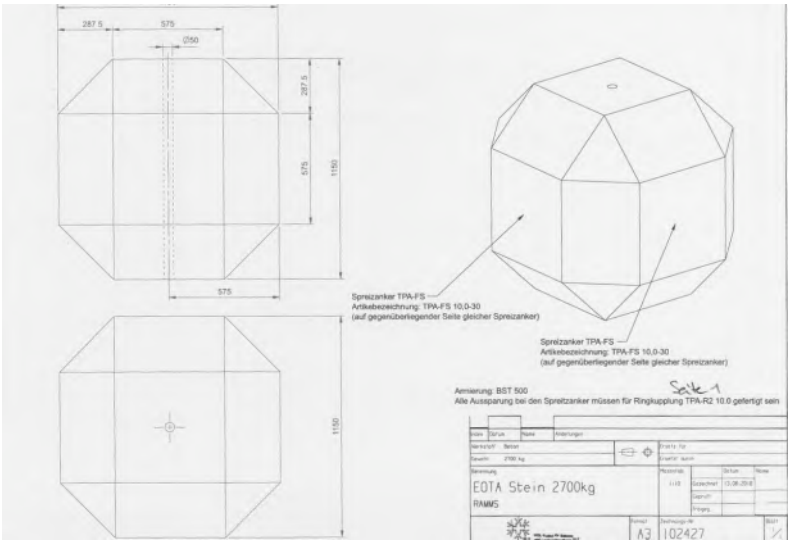

(a) Technical drawing of the equant, cubic $\text{EOTA}_{111}^{2600kg}$ rock.

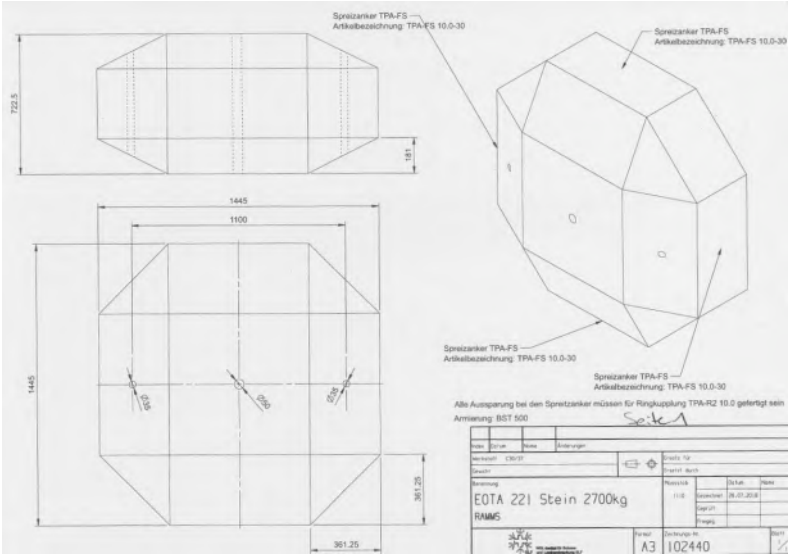

(b) Technical drawing of the wheel shaped, platy $\text{EOTA}_{221}^{2600kg}$ rock.

Figure 2.1.: Sketches of the a) equant, cubic and b) platy, wheel shaped EOTA rocks.

2.2.2. Flexible rockfall barrier setup

A six-field 2000 kJ flexible rockfall net with a construction height of 5 m is installed at the beginning of the runout zone. The exact elements of the installed rockfall barrier are summarized in Table 2.2 and the aberrations from standardized installation marked in Figure 2.2.

Table 2.2.: Elements of the 2000 kJ flexible rockfall barrier installed in Chant Sura

Net	ROCCO butterfly Wire Mesh	16/3/350
Middle/border post	Height 5 m Post spacing	Steel posts HEA-240 10 m
Ropes	Top support rope Bottom support rope Lateral anchor rope Upslope anchor rope Vertical rope	⌀ 22 mm GEOBINEX (2x) ⌀ 22 mm GEOBINEX (2x) ⌀ 22 mm GEOBINEX ⌀ 22 mm GEOBINEX ⌀ 22 mm
Brakes	Top support rope Bottom support rope Lateral anchor rope Upslope anchor rope	2x U-300-70/10 parallel on each side[a] 1x U-300-70/10 on each side 2x U-150-70/10 parallel on each side[a] 2x U-150-70/10 parallel per on rope 1 and 14[a] 2x U-150-70/10 parallel per anchor for middle ropes

[a]U-Brake U-300-R20 were used on the left side.

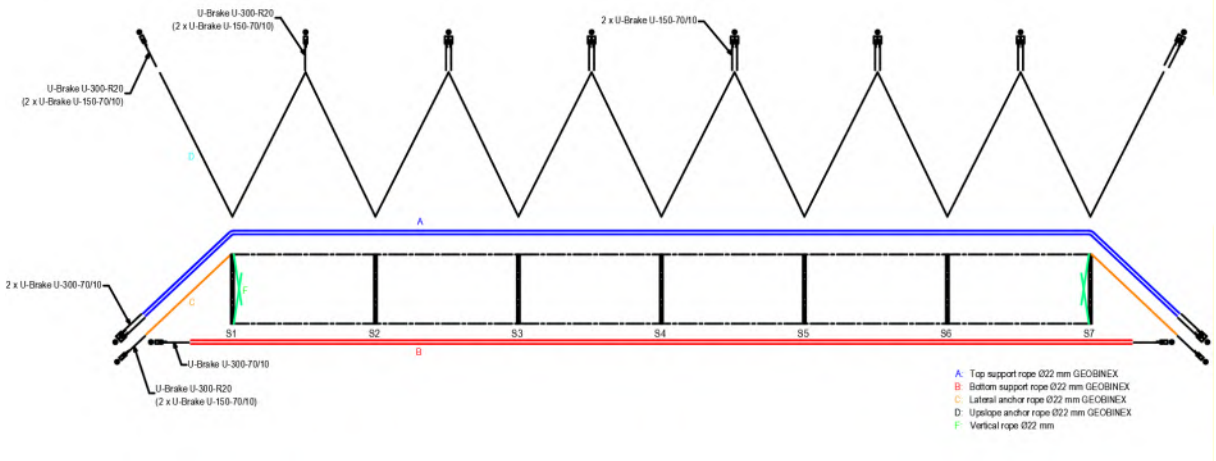

Figure 2.2.: Elements of the Chant Sura rockfall protection system. For details, a full size figure can be found in Appendix A.

The system is installed on hinged posts with support ropes attached to the base plate and top of the posts, plus upslope anchor ropes (see Figure 2.4 for the installation of the foundations and Figure 2.5 for the mounting and installation setup of the barrier). The ROCCO butterfly net is fastened to the support ropes and the border posts are held in place with lateral anchor ropes. At both sides of the barrier, U-Brakes are fixed to each support rope. For the tests in 2019, the first two upslope anchors and left lateral anchor were equipped with U-Brake U-300-R20 instead of the planned U-300-70/10 and U-150-70/10. The brakes that differ from the planned ones are shown in Figure 2.3.

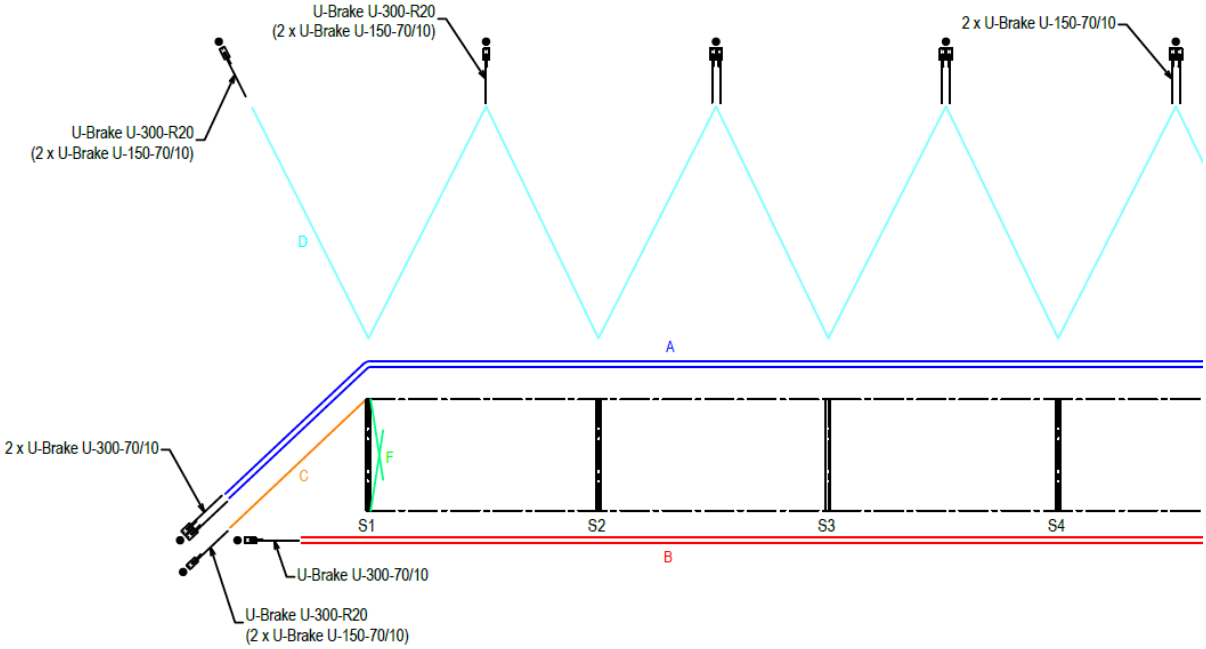

Figure 2.3.: Detailed view of the left side of the barrier. Utilized brakes are displayed (regular setup specifications inside brackets.

(a) Construction site with the 7 foundations. The vegetation marks the boundary between alpine meadow and scree field soil coverage.

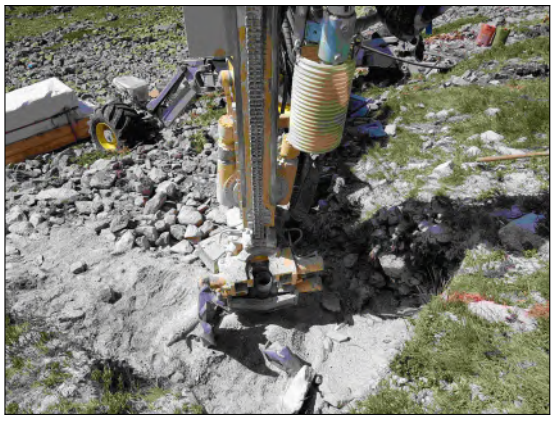

(b) Removal of the top-soil layer. The moraine material is 10 cm below the removed layer.

(c) Drilling through the moraine material. The anchors reach as deep as 6-7 m to the bedrock layer.

(d) Reinforcement cage for the base plate pad.

(e) Base plate pad ready for casting.

Figure 2.4.: Installation of the barrier foundations

(a) Pressure cells on the modified base plates.

(b) Base plates attached to the post ready for transport.

(c) Posts after helicopter aided installation hold by ratchet straps before mounting of the support.

(d) Transport of the ring nets by helicopter.

(e) Overview of the whole net system and placement of the ring net.

Figure 2.5.: Installation of posts and ring net.

2.3. Net instrumentation

The barrier post base plates were modified in order to install 300 kN load cells. Several ropes were instrumented with force cells with a load capacity of 500 kN to capture the response of the barrier over time. Figure 2.6 shows the mentioned modifications to the base plate to include the pressure load cells (see Figures 2.6a and 2.6b) and the placement of the load cells in the upslope anchor ropes (Figure 2.6c) and support ropes (Figure 2.6d). The translational and rotational deceleration of the rock is tracked with accelerometers and gyroscopes described in Section 2.2.1.

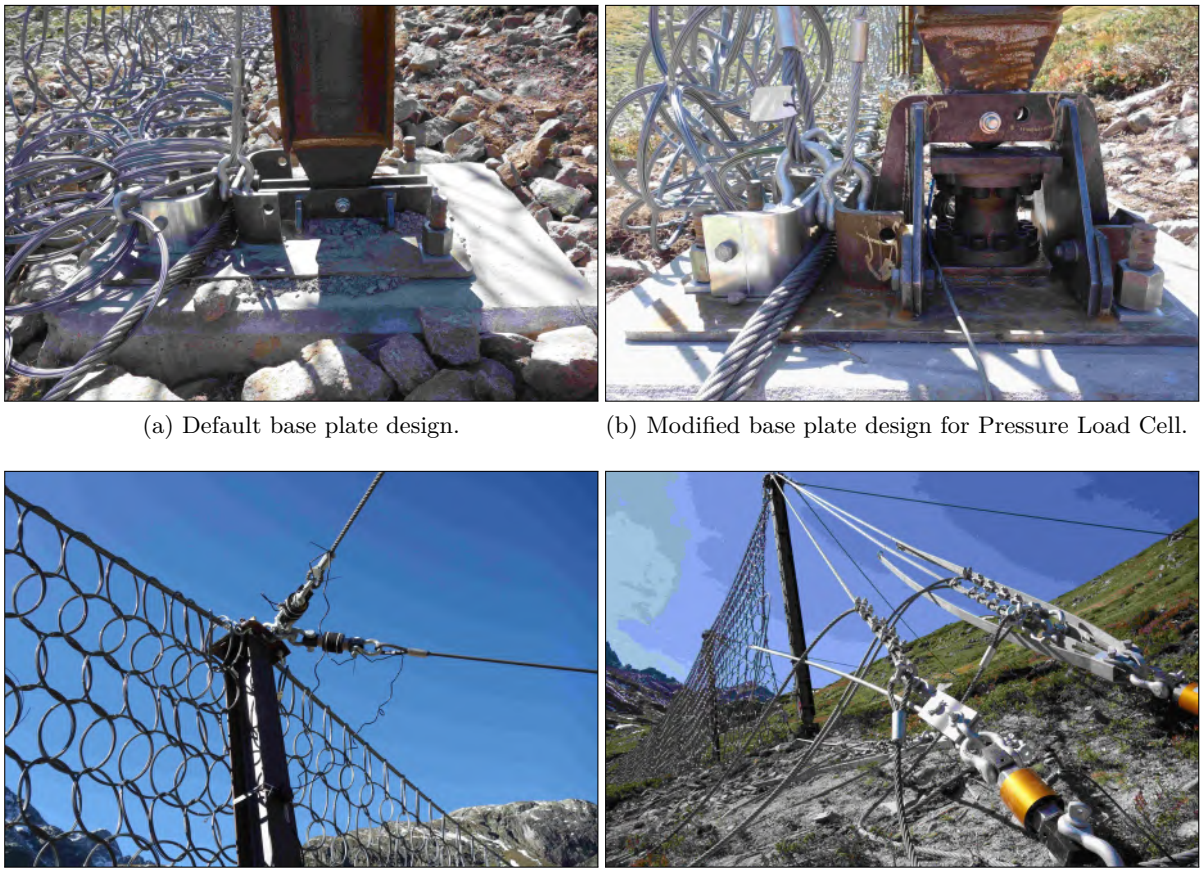

(a) Default base plate design.

(b) Modified base plate design for Pressure Load Cell.

(c) Load Cells on four upslope anchor ropes.

(d) Load Cells on Lateral, Top and Bottom anchor ropes.

Figure 2.6.: Measuring devices installed on the barrier.

The instrumentation used in the net is described in Table 2.3 and Figure 2.7. The three extra elements 15-17 displayed in Figure 2.7 not listed in the table, correspond to the additional wireless transmitters tested during some of the measurements. Those transceivers were tested in order to possibly eliminate physical sensor cabling in future experiments as cables are prone for failure in rugged environments. Redundant measurement setups allow for larger margin when evaluating new technology without compromising the data. The focus on instrumenting the east side of the 60 meter barrier corresponds to a higher number of blocks passing through this area during previous tests [1].

Table 2.3.: Net instrumentation setup. The positions are shown in Figure 2.7

Position	Description	Dynamic Range
1	Compressive force post 4	300 kN
2	Compressive force post 5	300 kN
3	Compressive force post 6	300 kN
4	Compressive force post 7	300 kN
5	Lateral anchor rope mountain	500 kN
6	Bottom support rope mountain	500 kN
7	Top support rope mountain	500 kN
8	Upslope anchor rope post 5 mountain	500 kN
9	Upslope anchor rope post 5 valley	500 kN
10	Upslope anchor rope post 6 mountain	500 kN
11	Upslope anchor rope post 6 valley	500 kN
12	Top support rope valley	500 kN
13	Bottom support rope valley	500 kN
14	Lateral anchor rope valley	500 kN

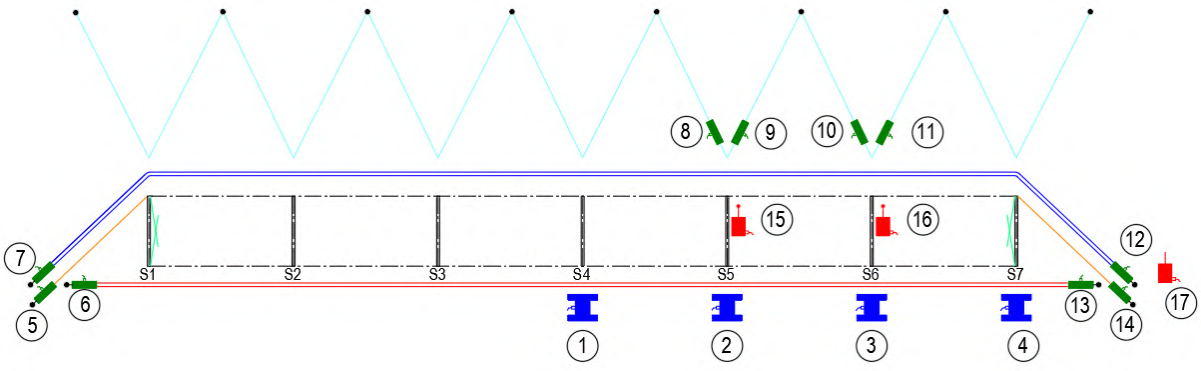

Figure 2.7.: Net instrumentation setup, numbering according Table 2.3.

3. Results

The first experimental testing with a 60 m long flexible barrier was successfully conducted in September 2019. To classify the impact points, we have divided and labelled each net field as shown in Figure 3.1. The discretization is used to analyse the net behavior response to impacts in different locations. Impact fields and impact points are shown in Tables 3.2 and 3.4.

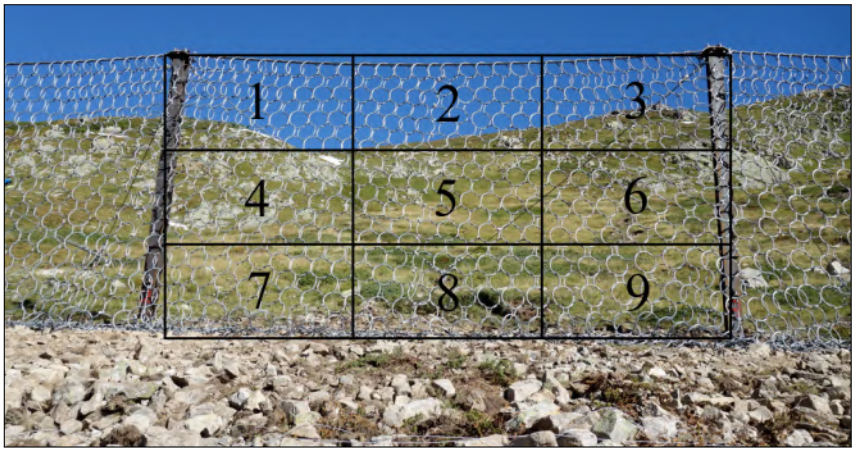

Figure 3.1.: Discretization of each net field to classify impact points.

Figure 3.2 and 3.3 show exemplary test results obtained with a 2600 kg equant shaped EOTA block. While the StoneNode data in Figure 3.2 displays the three-axial gyroscope readings alongside with its resultant and the measured accelerations upon individual impacts, the forces measured upon impact in the net are visualized in Figure 3.3.

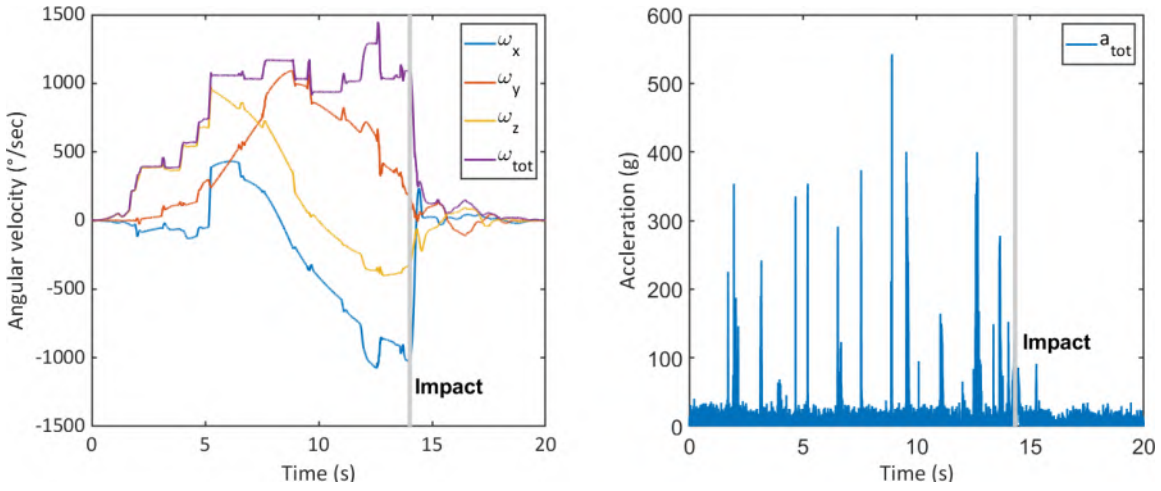

Figure 3.2.: StoneNode data corresponding to test 01, drop 09. The left panel is showing three-axial gyroscope readings alongside with its resultant, the right panel features the resultant measured accelerations upon individual impacts. The impact in the net is marked with a grey-line in both plots.

A complete list of all results is presented in the Appendix A: Chant Sura Pre-test, 13 September 2019 and Appendix B: Chant Sura GeoSummit, 4 October 2019. The fourteen devices are shown in the same figure to illustrate peak values and portray the scale among the different measurements.

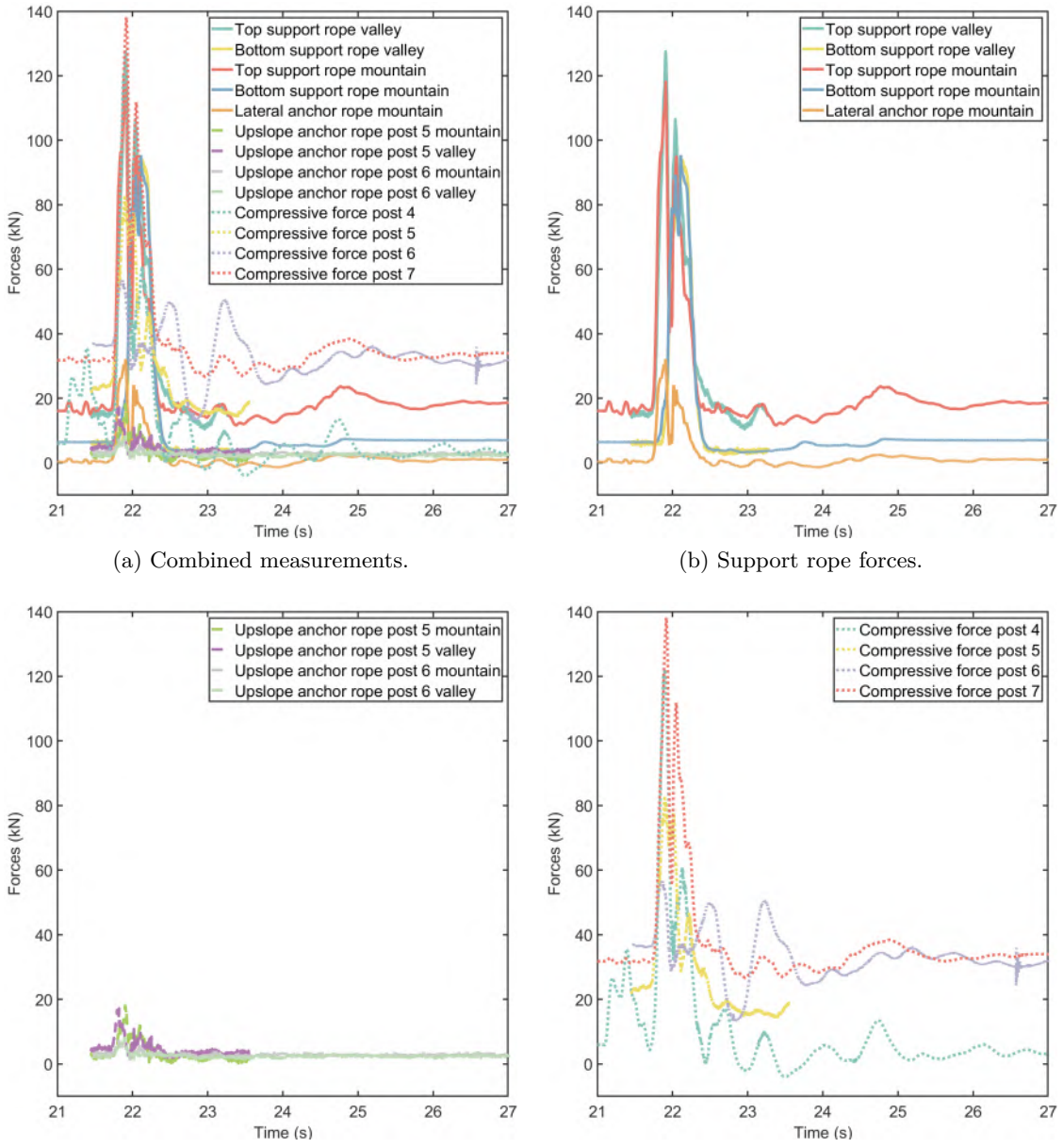

(a) Combined measurements.

(b) Support rope forces.

(c) Upslope rope forces.

(d) Post forces.

Figure 3.3.: Load cell data, corresponding to test 01, drop 09, subsequently labelled Run 1.9. The panels individually show a) all measurements, b) support ropes, c) upslope ropes and d) posts.

Forces measured in the net are compiled in Tables 3.1 and 3.3 and rock energies measured before impact are shown in Tables 3.2 and 3.4. The energies have been calculated using the video footage from different angles. Leading uncertainties arise from manual pinpointing the exact rock location and its transfer to a three-dimensional, geo-referenced position. With the

current workflow, the uncertainty of the energies is $< 20\%$. As two test days are presented, runs from the pre-test are labelled 1.1, 1.2, etc., runs from the second test are consequently labelled 2.1, 2.2, ….

3.1. Pre-test, 13 September, 2019

Load cell data and reconstructed energies from the pre-test: Run 1.5 is missing due to data acquisition failure. Tests 1.6 and 1.7 missed the barrier and did not result in load cell readings.

Table 3.1.: Force measurements from the pre-test.

	1.1	1.2	1.3	1.4	1.8	1.9
Top support rope valley	-	-	60	182	-	127
Bottom support rope valley	-	-	25	83	-	91
Lateral anchor rope valley	-	-	0.5	97.0	-	-
Compressive force post 7	120	52	-	-	-	138
Compressive force post 6	-	-	62	120	-	57
Compressive force post 5	-	-	-	134	200	81
Compressive force post 4	39	36	-	-	-	122
Upslope anchor rope post 5 mountain	-	-	-	14	60	18
Upslope anchor rope post 5 valley	-	-	-	13	88	16
Top support rope mountain	87	68	39	-	-	119
Bottom support rope mountain	48	28	39	-	-	95
Lateral anchor rope mountain	24	18	9	-	-	33

Table 3.2.: Reconstructed rock energies of barrier impacts from the pre-test.

Run Number/ Rock	Impact Field	Impact Point	E_{kin} (kJ)	E_{rot} (kJ)	E_{tot} (kJ)	E_{kin}/E_{rot}
1.1 Equant 800	6	8	98	29	127	3.4
1.2 Equant 800	4	8	69	13	82	5.3
1.3 Wheel 800	3	7	40	11	51	3.6
1.4 Equant 2600	3	5	120	64	185	1.9
1.5 Equant 2600	4	8	203	36	239	5.6
1.8 Wheel 2600	4	9	1003	103	1107	9.7
1.9 Equant 2600	3	8	415	69	483	6.0

3.2. GeoSummit test, 4 October, 2019

Load cell data and reconstructed energies from GeoSummit test: Here, runs 2.7., 2.8. and 2.11. missed the barrier.

Table 3.3.: Force measurements from GeoSummit test.

	2.1	2.2	2.3	2.4	2.5	2.6	2.9	2.10
Top support rope valley	81	193	81	13	92	49	32	183
Bottom support rope valley	61	79	61	17	193	183	15	99
Lateral anchor rope valley	16	13	31	68	318	213	48	105
Compressive force post 7	116	223	186	180	207	248	-	-
Compressive force post 6	12	10	-	80	172	160	-	
Compressive force post 5	31	107	-	69	84	127	8	-
Compressive force post 4	69	188	69	153	113	122	42	79
Upslope anchor rope post 6 mountain	26	20	-	8	36	31	147	-
Upslope anchor rope post 6 valley	60	74	-	10	12	18	50	-
Upslope anchor rope post 5 mountain	20	11	-	164	198	224	25	-
Upslope anchor rope post 5 valley	112	79	-	73	101	123	6	-
Top support rope mountain	103	21	160	208	246	222	90	156
Bottom support rope mountain	69	136	93	101	128	148	37	93
Lateral anchor rope mountain	34	83	51	85	114	134	44	61

Table 3.4.: Reconstructed rock energies of barrier impacts from the GeoSummit test.

Run Number/ Rock	Impact Field	Impact Point	E_{kin} (kJ)	E_{rot} (kJ)	E_{tot} (kJ)	E_{kin}/E_{rot}
2.1 Equant 800	4	8	160	-	-	-
2.2 Equant 2600	3	7	619	161	780	3.8
2.3 Equant 2600	5	7	619	104	723	6.0
2.4 Equant 2600	2	9	619	154	773	4.0
2.5 Wheel 2600	4	9	924	145	1069	6.4
2.6 Wheel 2600	4	8	749	150	899	5.0
2.9 Equant 2600	5	9	520	161	681	3.2

3.2.1. Post impact in run 2.4.

One of the goals of testing in real conditions is to induce impact configurations absent in standard testing procedures. In the test 2.4. a direct impact of an equant EOTA boulder of 2600 kg on post 3 was recorded. Figure 3.4 shows the damage to the post. The structural integrity of the entire barrier is only minimally affected as more tests were conducted.

Figure 3.4.: Close-up images of post number 3 after impact of a block of 2600 kg. The post is deformed but functional, as five more impacts on the barrier were recorded.

Figure 3.5 shows the measured forces in the net and the accelerometer data. Figure 3.5a features the support ropes readings, displaying a maximal load of 207 kN on the top support rope. Figure 3.5b shows the forces on the four instrumented posts. Post 4 recorded a peak value of 153 kN. This post was the closest instrumented post to the impacted one. Figure 3.5c shows a zoomed in cut of the StoneNode accelerometer data on the last jump and net impact at about 15.5 s. The velocity of the block was approximately 22 m/s and 1550 °/s with a total energy of 772 kJ.

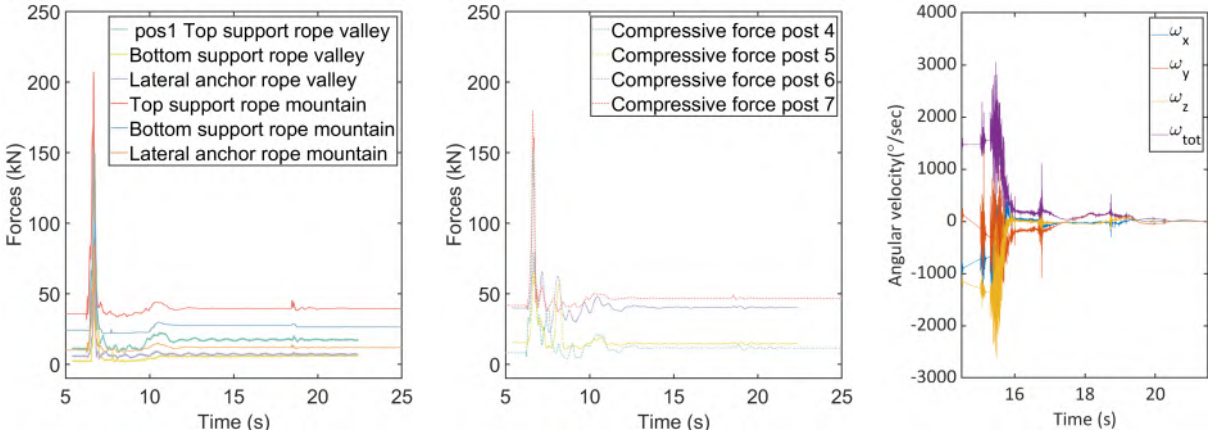

(a) Support rope forces (b) Post forces (c) StoneNode readings

Figure 3.5.: Measurements from run 2.4. where a post impact was recorded. The individual panels feature a) the support ropes forces, b) the post forces and c) StoneNode accelerometer readings. Note, the time scales between the force sensors and StoneNode are not calibrated.

4. Conclusions

The first experimental tests were successfully conducted at the Chant Sura test site with a 2000 kJ flexible barrier. In-situ instrumentation combined with the instrumented barrier allows for a comprehensive approach to measure acting forces and impulses during contact situations. The barrier post base plates were modified in order to install 300 kN load cells. Anchor cables were instrumented with force cells up to 500 kN to capture the response of the net over time. The translational and rotational deceleration of the rock was tracked with accelerometers and gyroscopes embedded inside a StoneNode [6].

The experimental setup at Chant Sura is an extension to the regular drop tests conducted by Geobrugg AG. They provide valuable insight not only due to the realistic impact behaviour of the rocks, but also allow to scrutinize the effect of rock shape and mass with respect to the acting forces. Rolling tests are not used as a certification method due to their lack of reliability: Reproducing identical conditions on a rolling test in natural terrain is almost impossible. Nonetheless, rolling tests are the only test able to produce realistic rotational energies and thus mimicking real case loadings. Calculated energies obtained from the tests show that rotational energies can amount for 15 to 30% of the block energy. Thus, even the first tests reveal the importance of studying the role of rotational energies in rockfalls in general and barrier interaction in particular.

The first tests show low impact energies for blocks of 800 kg. For blocks of 2700 kg, the energies can reach 1000 kJ. Larger blocks need to be released in order to load the nets near their design loads. Although still constrained by the limited number of drops, the tests show the problems of rock shape: Cubic shaped rocks tend to follow less erratic trajectories and hence are more predictable. Wheel shaped rocks start tumbling randomly. The transition time from wobbling to a wheel-like descending motion is a key factor determining the impacting rotational energy. The longer an undisturbed rotation around its major axis of inertia lasts, only insignificantly disturbed by the rock-ground interactions, the larger becomes the portion of rotational energy upon barrier impact.

This report provides a summary of the measured forces of the 2019 measurement campaign. We will further analyse the breaking motions, with emphasis on the energy dissipation mechanisms and rock deceleration upon impact into the flexible barrier. Further tests will be conducted to obtain additional data on single field impacts or special load cases to a flexible rockfall barrier under realistic conditions.

Bibliography

[1] A. Caviezel, S. E. Demmel, A. Ringenbach, Y. Bühler, G. Lu, M. Christen, C. E. Dinneen, L. A. Eberhard, D. von Rickenbach, and P. Bartelt. Reconstruction of four-dimensional rockfall trajectories using remote sensing and rock-based accelerometers and gyroscopes. *Earth Surface Dynamics*, 7(1):199–210, 2019.

[2] A. Caviezel and W. Gerber. Brief Communication: Measuring rock decelerations and rotation changes during short-duration ground impacts. *Natural Hazards and Earth System Sciences*, 18(11):3145–3151, 2018.

[3] A. Caviezel, M. Schaffner, L. Cavigelli, P. Niklaus, Y. Bühler, P. Bartelt, M. Magno, and L. Benini. Design and Evaluation of a Low-Power Sensor Device for Induced Rockfall Experiments. *IEEE Transactions on Instrumentation and Measurement*, 67(4):767–779, 2018.

[4] R. I. Leine, A. Schweizer, M. Christen, J. Glover, P. Bartelt, and W. Gerber. Simulation of rockfall trajectories with consideration of rock shape. *Multibody System Dynamics*, 32(2):241–271, 2014.

[5] G. Lu, A. Caviezel, M. Christen, Y. Bühler, and P. Bartelt. Modelling rockfall dynamics using (convex) non-smooth mechanics. *Numerical Methods in Geotechnical Engineering IX*, pages 575–583, 2018.

[6] P. Niklaus, T. Birchler, T. Aebi, M. Schaffner, L. Cavigelli, A. Caviezel, M. Magno, and L. Benini. StoneNode: A low-power sensor device for induced rockfall experiments. In *2017 IEEE Sensors Applications Symposium (SAS)*, pages 1–6, Glassboro, NJ, USA, 2017. IEEE.

Appendices

A. Chant Sura pre-test, 13 September 2019

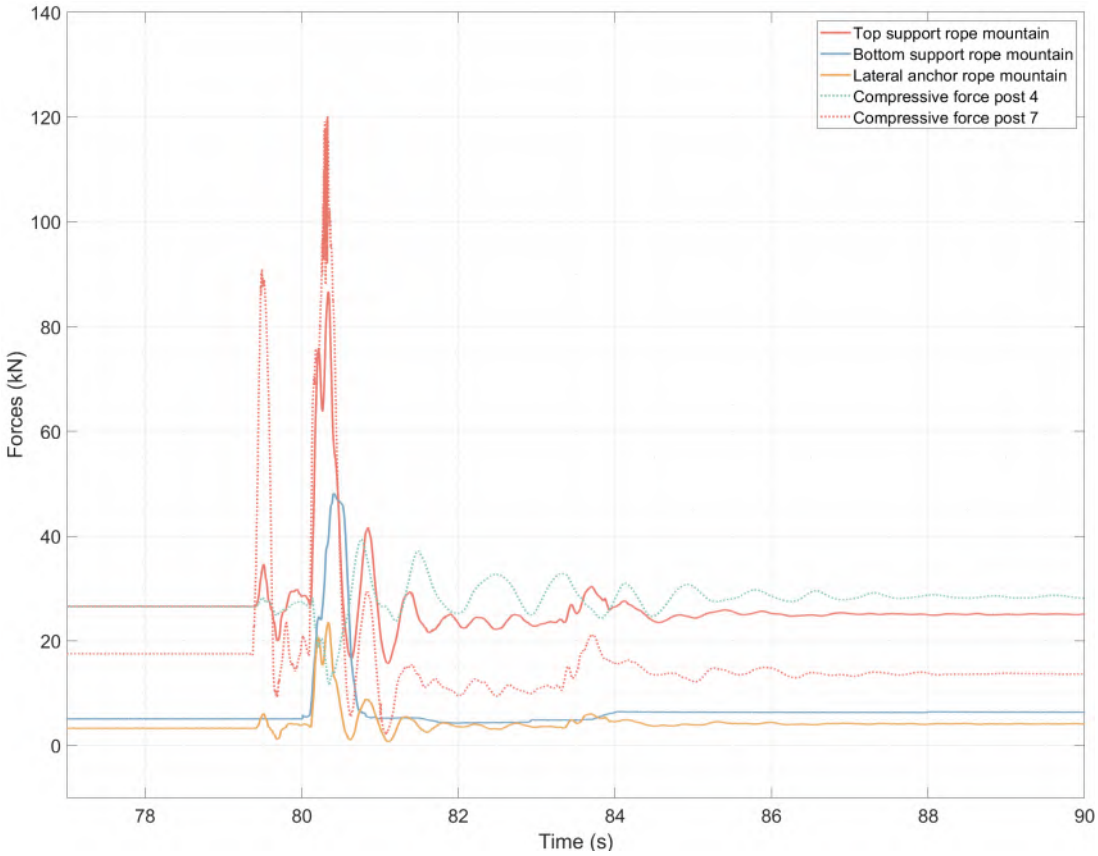

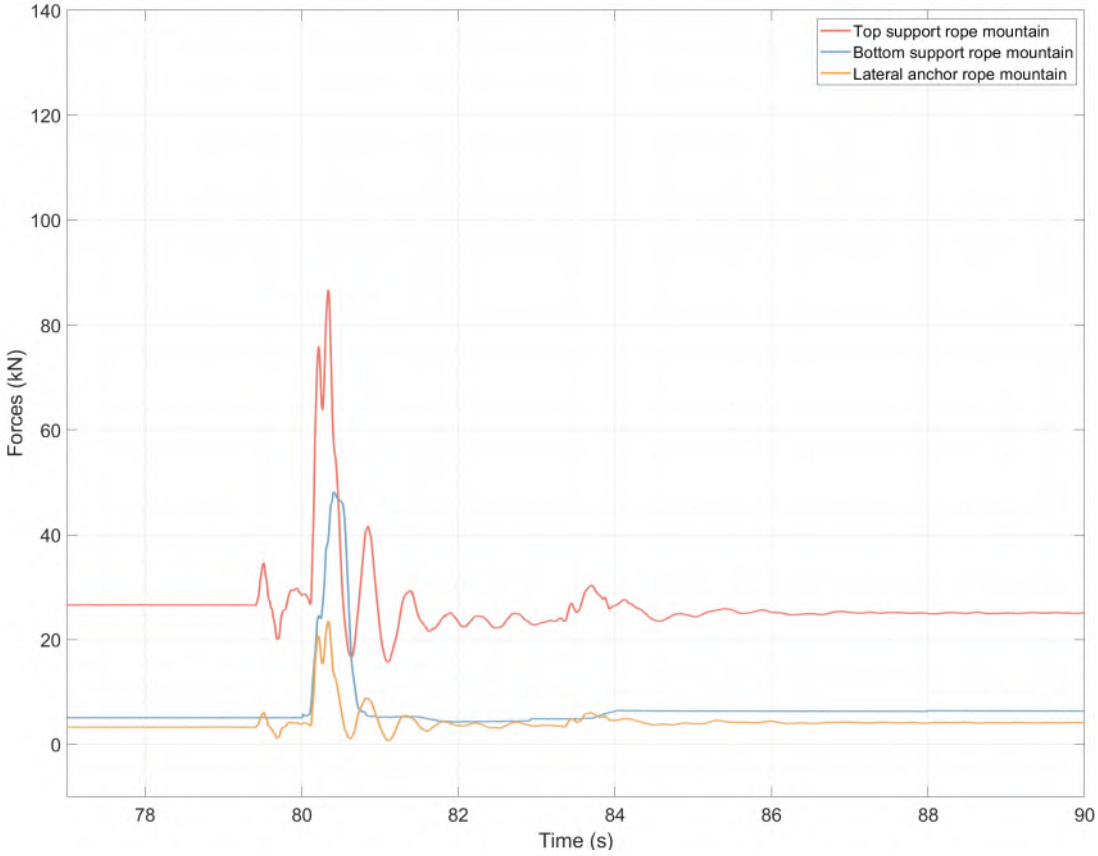

INNONETS PROJEKT		Test Nr: 01	Drop Nr: 01
Rock Rolling Test	Date: 13.09.2019	Block mass 840kg	Block type: EOTA111
Location: Chant Sura	Flexible Barrier 2000kJ	Impact Field: 3	Impact point: 8

Remarks: Ground contact directly after net contact.

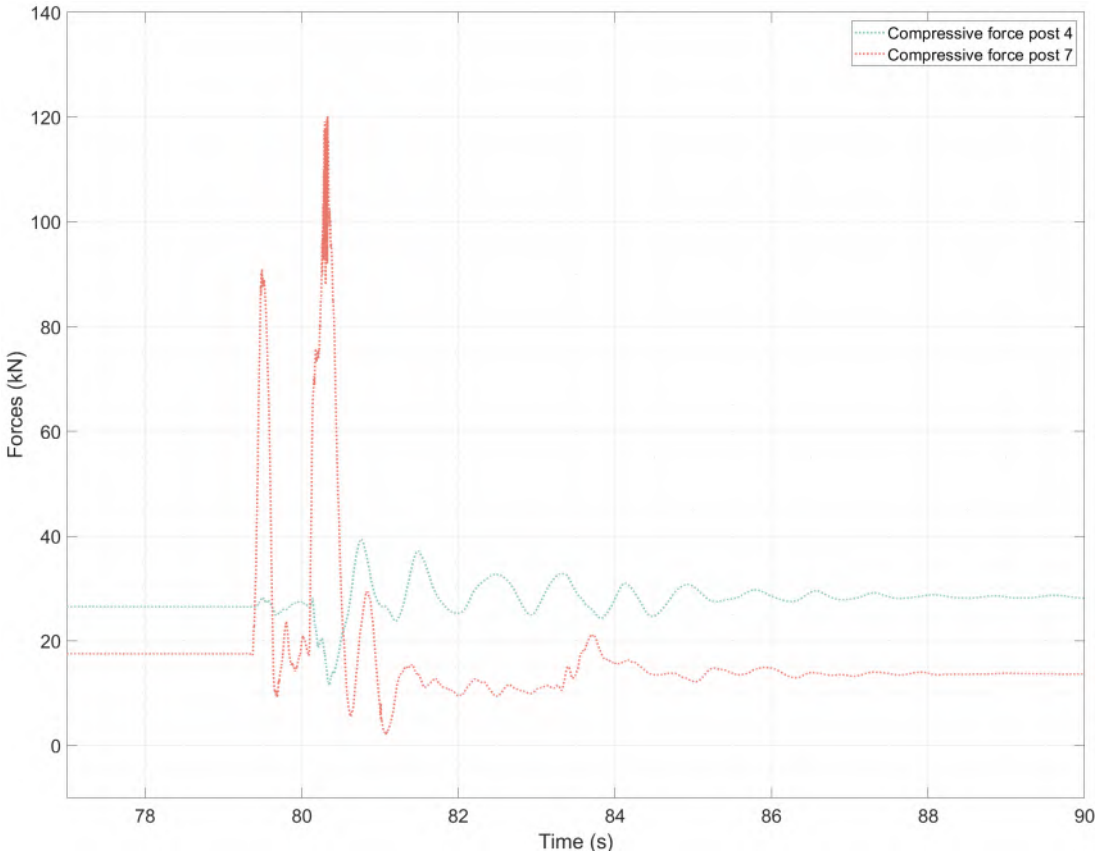

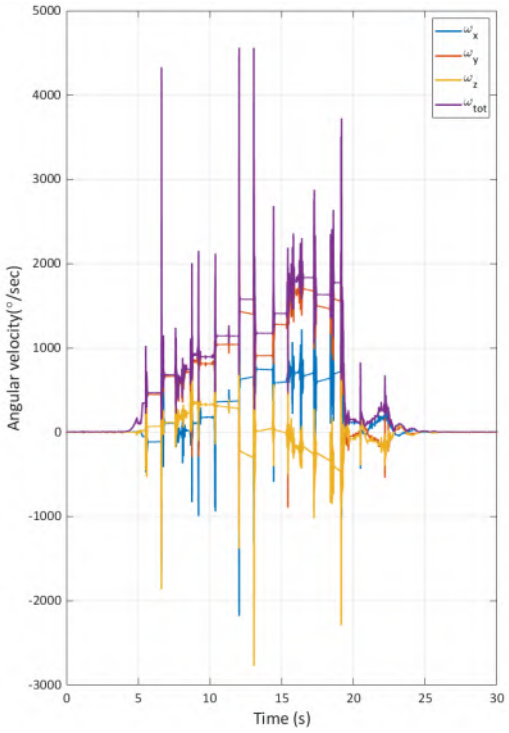

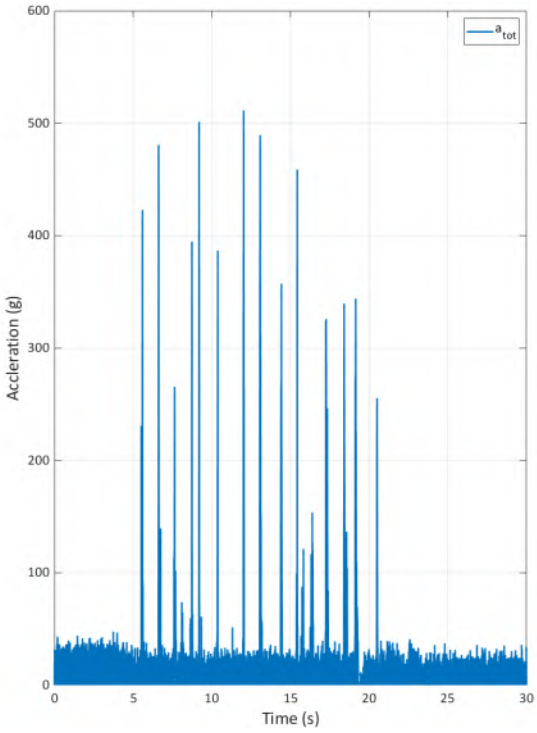

INNONETS PROJEKT		Test Nr: 01	Drop Nr: 01
Rock Rolling Test	Date: 13.09.2019	Block mass 840kg	Block type: EOTA111
Location: Chant Sura	Flexible rockfall Flexible Barrier 2000kJ	Impact Field: 3	Impact point: 8

Remarks: Ground contact directly after net contact.

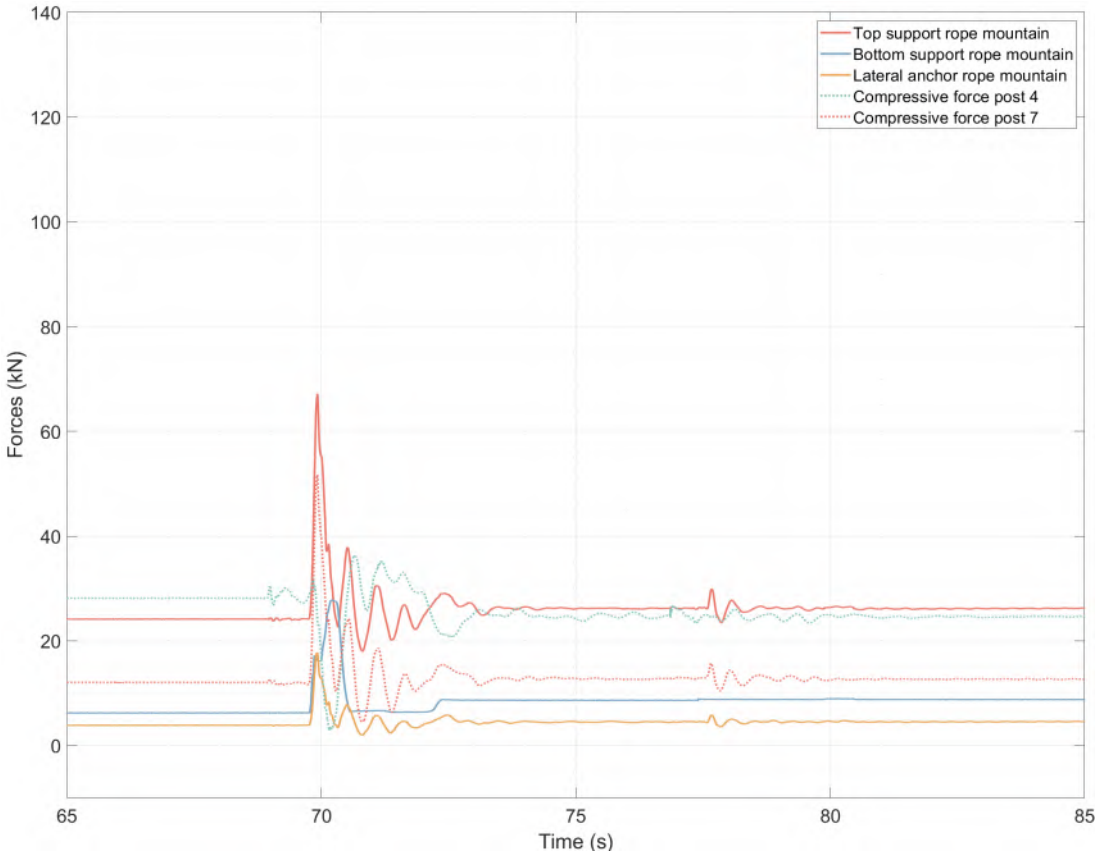

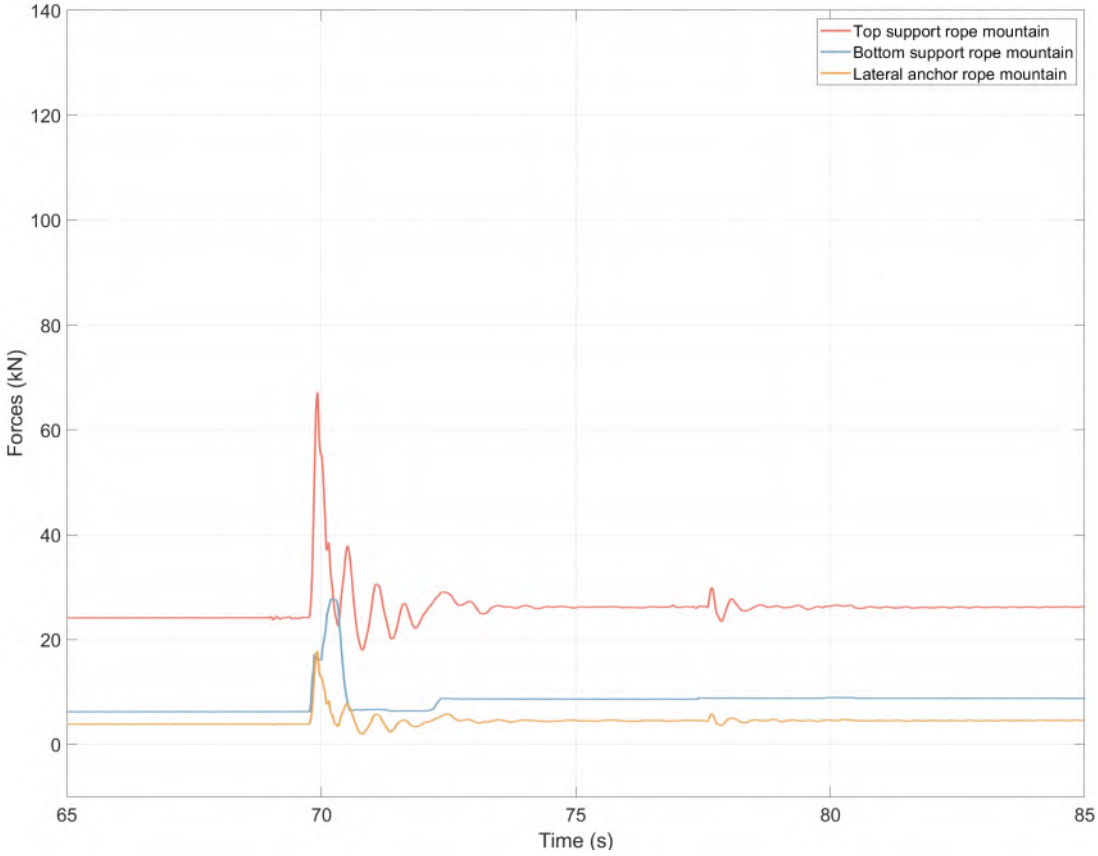

INNONETS PROJEKT		Test Nr: 01	Drop Nr: 02
Rock Rolling Test	Date: 13.09.2019	Block mass 840kg	Block type: EOTA111
Location: Chant Sura	Flexible Barrier 2000kJ	Impact Field: 4	Impact point: 8

Remarks: Ground contact 1m after net contact.

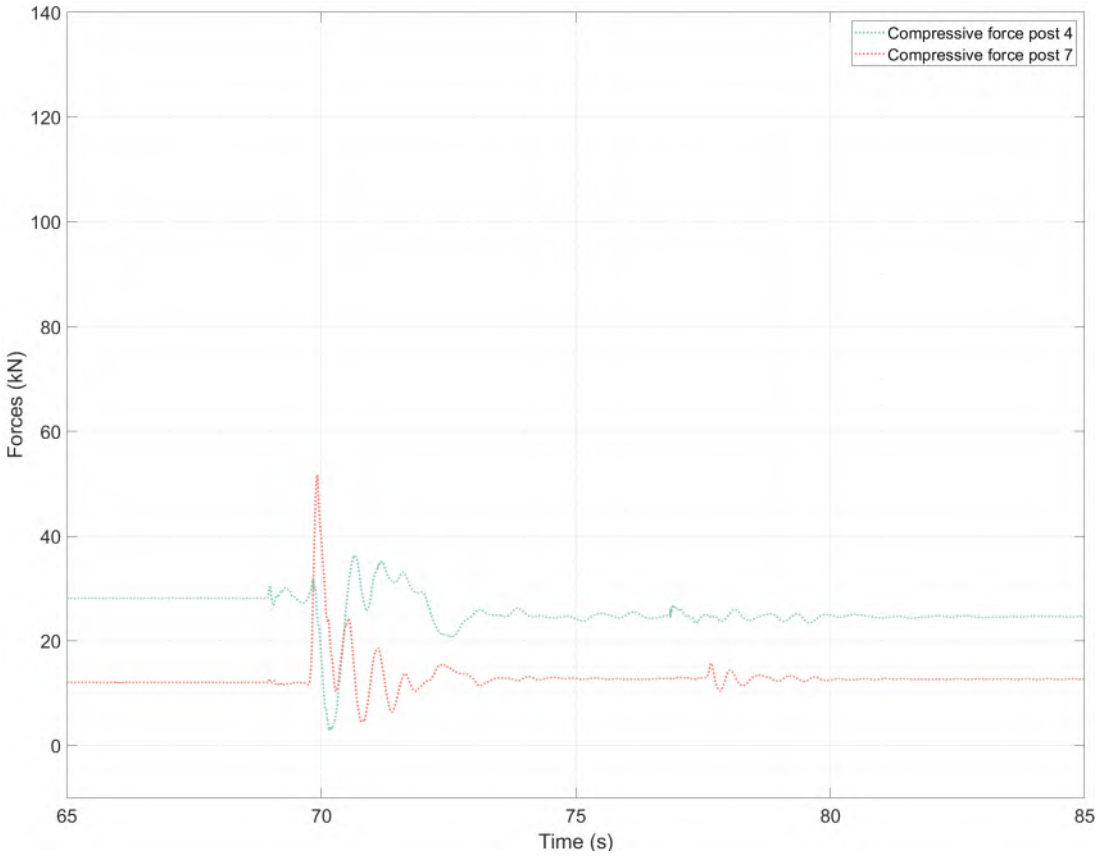

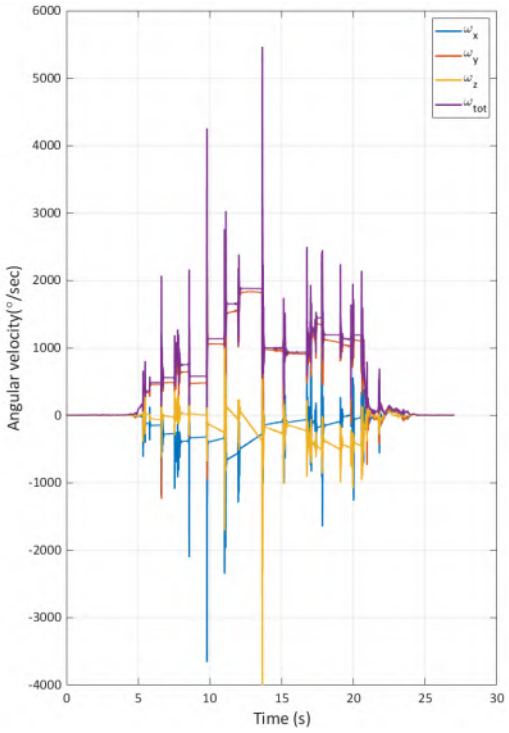

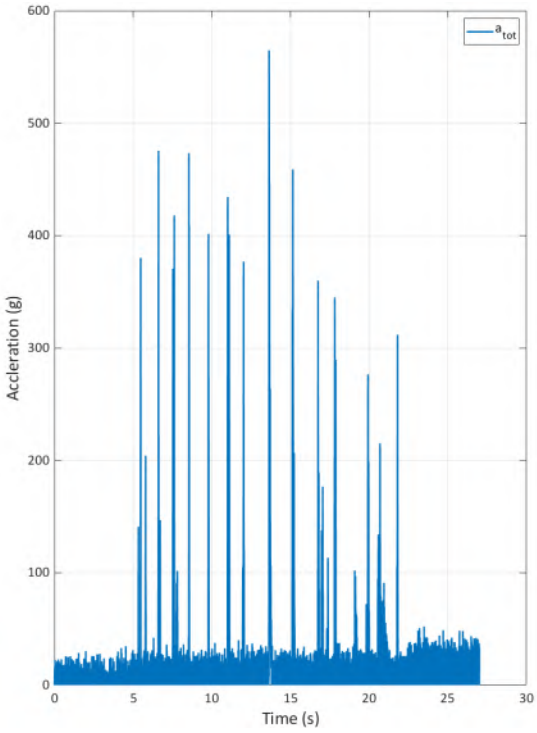

INNONETS PROJEKT		Test Nr: 01	Drop Nr: 02
Rock Rolling Test	Date: 13.09.2019	Block mass 840kg	Block type: EOTA111
Location: Chant Sura	Flexible Barrier 2000kJ	Impact Field: 4	Impact point: 8

Remarks: Ground contact 1m after net contact.

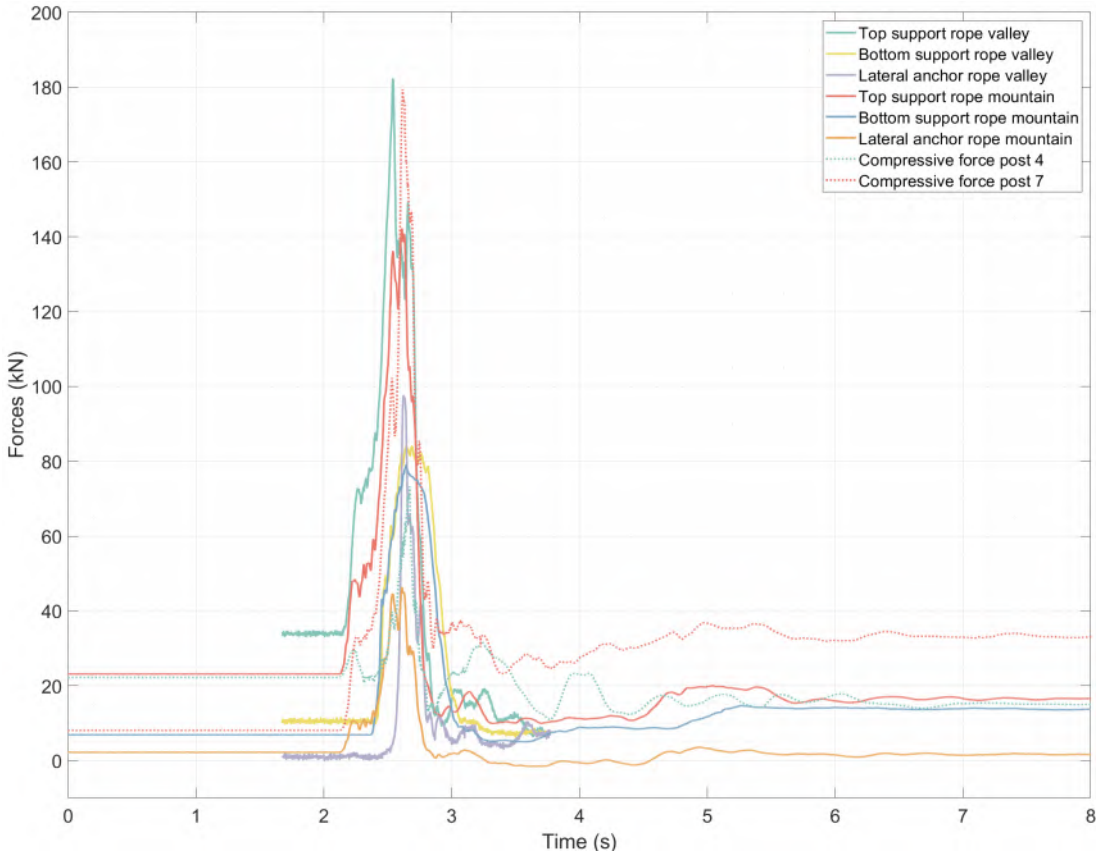

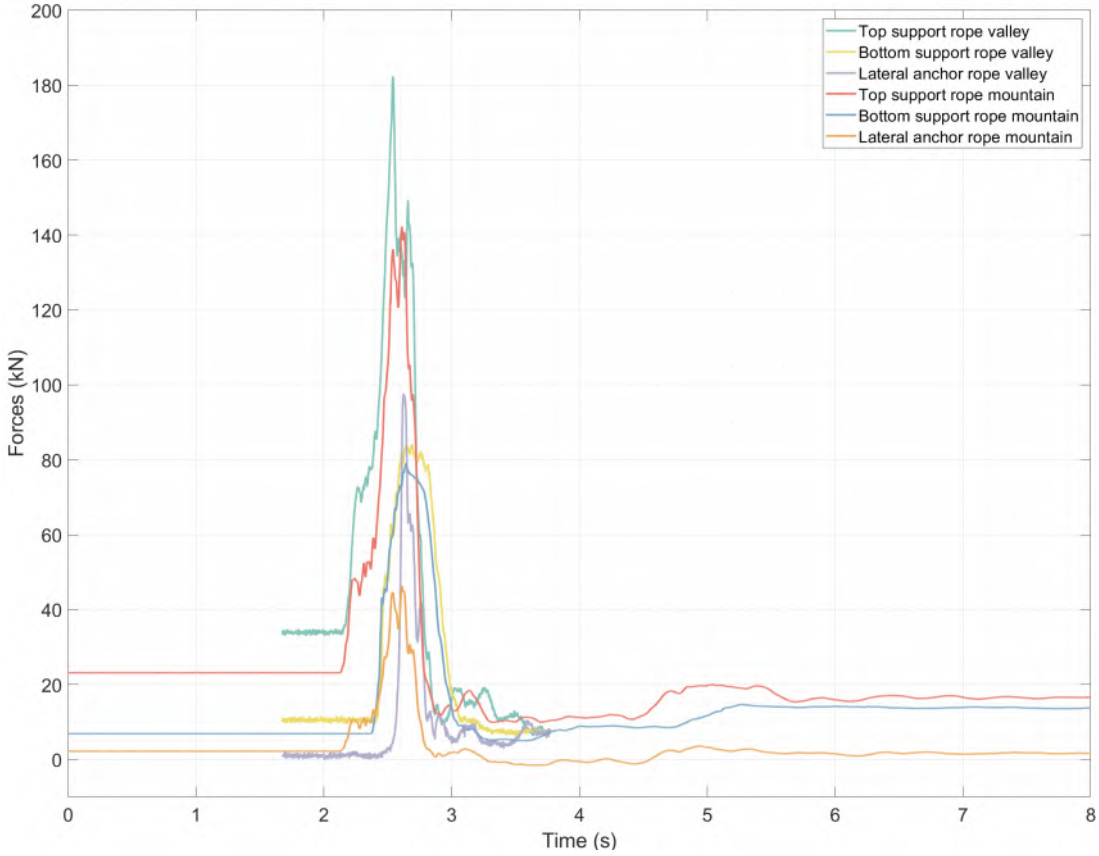

INNONETS PROJEKT		Test Nr: 01	Drop Nr: 04
Rock Rolling Test	Date: 13.09.2019	Block mass 2600kg	Block type: EOTA111
Location: Chant Sura	Flexible Barrier 2000kJ	Impact Field: 3	Impact point: 5

Remarks: Block hit before impact. Big energy dissipation, big jump.

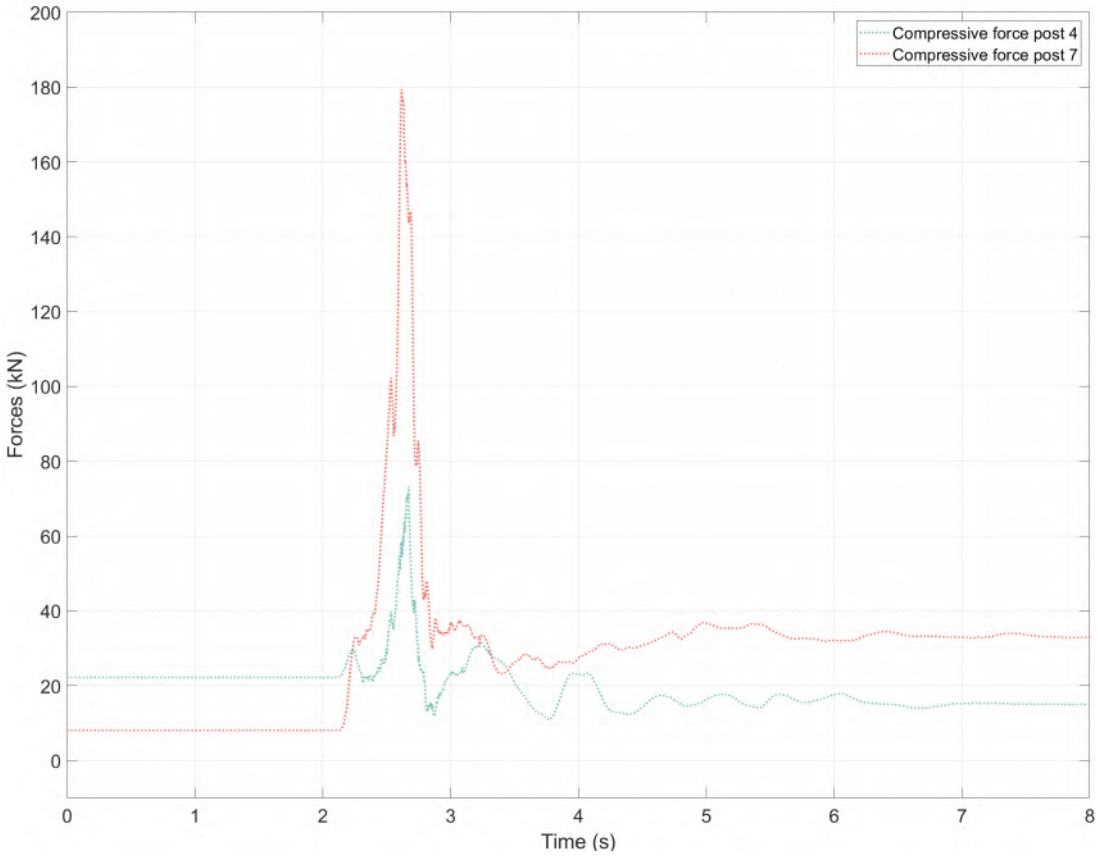

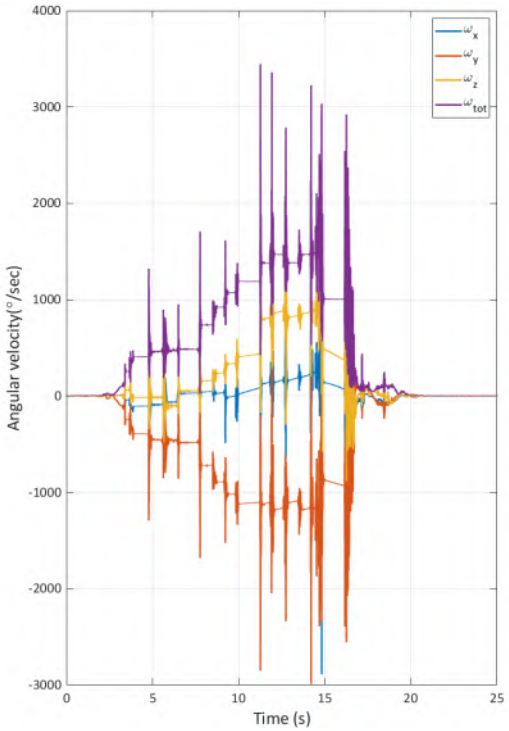

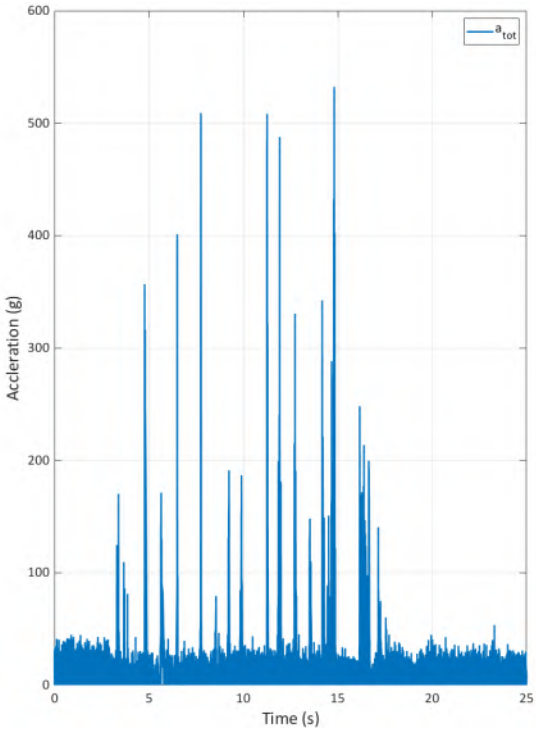

INNONETS PROJEKT		Test Nr: 01	Drop Nr: 04
Rock Rolling Test	Date: 13.09.2019	Block mass 2600kg	Block type: EOTA111
Location: Chant Sura	Flexible Barrier 2000kJ	Impact Field: 3	Impact point: 5

Remarks: Block hit before impact. Big energy dissipation, big jump.

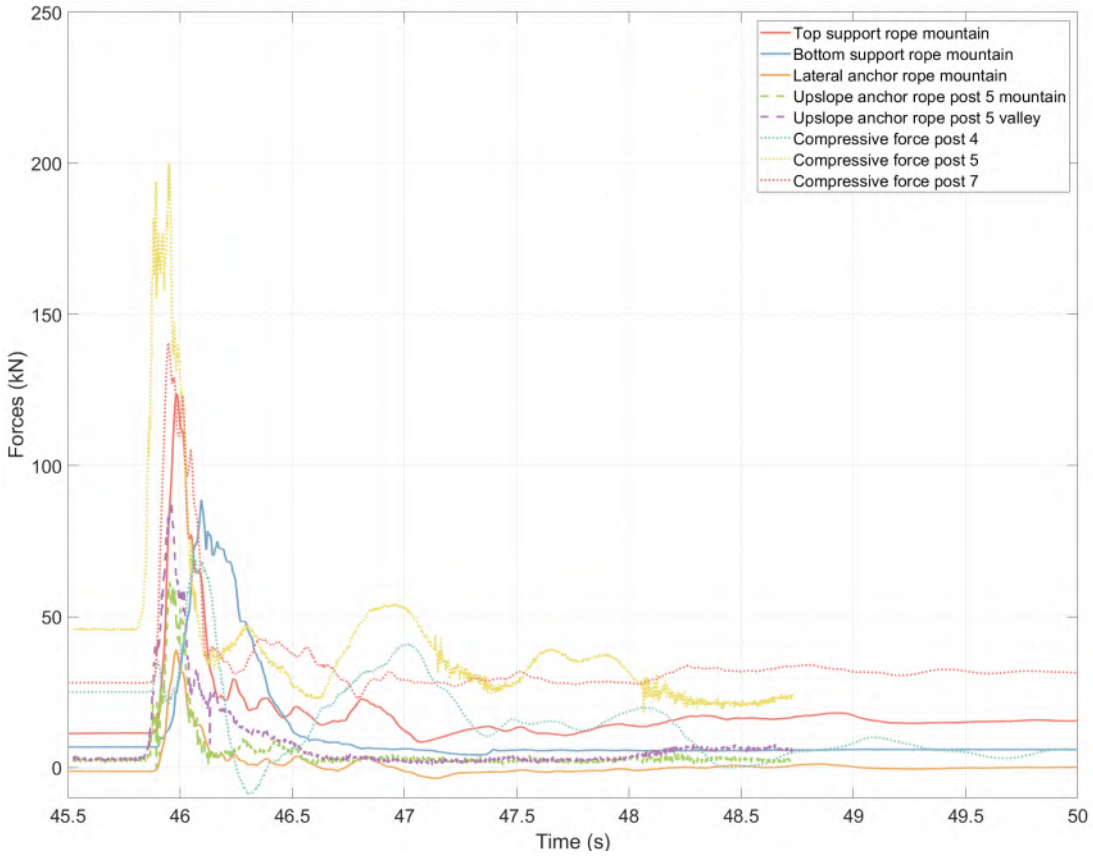
Top support rope mountain
Bottom support rope mountain
Lateral anchor rope mountain
Upslope anchor rope post 5 mountain
Upslope anchor rope post 5 valley
Compressive force post 4
Compressive force post 5
Compressive force post 7
Forces (kN)
Time (s)
250
200
150
100
50
0
45.5
46
46.5
47
47.5
48
48.5
49
49.5
50

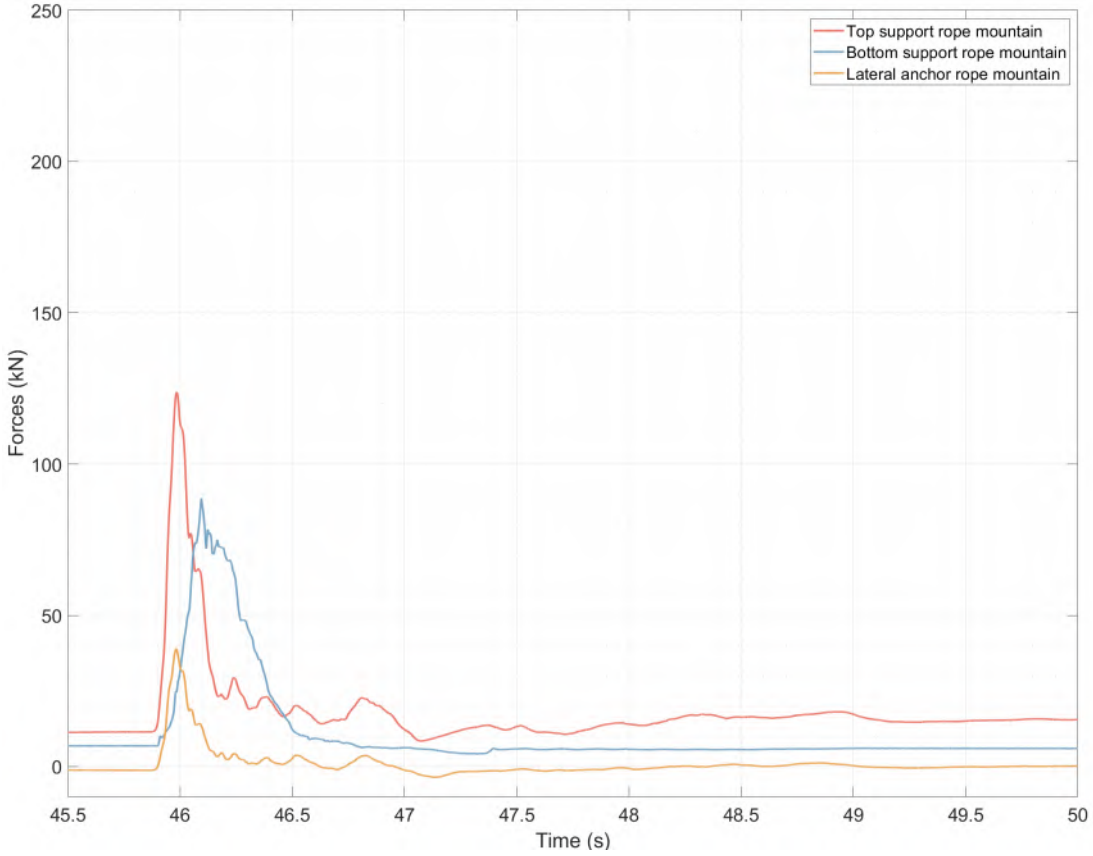
Top support rope mountain
Bottom support rope mountain
Lateral anchor rope mountain
Forces (kN)
Time (s)
250
200
150
100
50
0
45.5
46
46.5
47
47.5
48
48.5
49
49.5
50

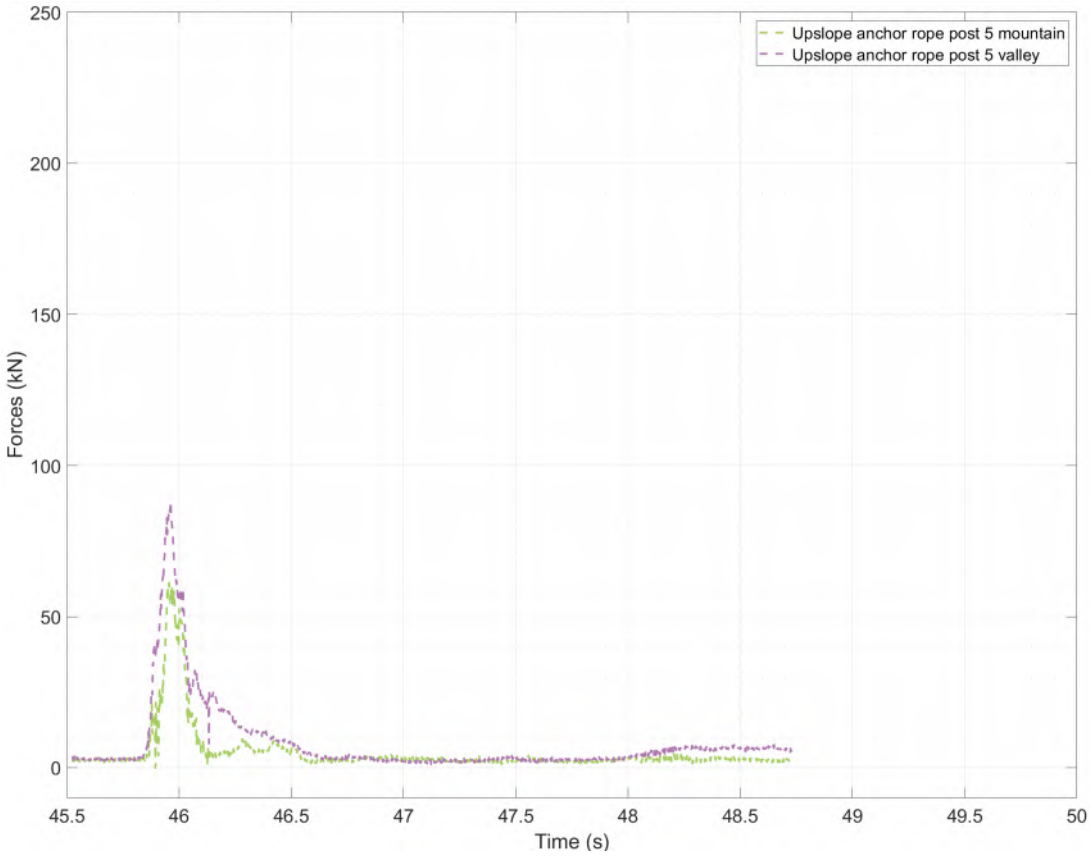
Upslope anchor rope post 5 mountain
Upslope anchor rope post 5 valley
Forces (kN)
Time (s)
250
200
150
100
50
0
45.5
46
46.5
47
47.5
48
48.5
49
49.5
50

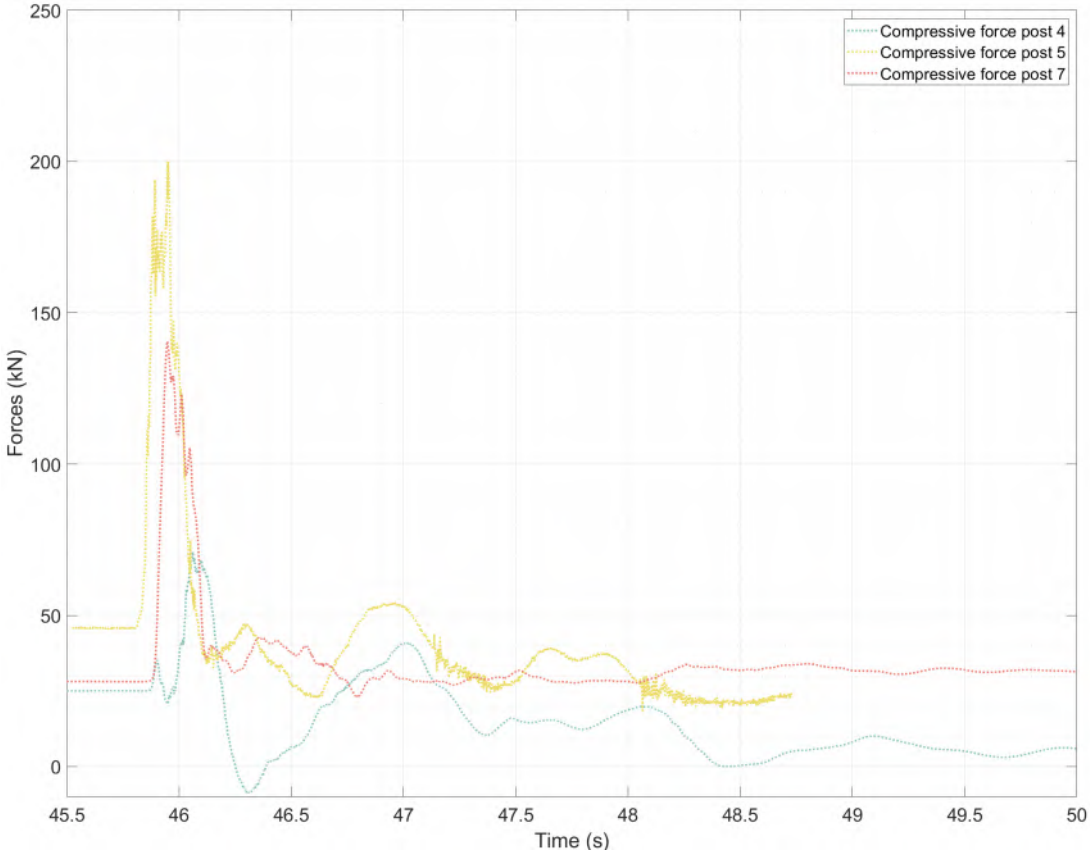
Compressive force post 4
Compressive force post 5
Compressive force post 7
Forces (kN)
Time (s)
250
200
150
100
50
0
45.5
46
46.5
47
47.5
48
48.5
49
49.5
50

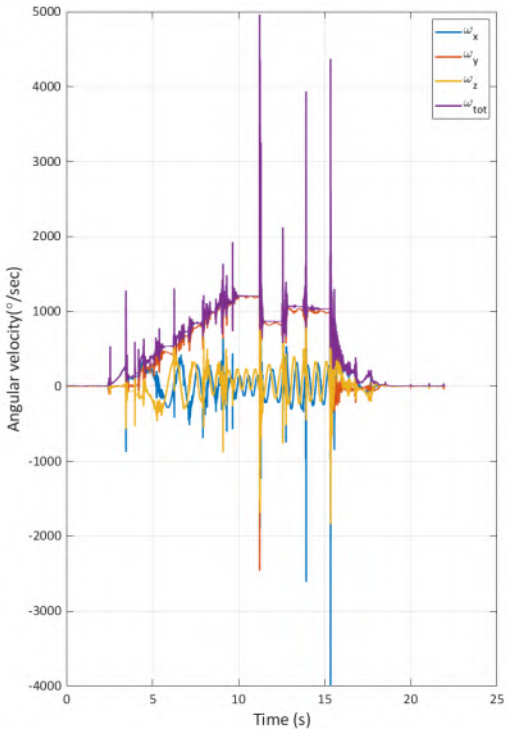
Angular velocity(°/sec)
Time (s)
ω_x
ω_y
ω_z
ω_{tot}

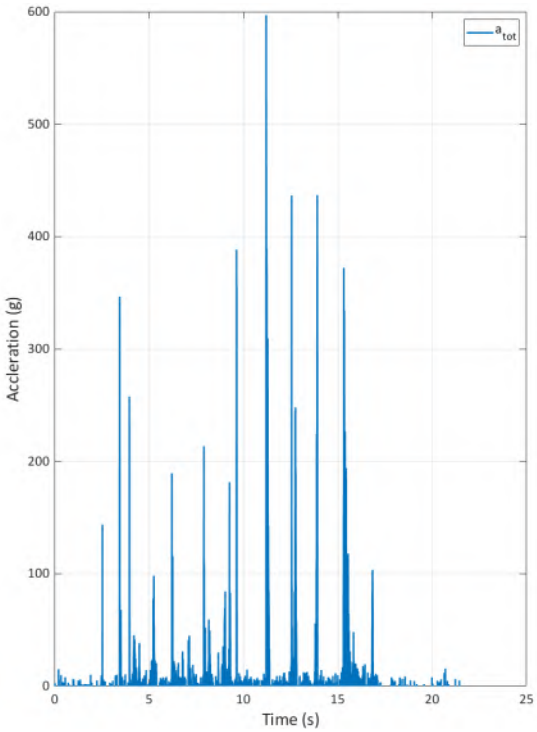
Accleration (g)
Time (s)
a_{tot}

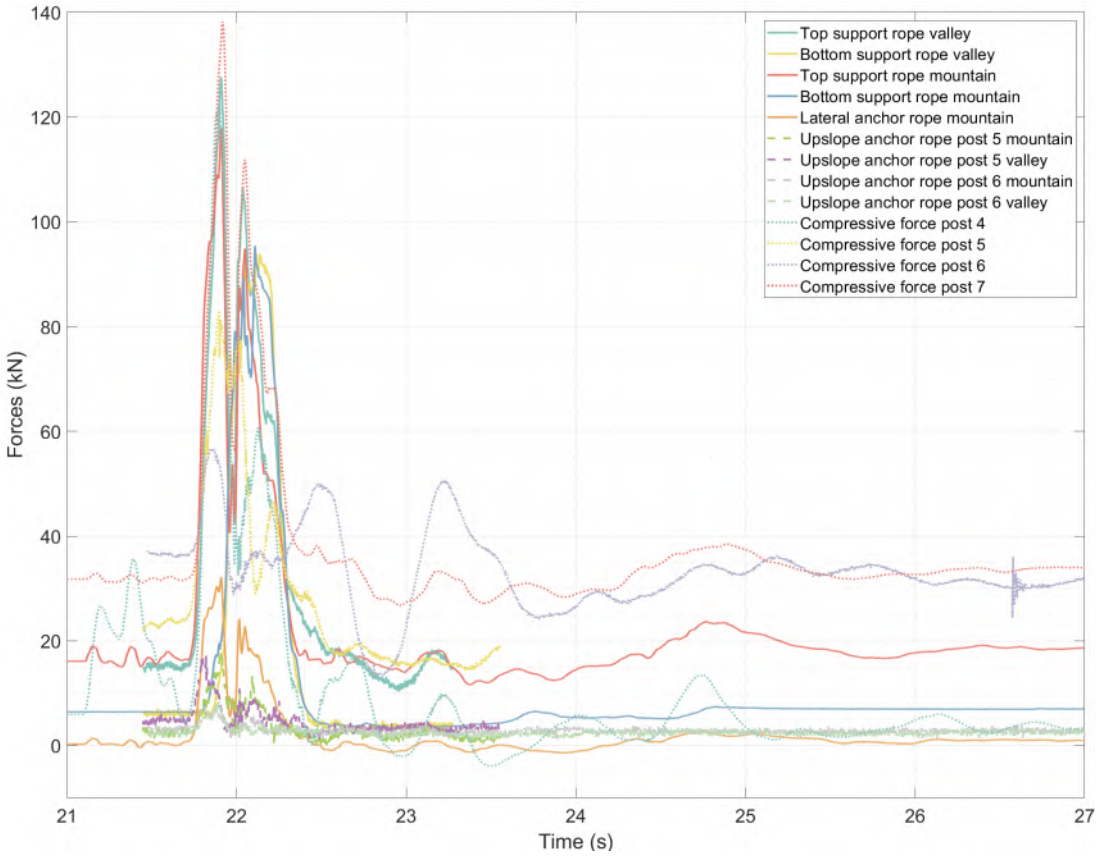

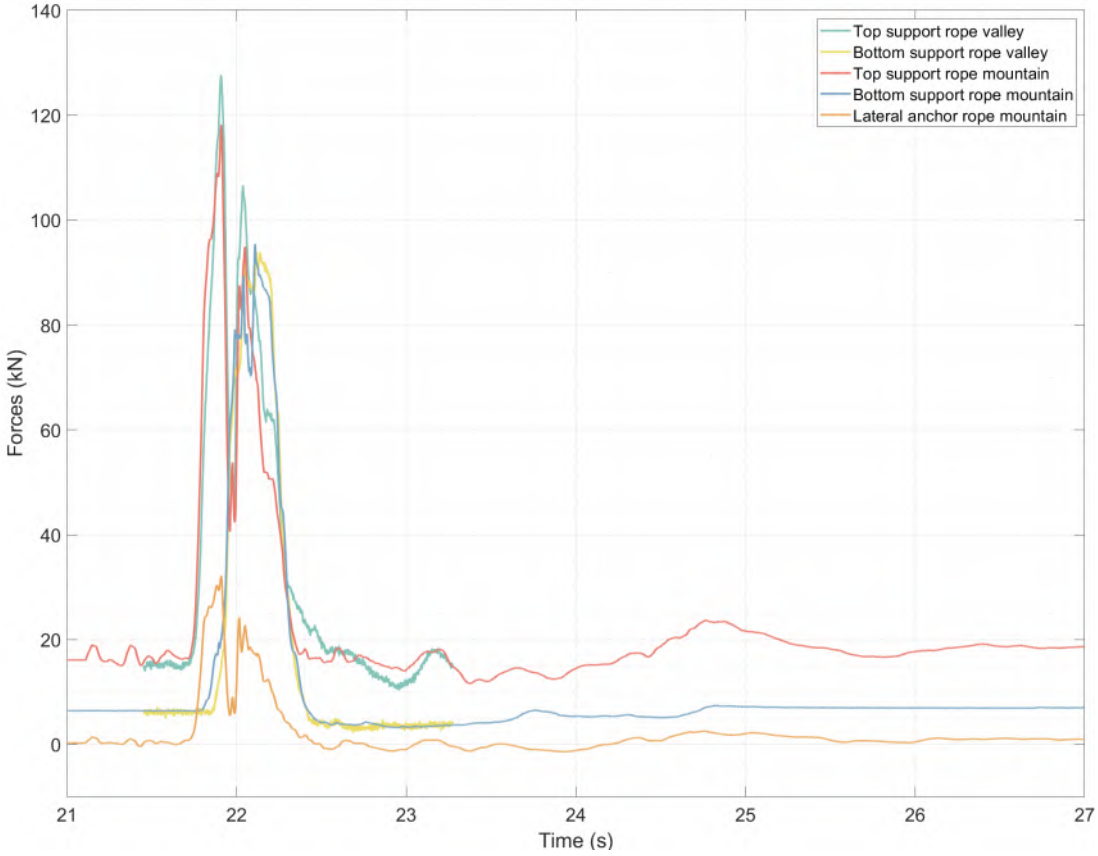

INNONETS PROJEKT		Test Nr: 01	Drop Nr: 09
Rock Rolling Test	Date: 13.09.2019	Block mass 2600kg	Block type: EOTA111
Location: Chant Sura	Flexible Barrier 2000kJ	Impact Field: 3	Impact point: 8

Remarks: No ground contact during deceleration in the net

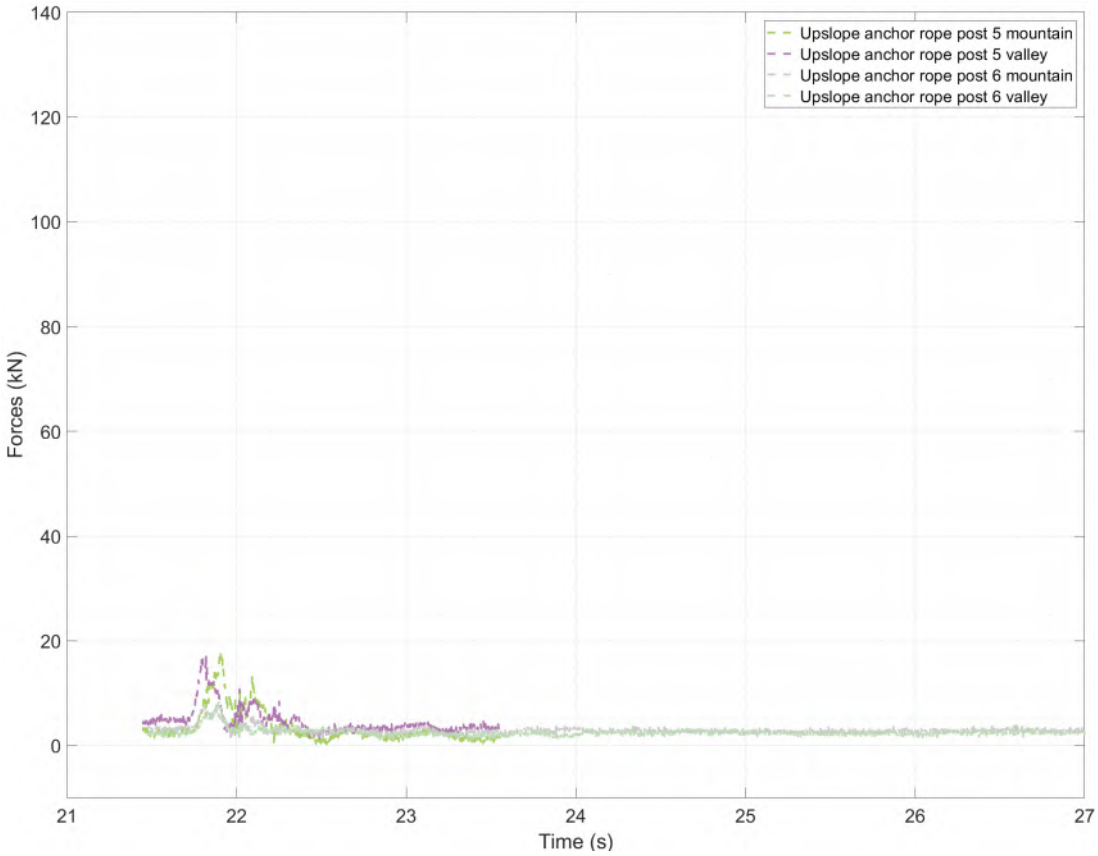

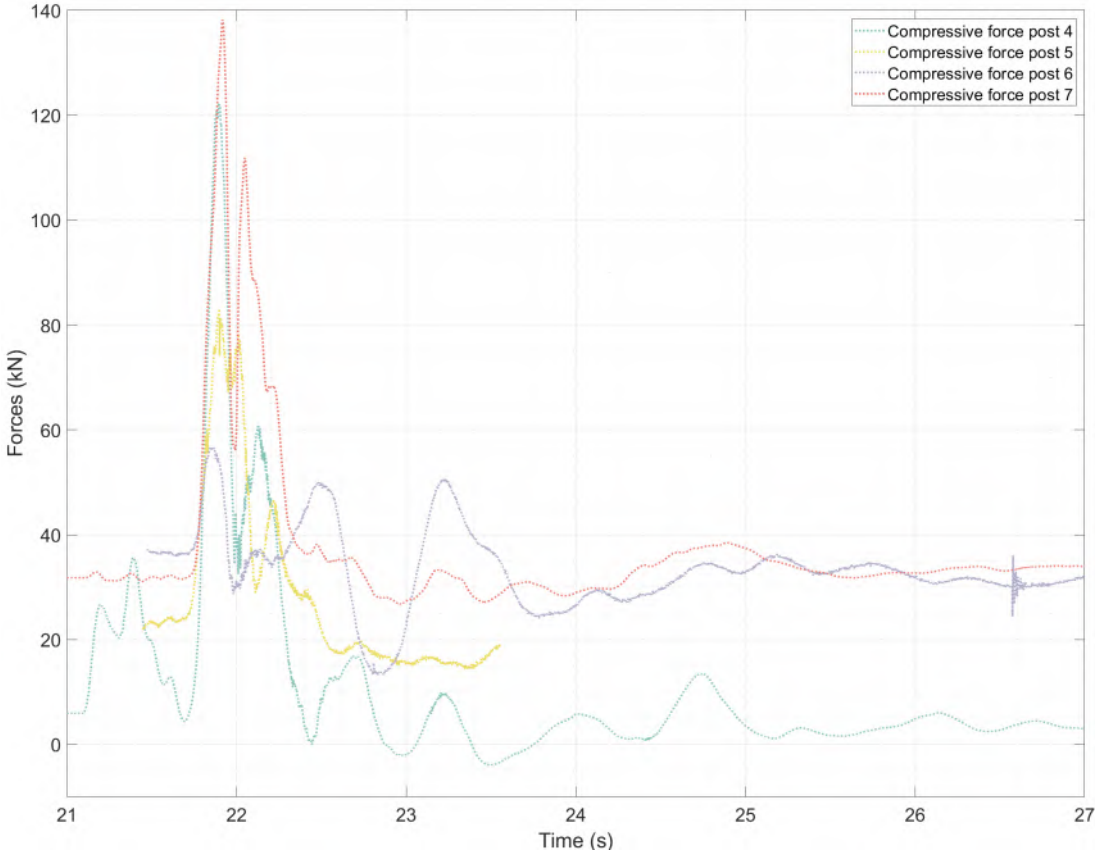

INNONETS PROJEKT		Test Nr: 01	Drop Nr: 09
Rock Rolling Test	Date: 13.09.2019	Block mass 2600kg	Block type: EOTA111
Location: Chant Sura	Flexible Barrier 2000kJ	Impact Field: 3	Impact point: 8

Remarks: No ground contact during deceleration in the net

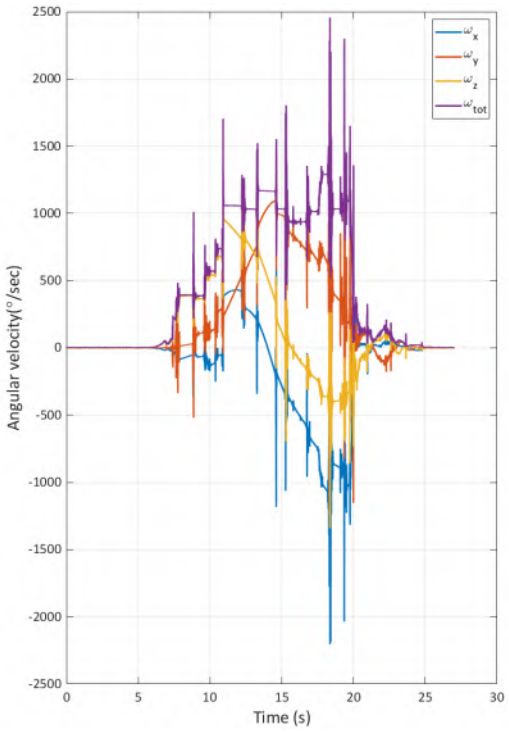

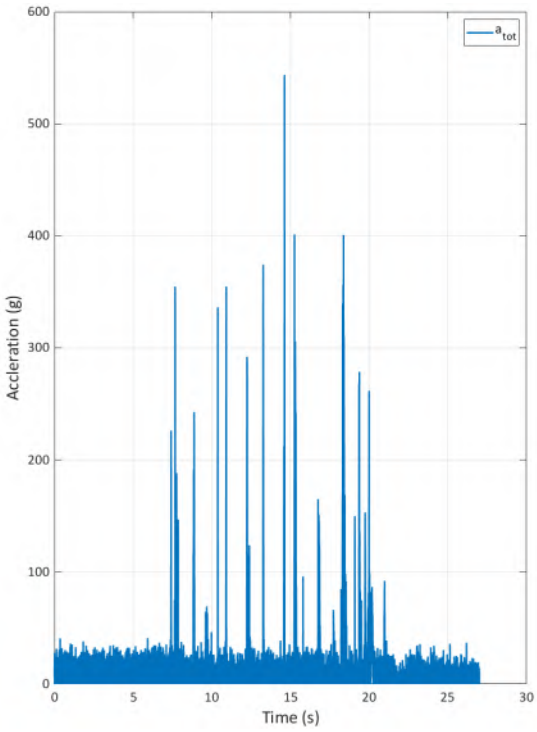

INNONETS PROJEKT		Test Nr: 01	Drop Nr: 09
Rock Rolling Test	Date: 13.09.2019	Block mass 2600kg	Block type: EOTA111
Location: Chant Sura	Flexible Barrier 2000kJ	Impact Field: 3	Impact point: 8

Remarks: No ground contact during deceleration in the net

B. Chant Sura GeoSummit test, 4 October 2019

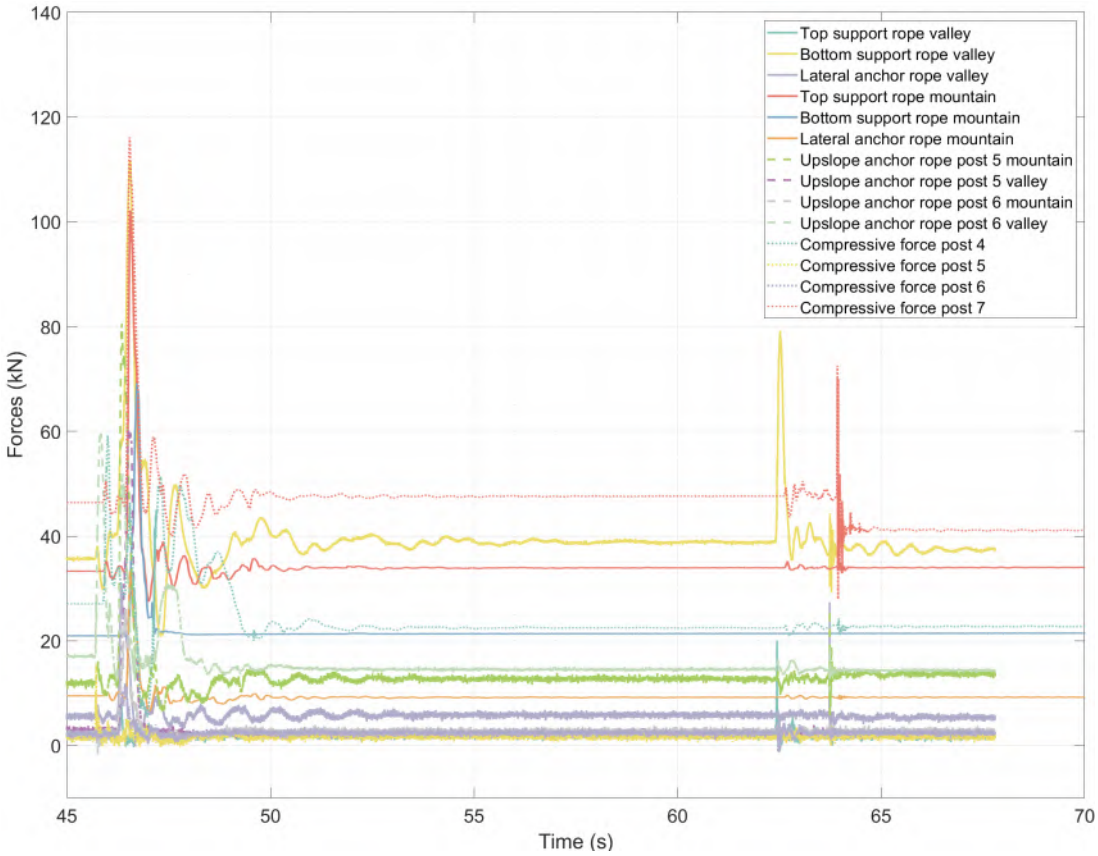

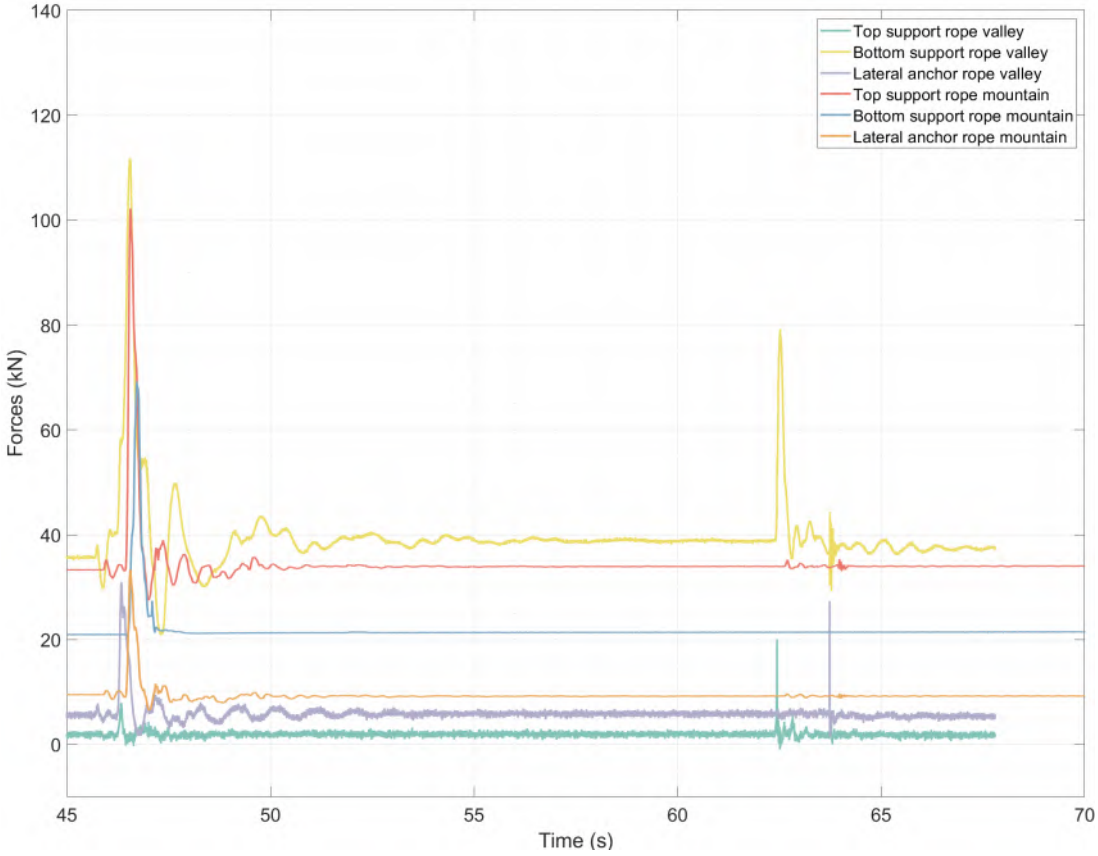

INNONETS PROJEKT		Test Nr: 02	Drop Nr: 01
Rock Rolling Test	Date: 04.10.2019	Block mass 840kg	Block type: EOTA111
Location: Chant Sura	Flexible Barrier 2000kJ	Impact Field: 4	Impact point: 8

Remarks: Ground contact aprox. 1.5m after net contact. Rolling over upslope valley anchor rope.

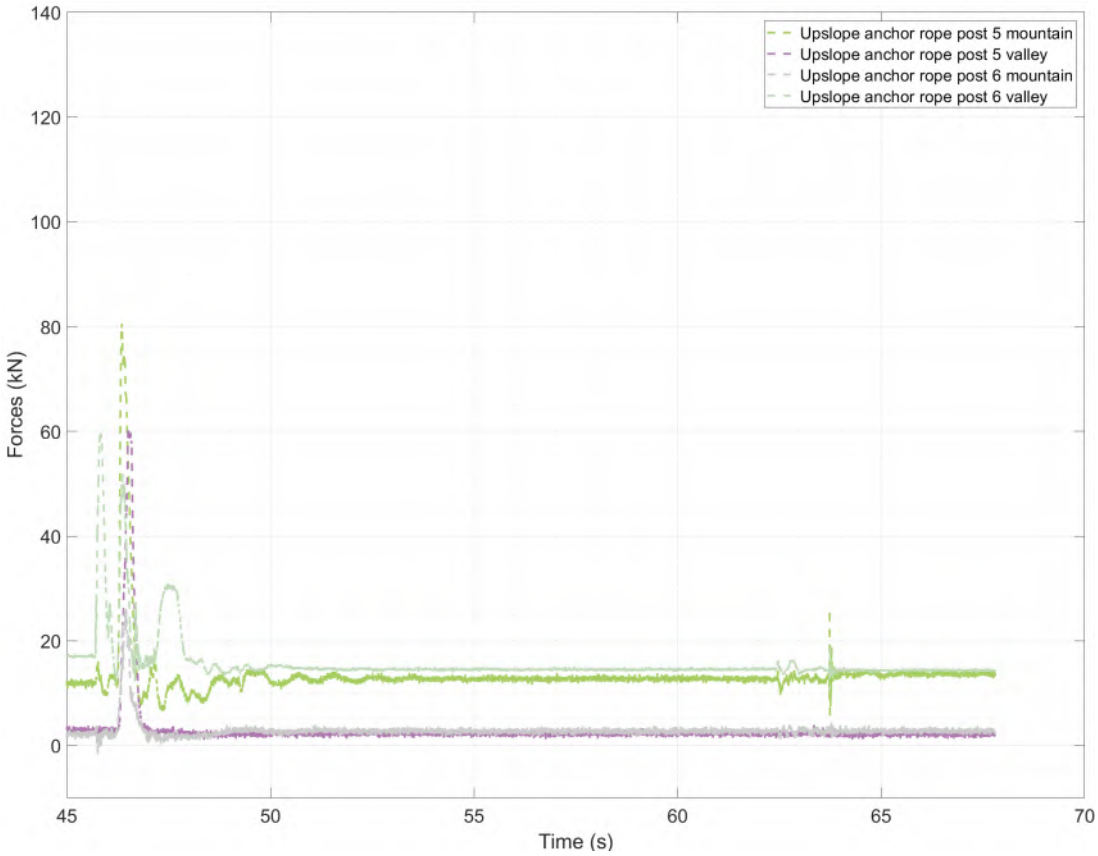

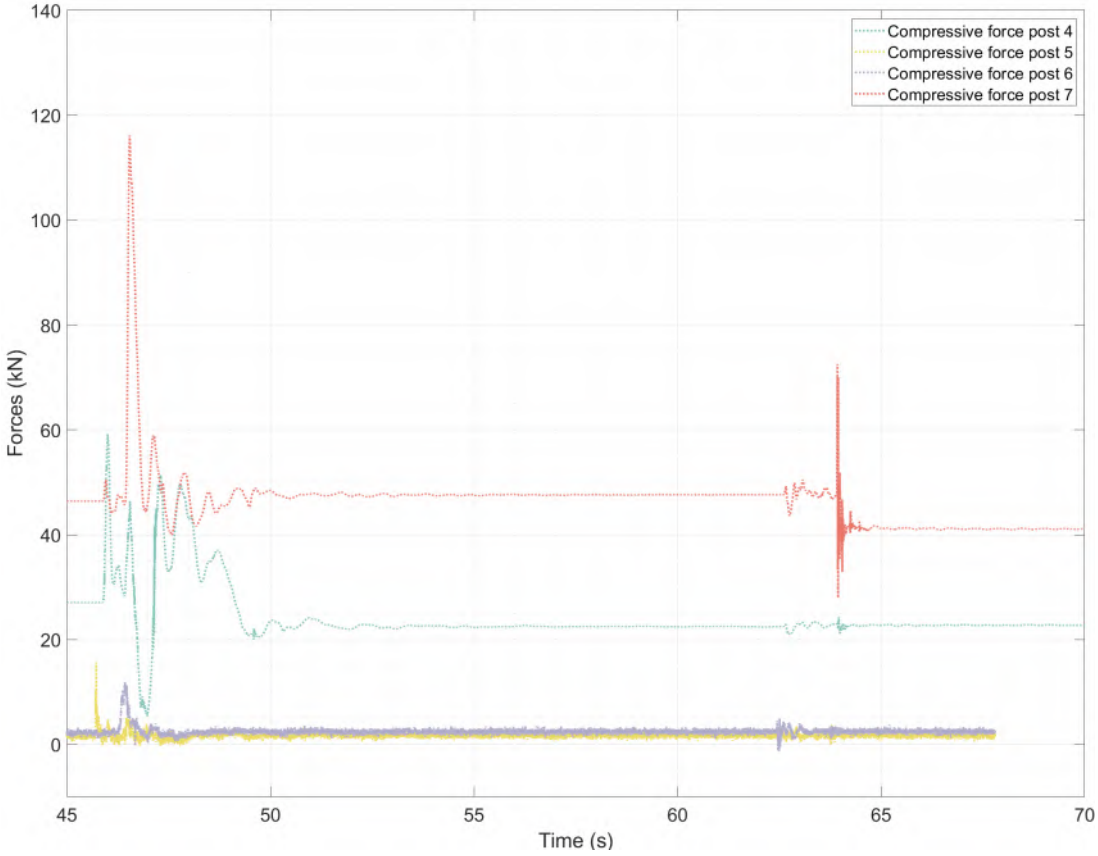

INNONETS PROJEKT		Test Nr: 02	Drop Nr: 01
Rock Rolling Test	Date: 04.10.2019	Block mass 840kg	Block type: EOTA111
Location: Chant Sura	Flexible Barrier 2000kJ	Impact Field: 4	Impact point: 8

Remarks: Ground contact aprox. 1.5m after net contact. Rolling over upslope valley anchor rope.

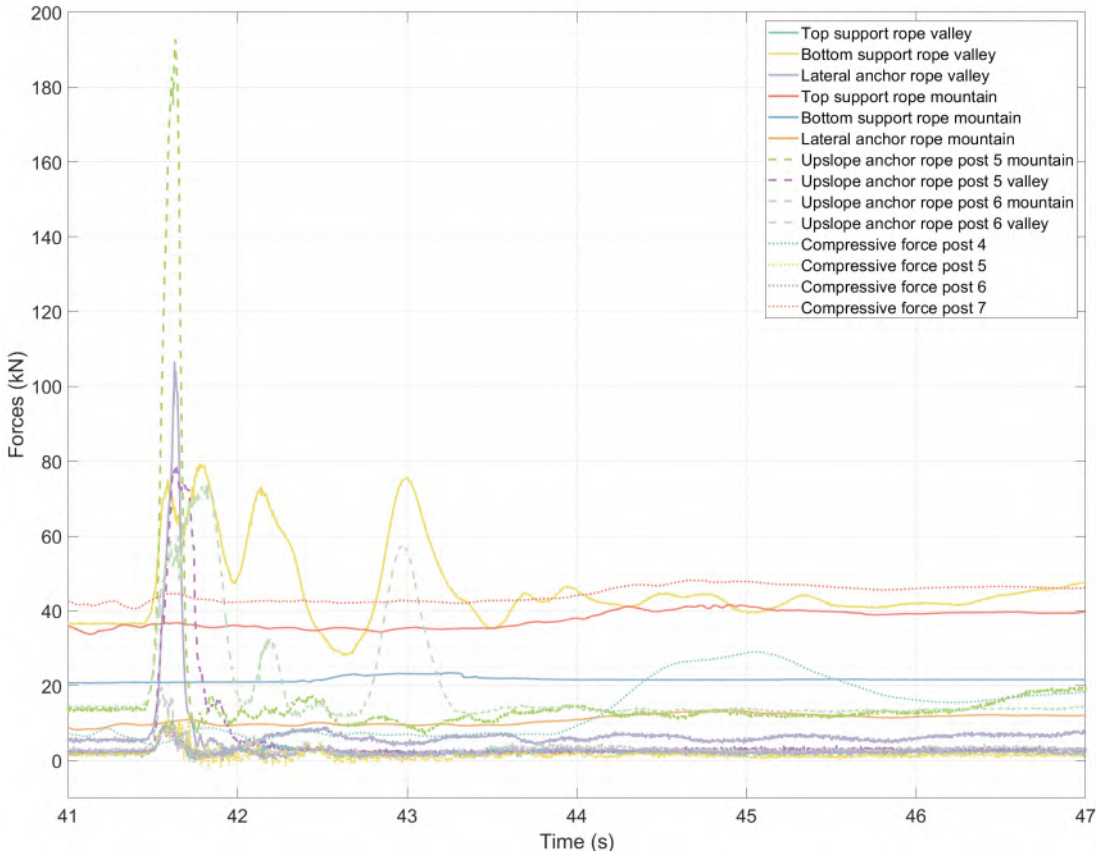

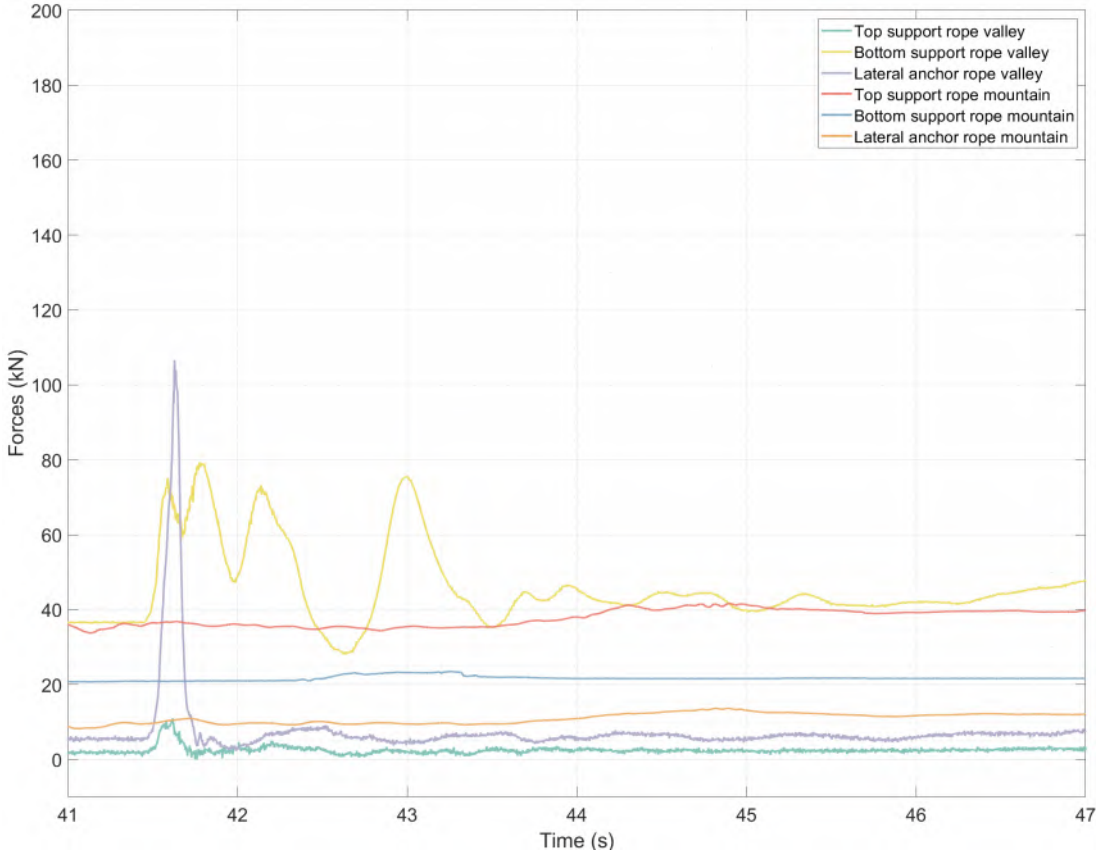

INNONETS PROJEKT		Test Nr: 02	Drop Nr: 02
Rock Rolling Test	Date: 04.10.2019	Block mass 2600kg	Block type: EOTA111
Location: Chant Sura	Flexible Barrier 2000kJ	Impact Field: 3	Impact point: 7

Remarks: No ground contact during deceleration in the net.

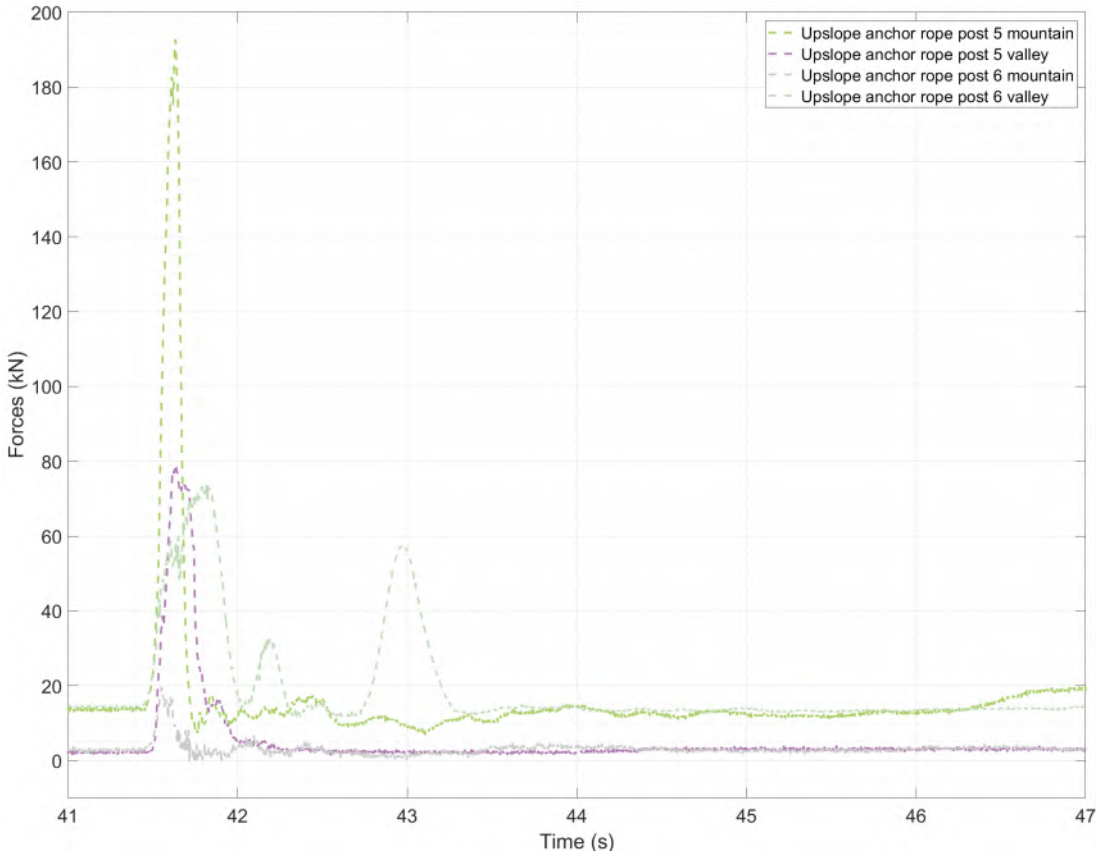
Upslope anchor rope post 5 mountain
Upslope anchor rope post 5 valley
Upslope anchor rope post 6 mountain
Upslope anchor rope post 6 valley
Forces (kN)
Time (s)

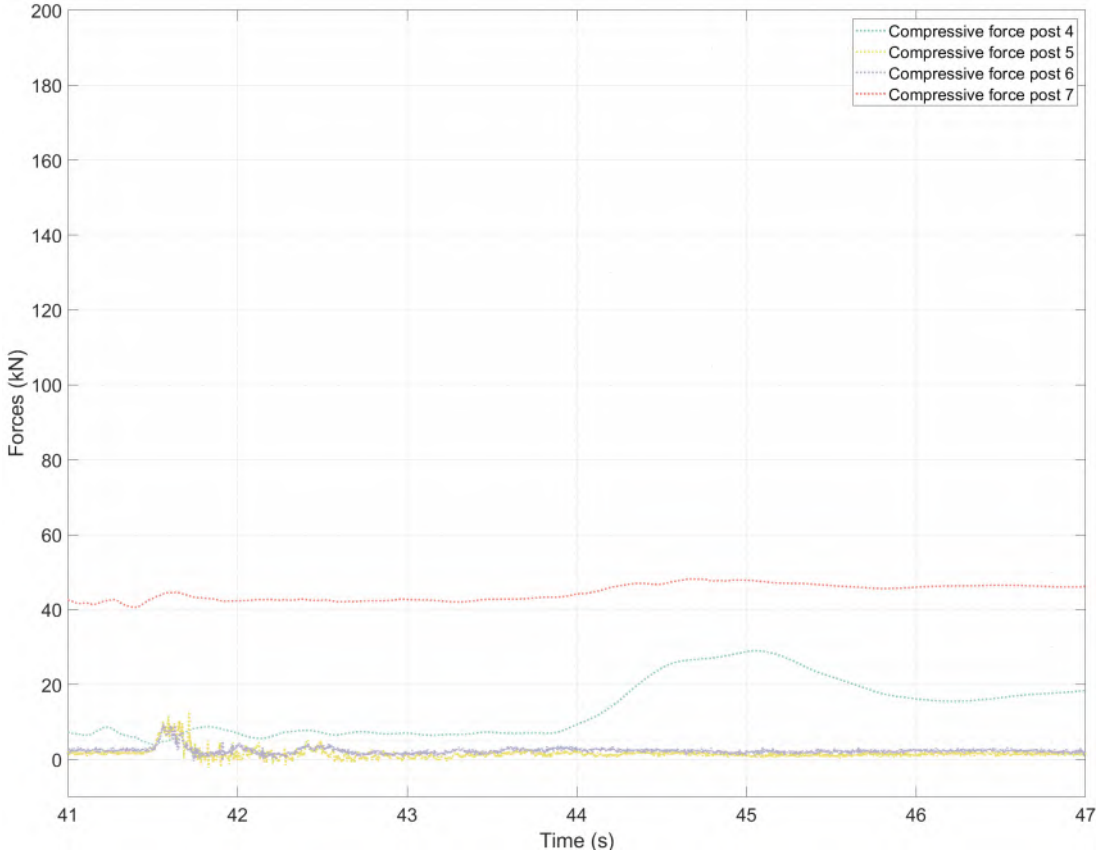
Compressive force post 4
Compressive force post 5
Compressive force post 6
Compressive force post 7
Forces (kN)
Time (s)

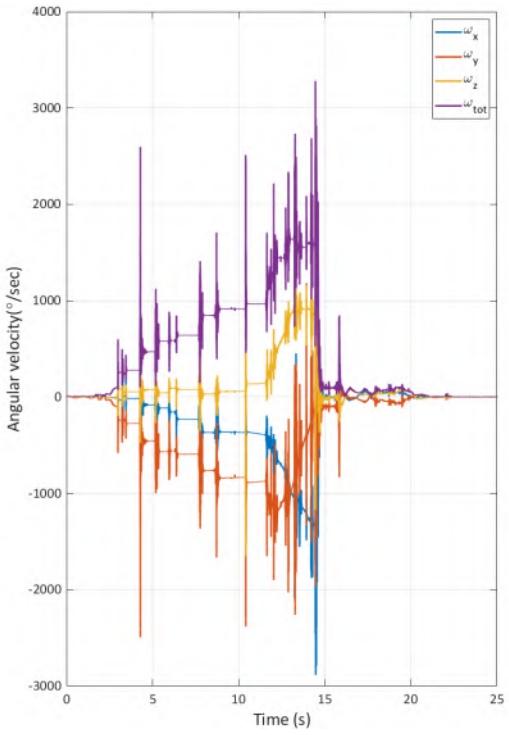

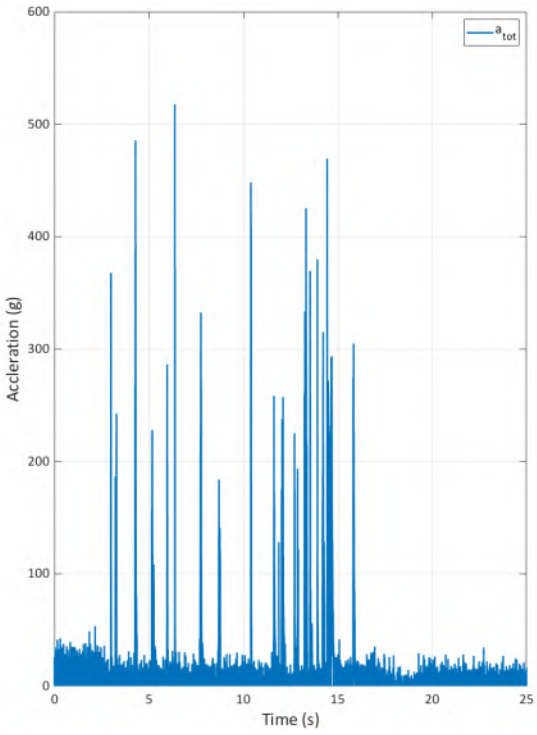

INNONETS PROJEKT		Test Nr: 02	Drop Nr: 02
Rock Rolling Test	Date: 04.10.2019	Block mass 2600kg	Block type: EOTA111
Location: Chant Sura	Flexible Barrier 2000kJ	Impact Field: 3	Impact point: 7

Remarks: No ground contact during deceleration in the net.

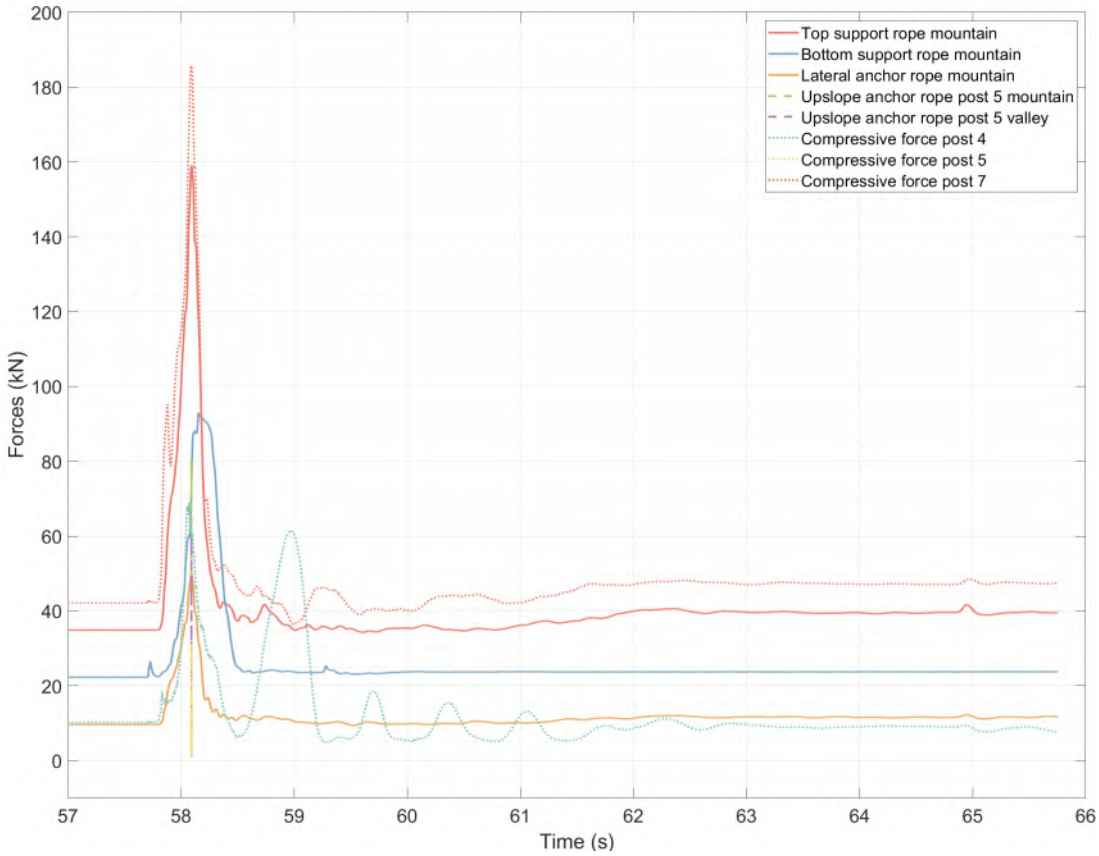

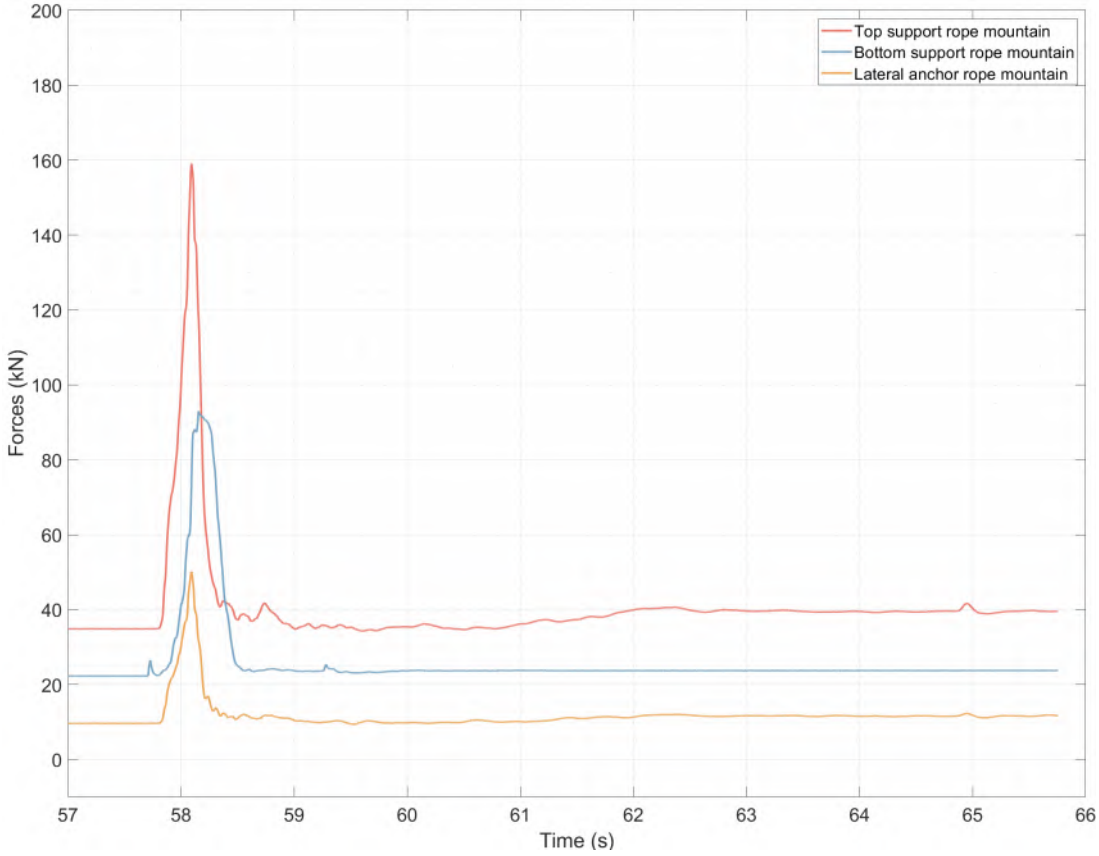

INNONETS PROJEKT		Test Nr: 02	Drop Nr: 03
Rock Rolling Test	Date: 04.10.2019	Block mass 2600kg	Block type: EOTA111
Location: Chant Sura	Flexible Barrier 2000kJ	Impact Field: 5	Impact point: 7

Remarks: Ground contact directely before net contact.

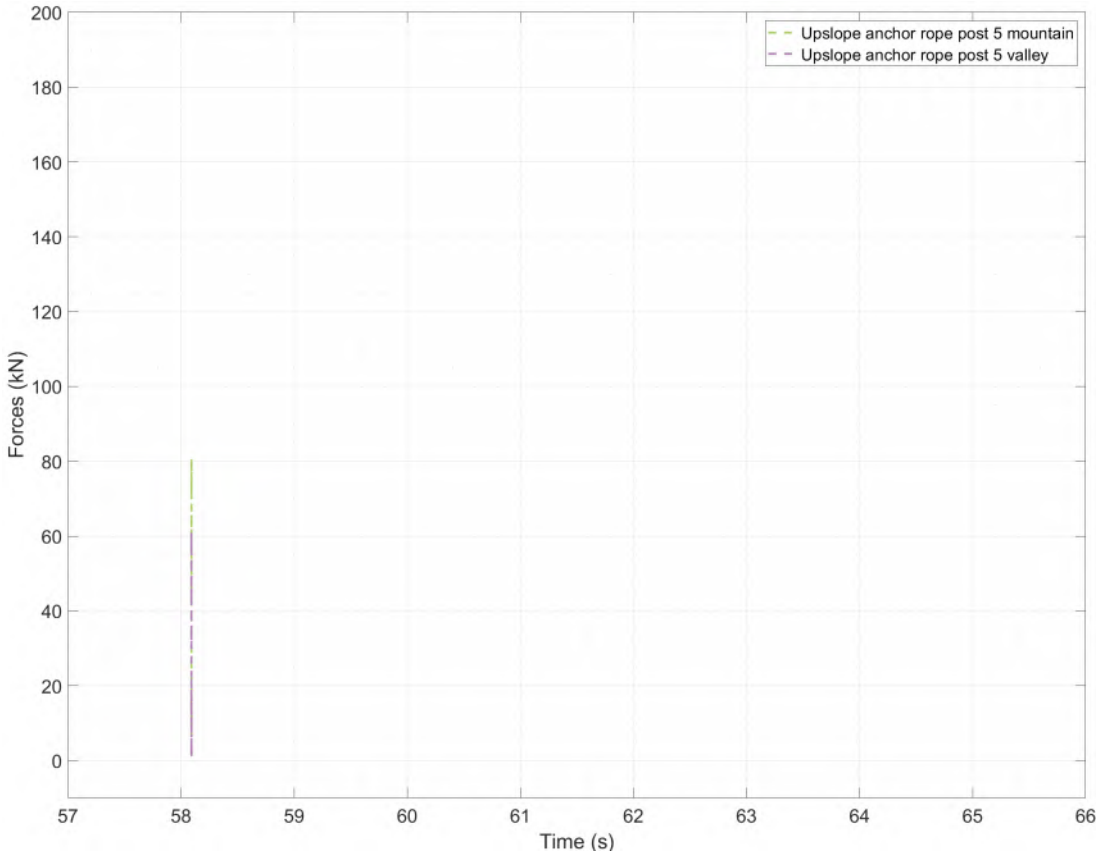
Upslope anchor rope post 5 mountain
Upslope anchor rope post 5 valley
Forces (kN)
Time (s)

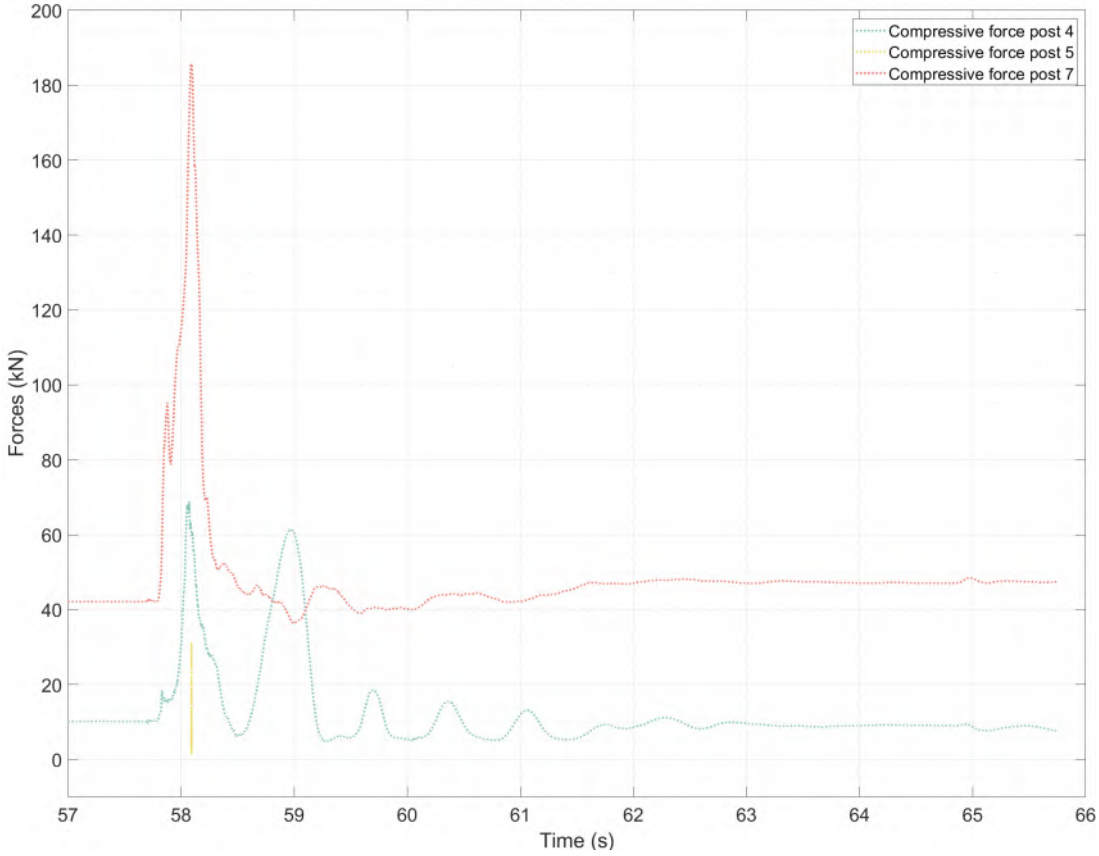
Compressive force post 4
Compressive force post 5
Compressive force post 7
Forces (kN)
Time (s)

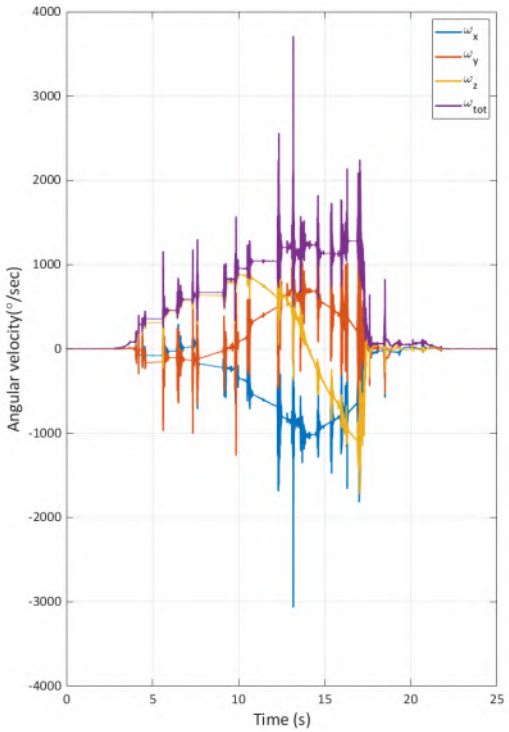

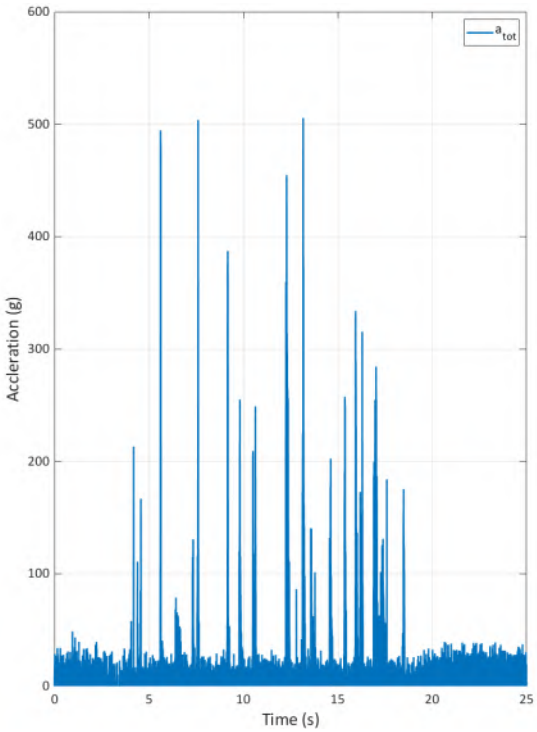

INNONETS PROJEKT		Test Nr: 02	Drop Nr: 03
Rock Rolling Test	Date: 04.10.2019	Block mass 2600kg	Block type: EOTA111
Location: Chant Sura	Flexible Barrier 2000kJ	Impact Field: 5	Impact point: 7

Remarks: Ground contact directely before net contact.

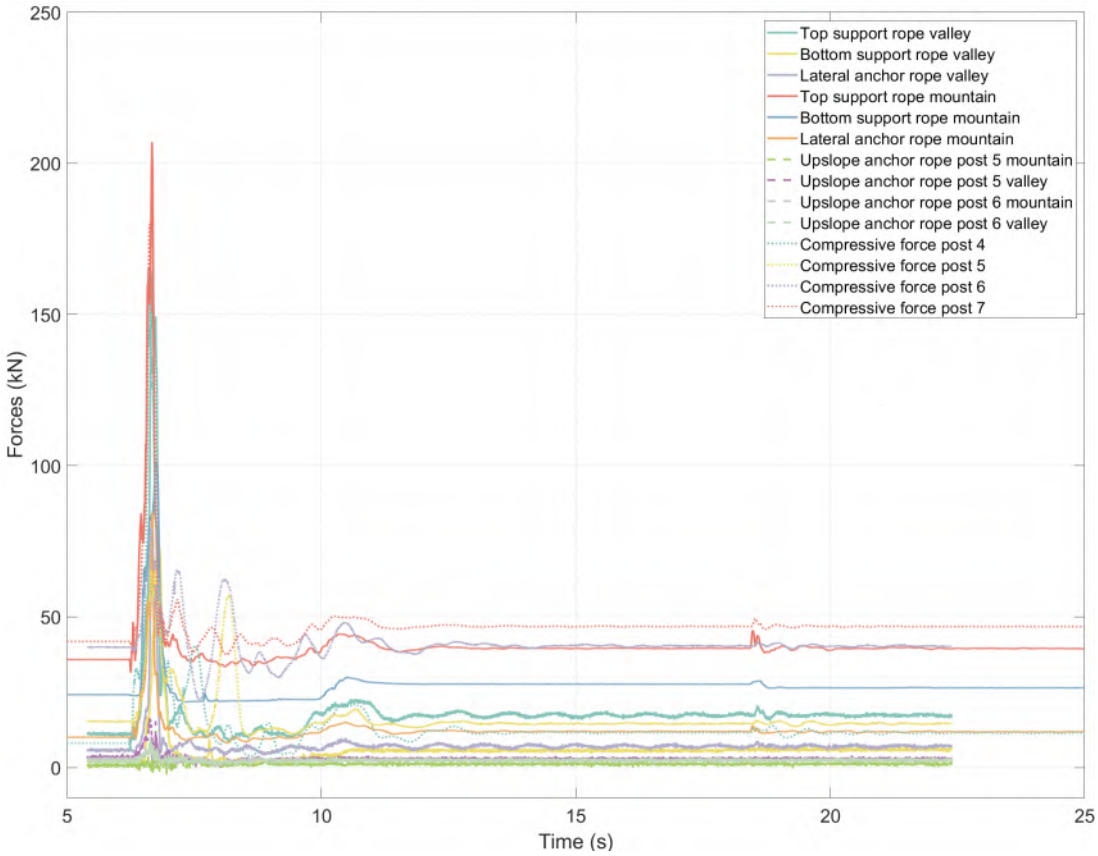

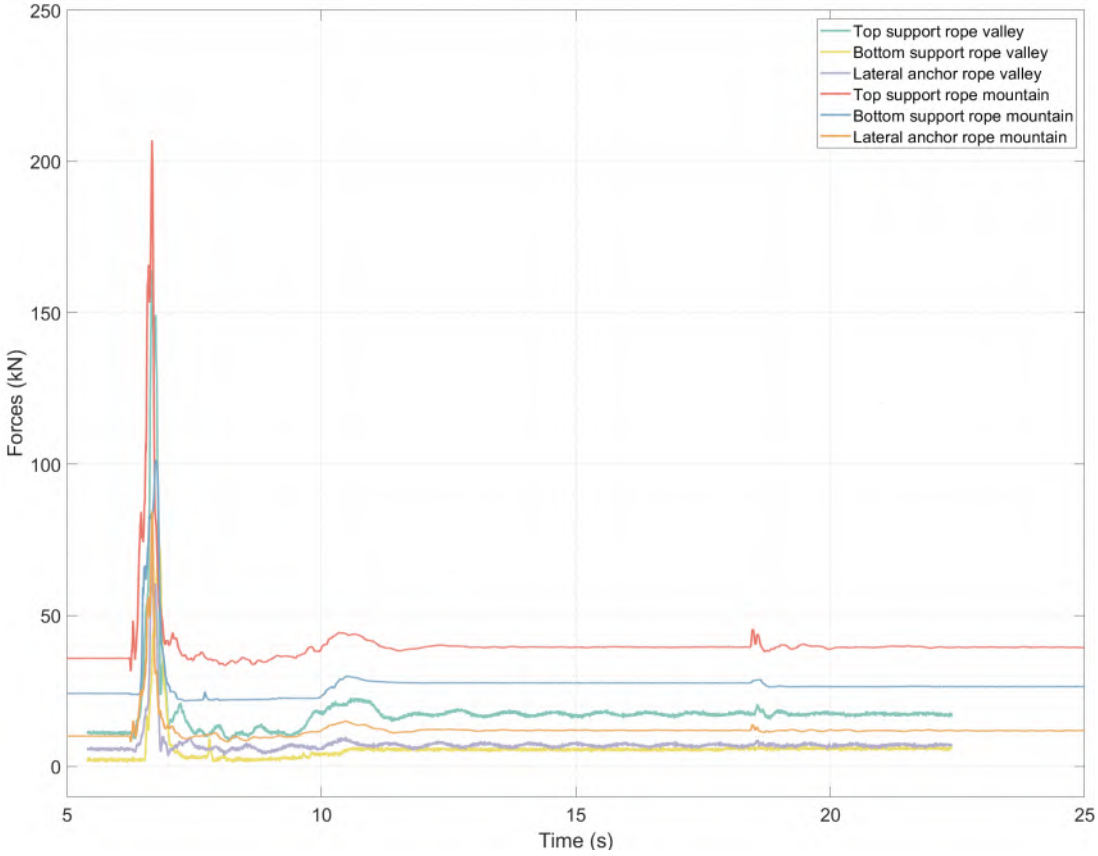

INNONETS PROJEKT		Test Nr: 02	Drop Nr: 04
Rock Rolling Test	Date: 04.10.2019	Block mass 2600kg	Block type: EOTA111
Location: Chant Sura	Flexible Barrier 2000kJ	Impact Field: 2	Impact point: 9

Remarks: No ground contact during deceleration in the net. Post hit no.3 bottom part.

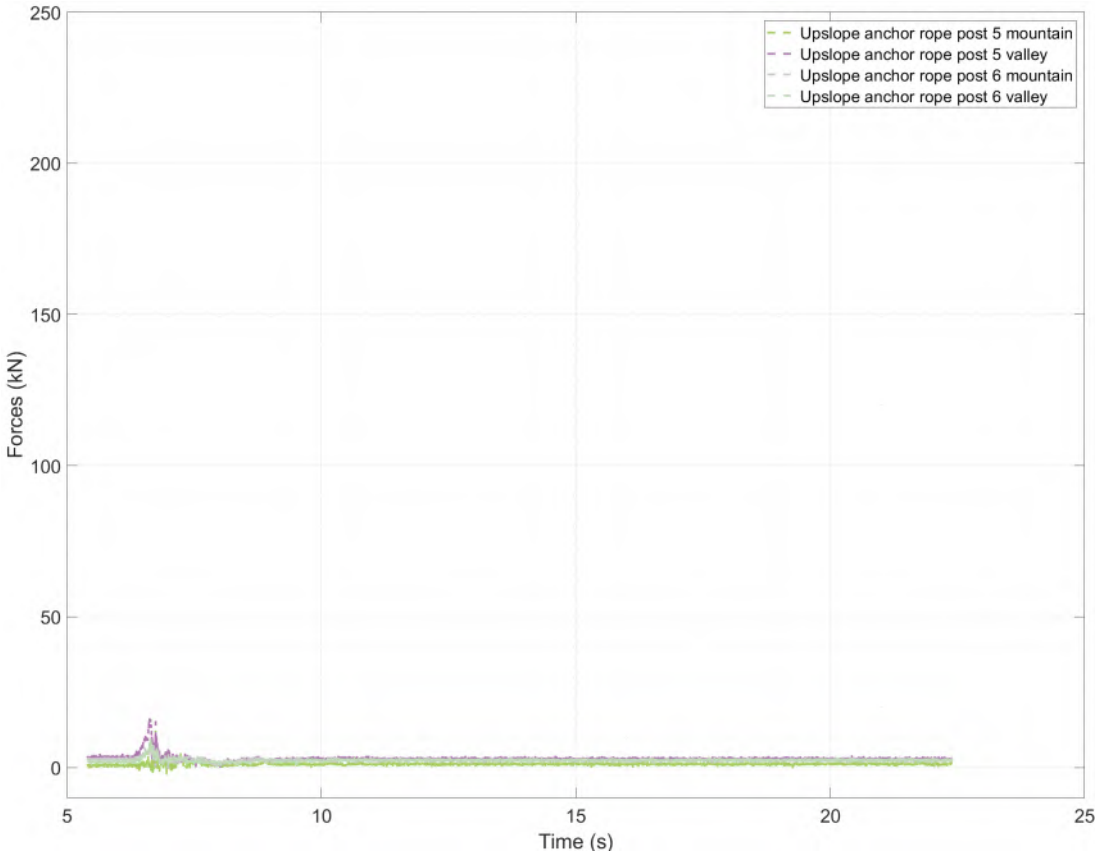

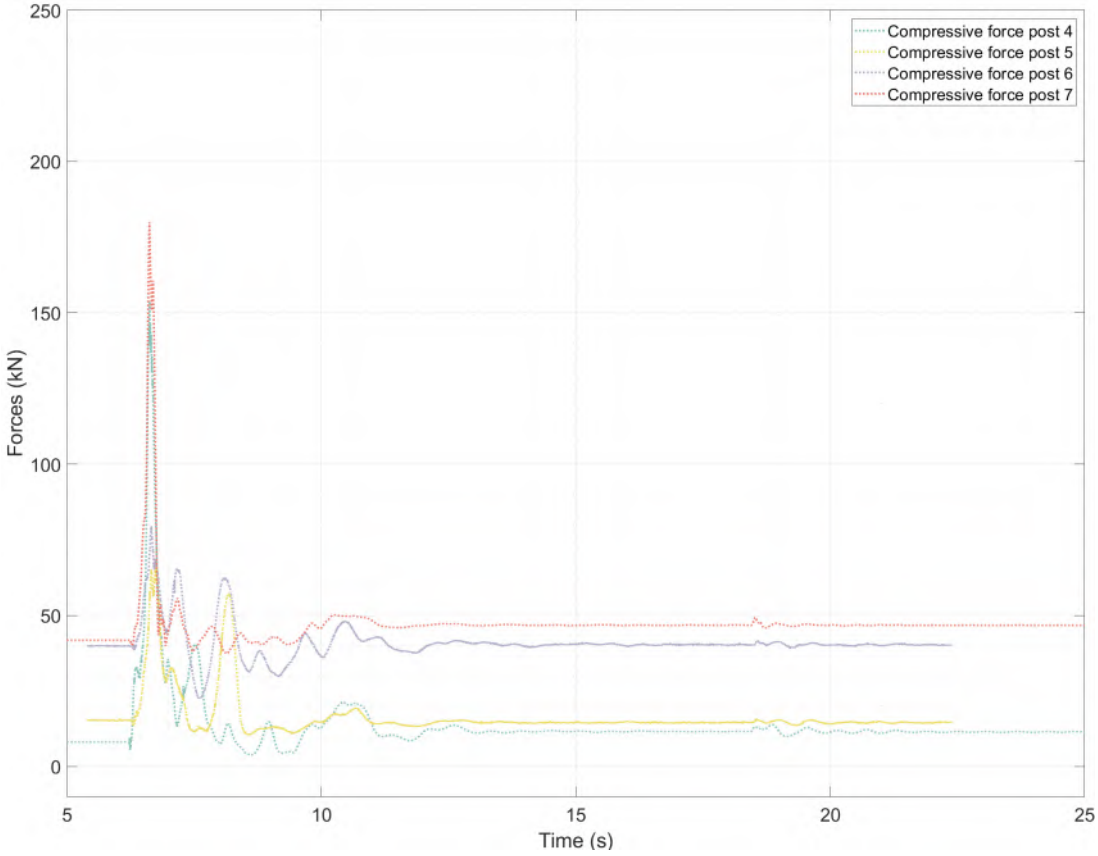

INNONETS PROJEKT		Test Nr: 02	Drop Nr: 04
Rock Rolling Test	Date: 04.10.2019	Block mass 2600kg	Block type: EOTA111
Location: Chant Sura	Flexible Barrier 2000kJ	Impact Field: 2	Impact point: 9

Remarks: No ground contact during deceleration in the net. Post hit no.3 bottom part.

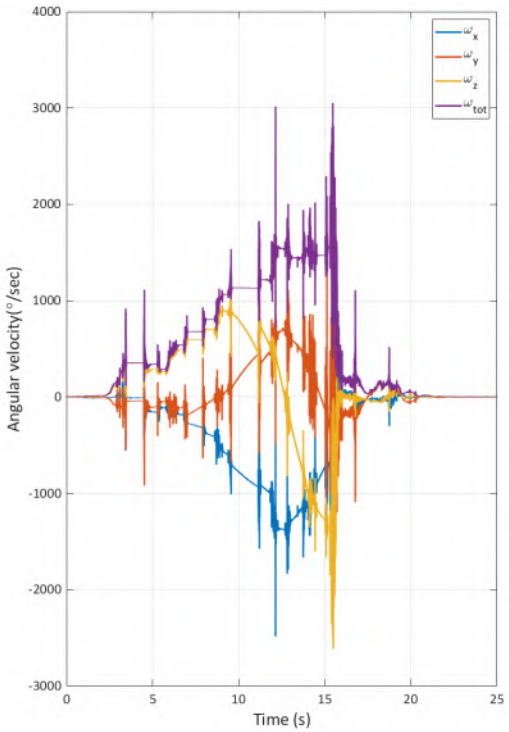
Angular velocity(°/sec)
Time (s)
ω x
ω y
ω z
ω tot

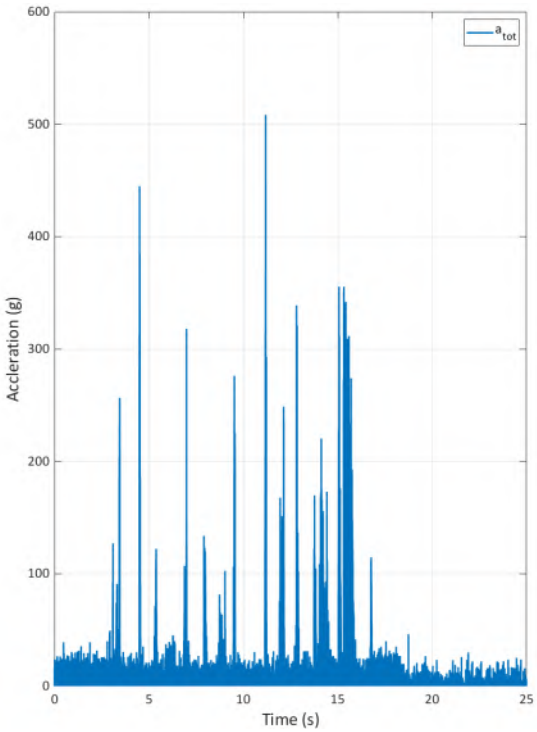
Accleration (g)
Time (s)
a tot

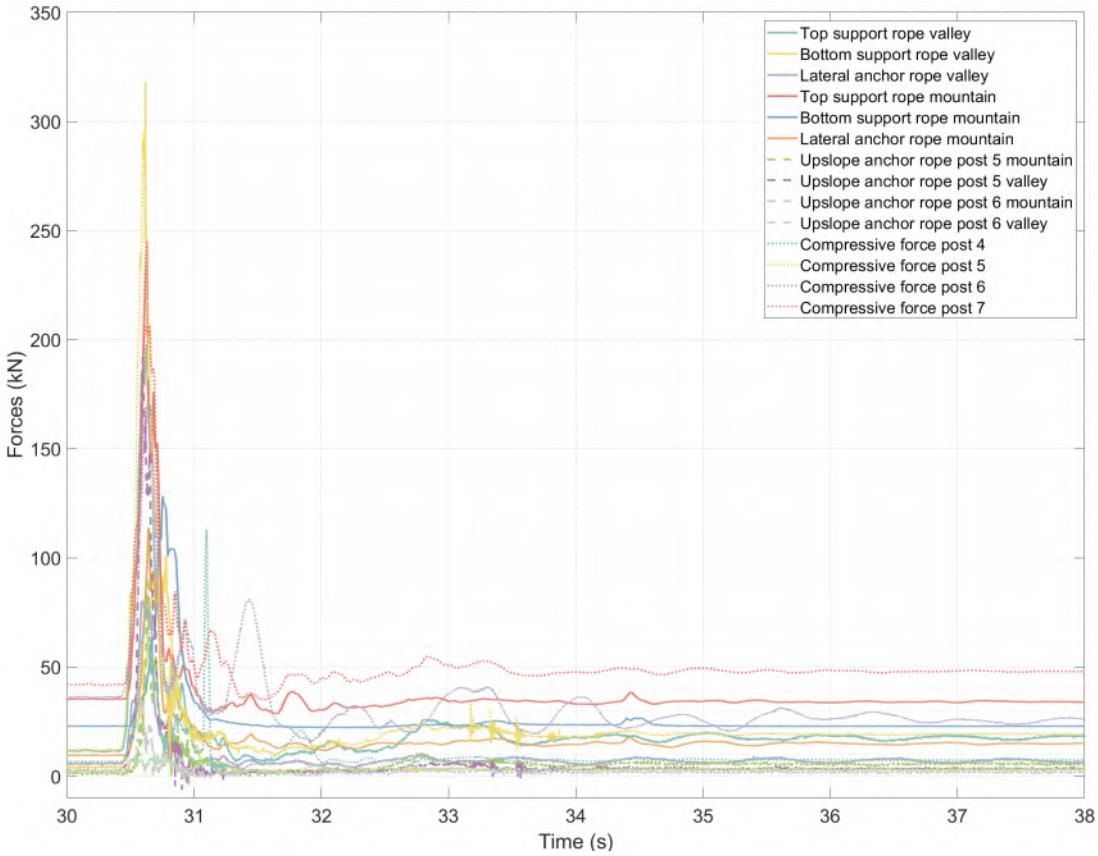
Top support rope valley
Bottom support rope valley
Lateral anchor rope valley
Top support rope mountain
Bottom support rope mountain
Lateral anchor rope mountain
Upslope anchor rope post 5 mountain
Upslope anchor rope post 5 valley
Upslope anchor rope post 6 mountain
Upslope anchor rope post 6 valley
Compressive force post 4
Compressive force post 5
Compressive force post 6
Compressive force post 7
Forces (kN)
Time (s)

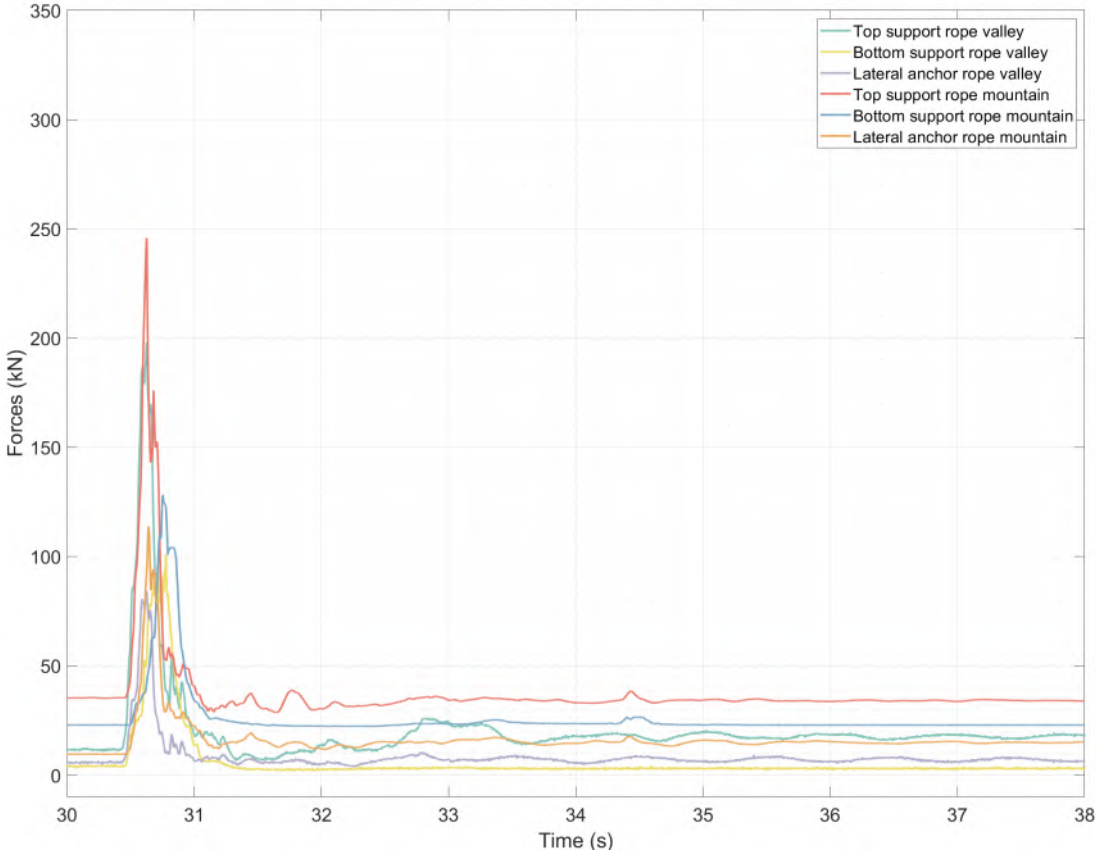
Top support rope valley
Bottom support rope valley
Lateral anchor rope valley
Top support rope mountain
Bottom support rope mountain
Lateral anchor rope mountain
Forces (kN)
Time (s)

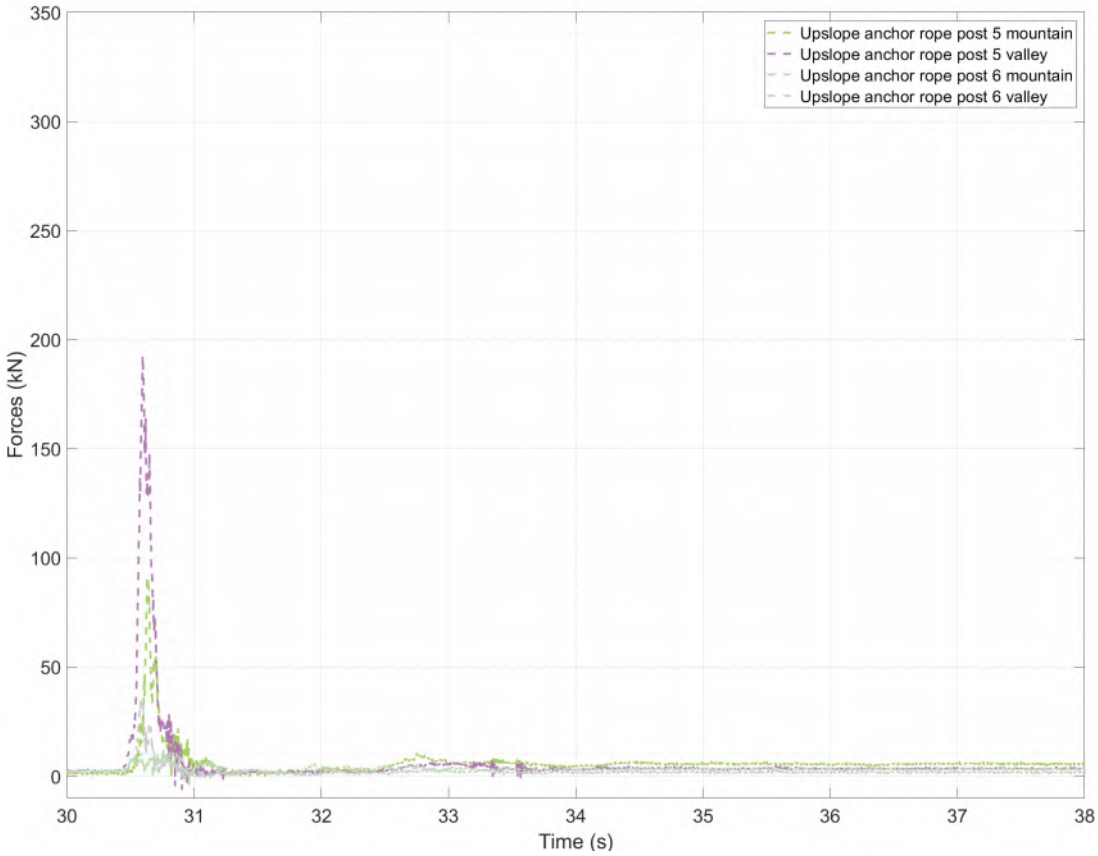

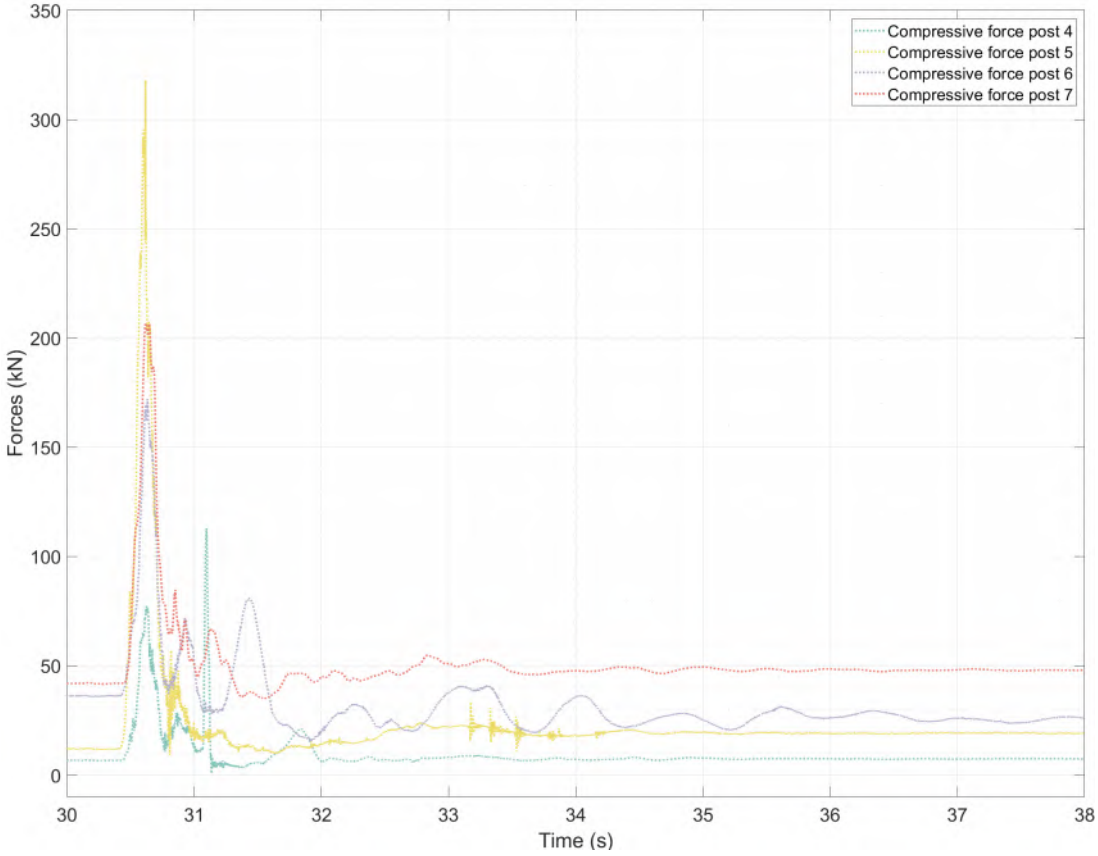

INNONETS PROJEKT		Test Nr: 02	Drop Nr: 05
Rock Rolling Test	Date: 04.10.2019	Block mass 2600kg	Block type: EOTA221
Location: Chant Sura	Flexible Barrier 2000kJ	Impact Field: 4	Impact point: 9

Remarks: Ground Contact aprox. 1.5m after net contact.

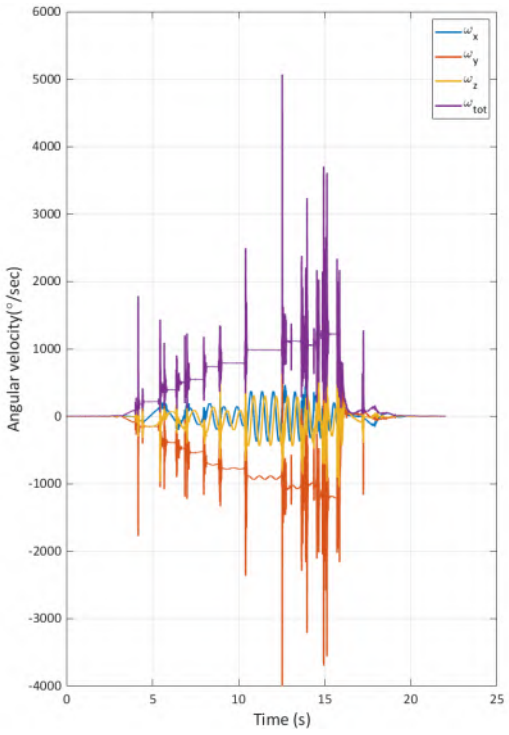
Angular velocity(°/sec)
Time (s)
ω_x
ω_y
ω_z
ω_{tot}

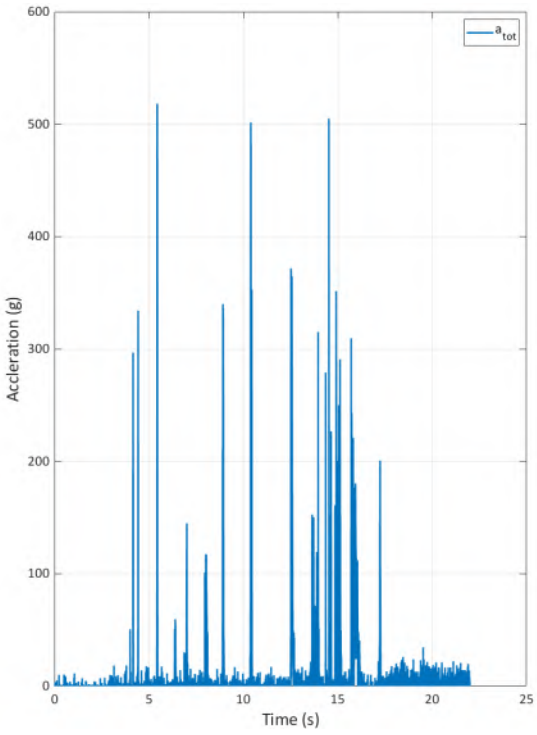
Accleration (g)
Time (s)
a_{tot}

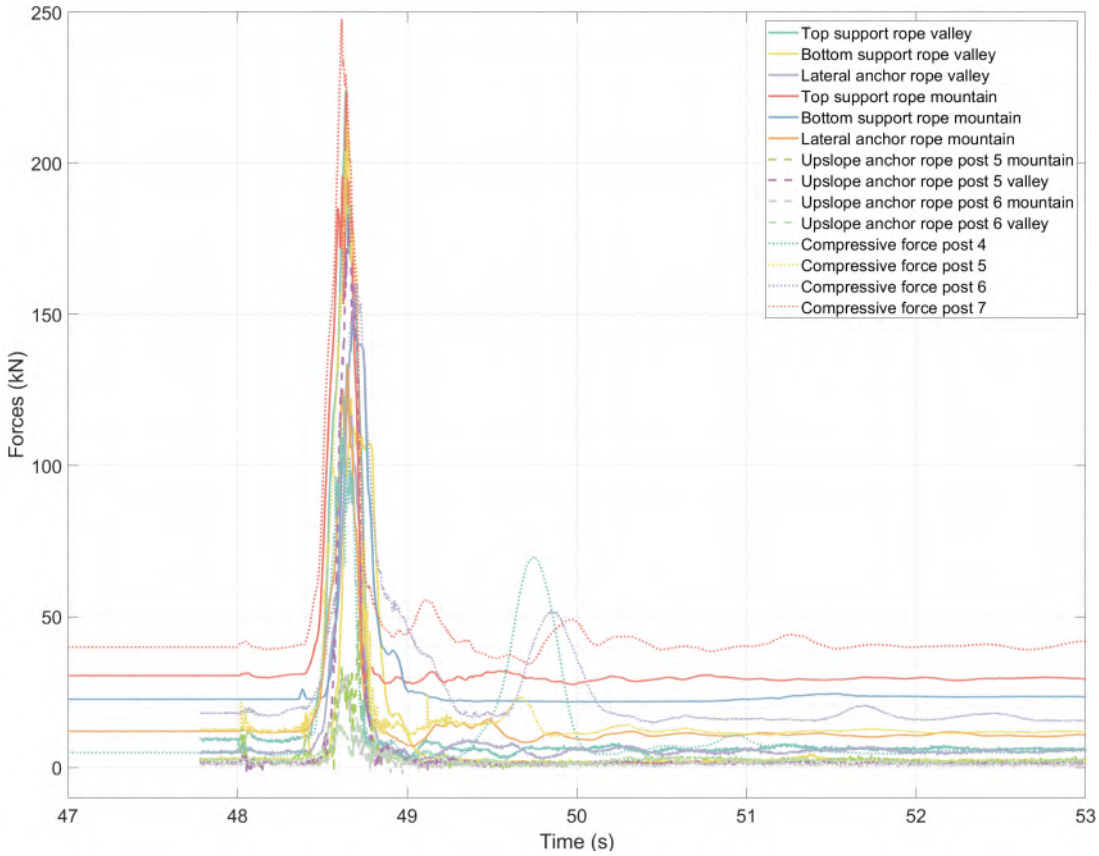
Top support rope valley
Bottom support rope valley
Lateral anchor rope valley
Top support rope mountain
Bottom support rope mountain
Lateral anchor rope mountain
Upslope anchor rope post 5 mountain
Upslope anchor rope post 5 valley
Upslope anchor rope post 6 mountain
Upslope anchor rope post 6 valley
Compressive force post 4
Compressive force post 5
Compressive force post 6
Compressive force post 7
Forces (kN)
Time (s)
250
200
150
100
50
0
47
48
49
50
51
52
53

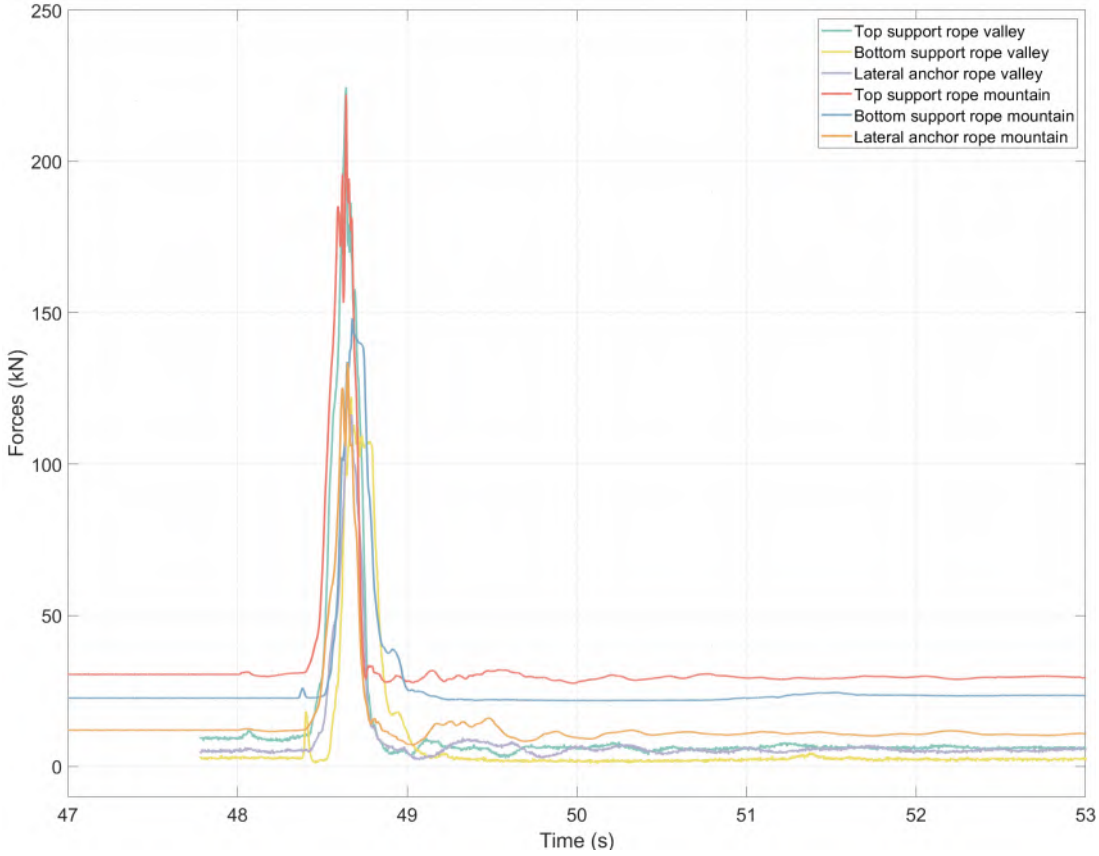
Top support rope valley
Bottom support rope valley
Lateral anchor rope valley
Top support rope mountain
Bottom support rope mountain
Lateral anchor rope mountain
Forces (kN)
Time (s)
250
200
150
100
50
0
47
48
49
50
51
52
53

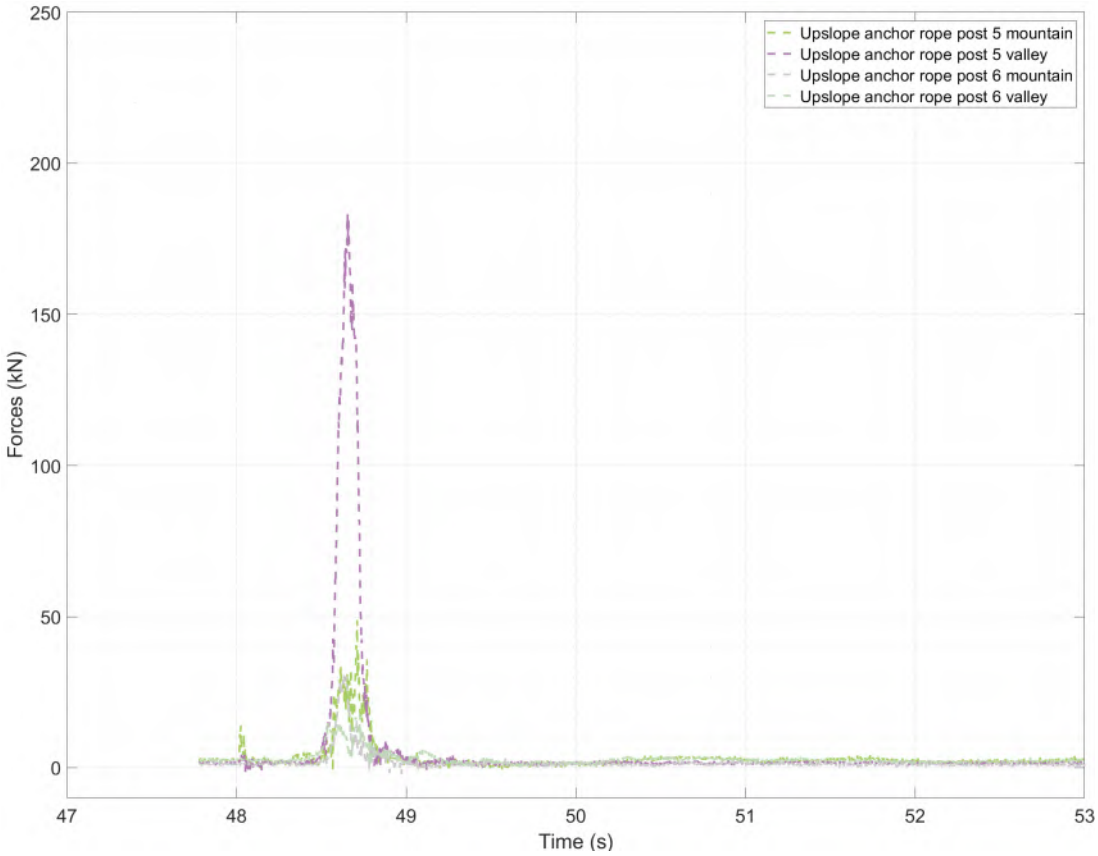
Upslope anchor rope post 5 mountain
Upslope anchor rope post 5 valley
Upslope anchor rope post 6 mountain
Upslope anchor rope post 6 valley
Forces (kN)
Time (s)

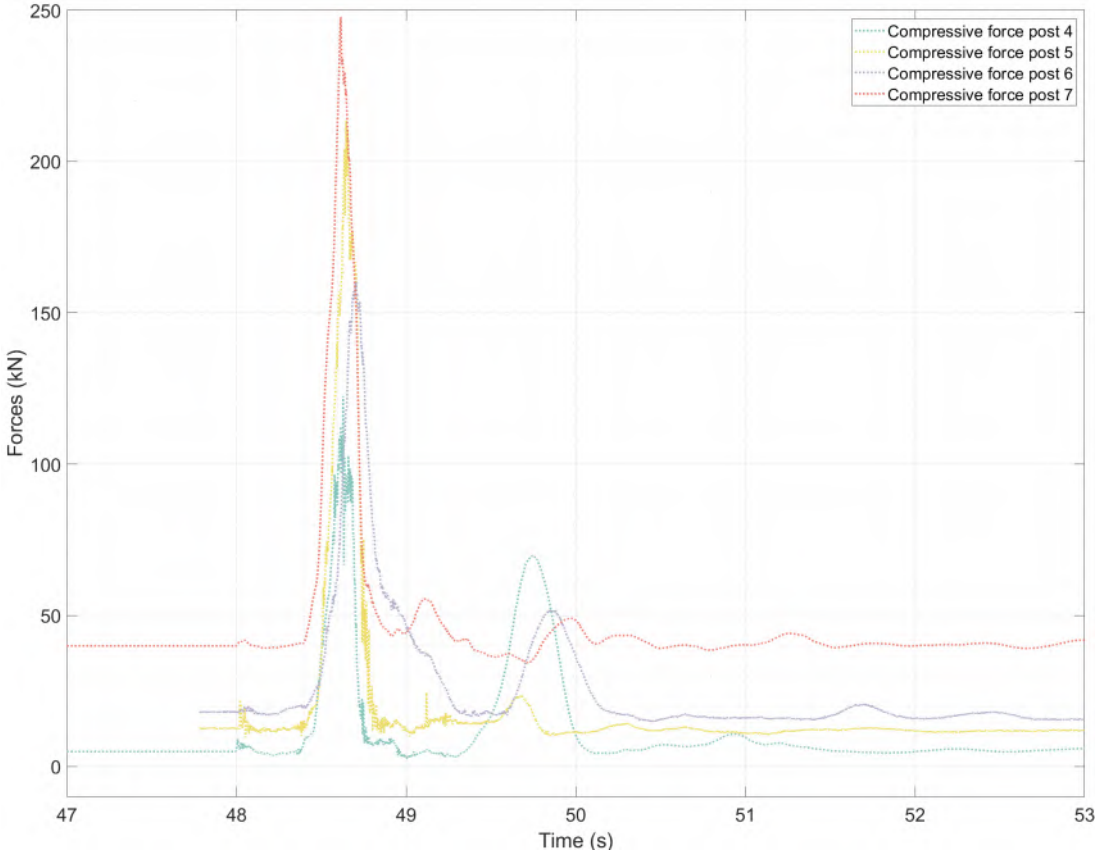
Compressive force post 4
Compressive force post 5
Compressive force post 6
Compressive force post 7
Forces (kN)
Time (s)

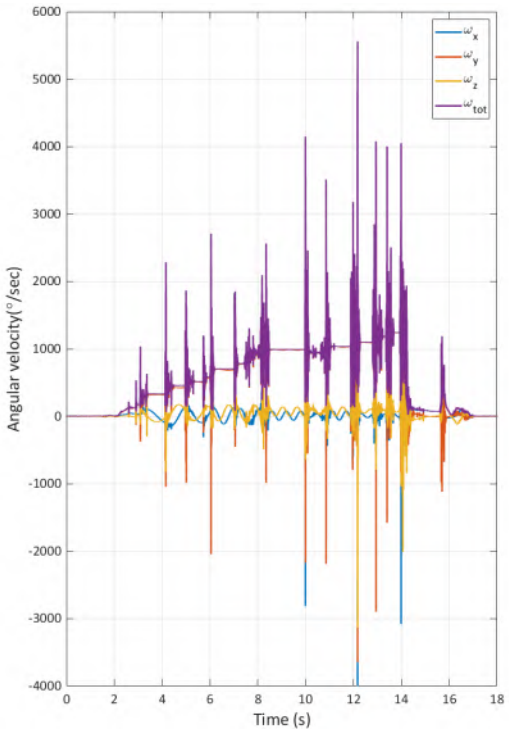
Angular velocity(°/sec)
Time (s)
ω_x
ω_y
ω_z
ω_{tot}

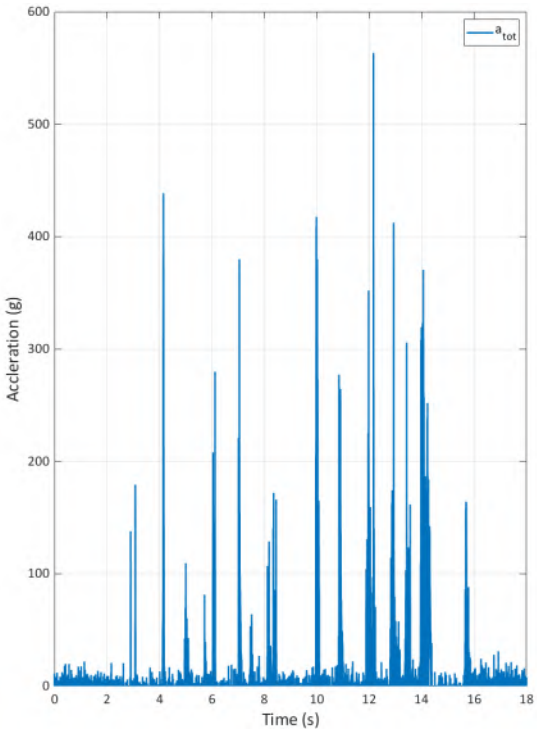
Accleration (g)
Time (s)
a_{tot}

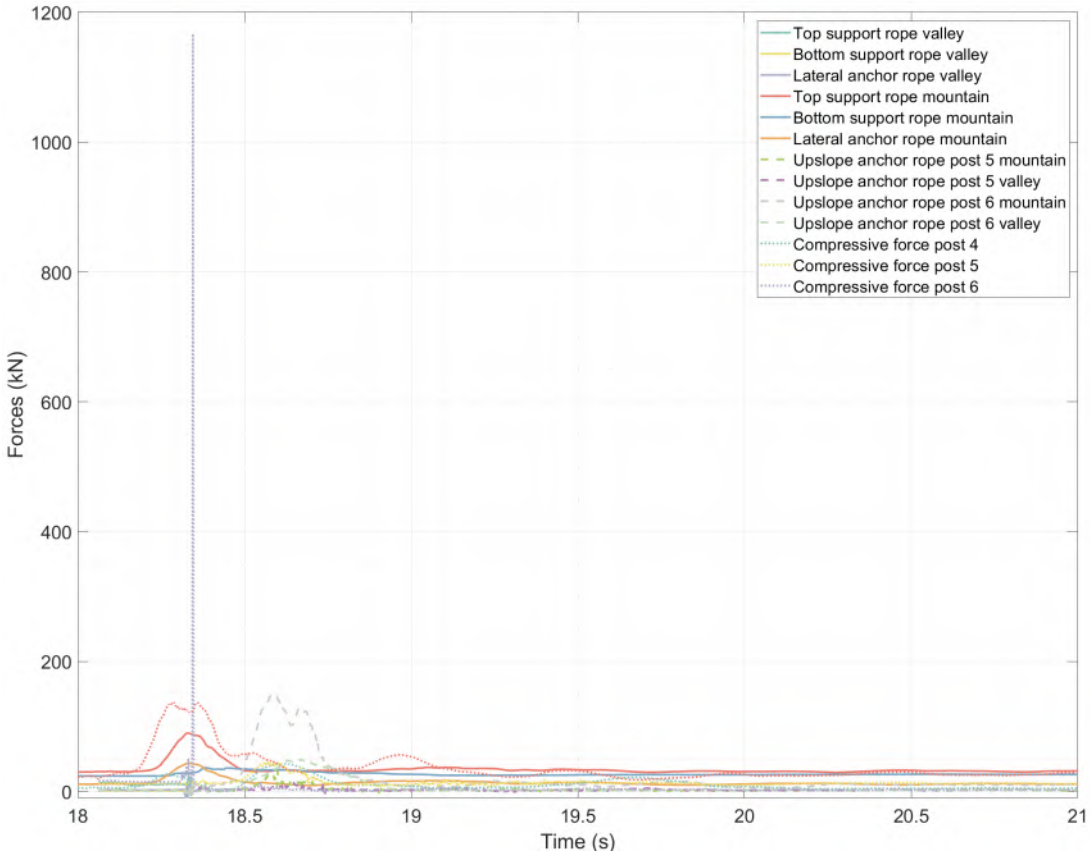

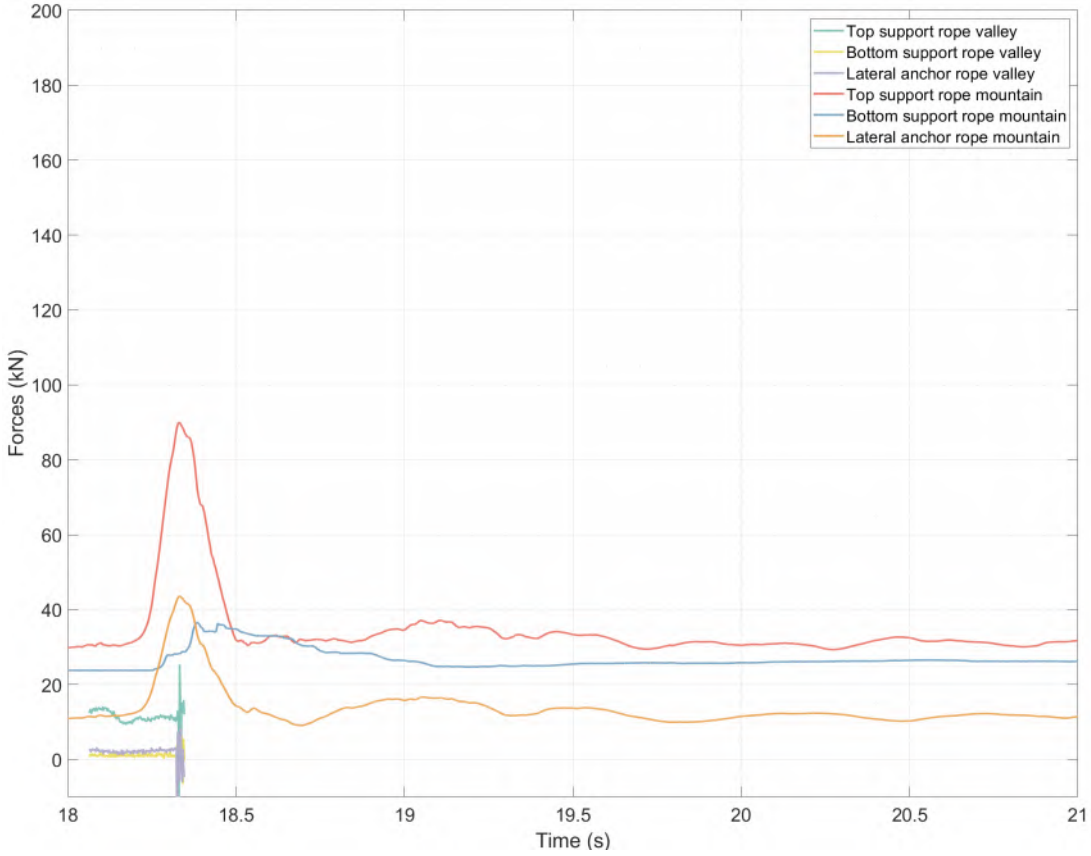

INNONETS PROJEKT		Test Nr: 02	Drop Nr: 09
Rock Rolling Test	Date: 04.10.2019	Block mass 2600kg	Block type: EOTA111
Location: Chant Sura	Flexible Barrier 2000kJ	Impact Field: 5	Impact point: 9

Remarks: Post hit No.6 bottom part.

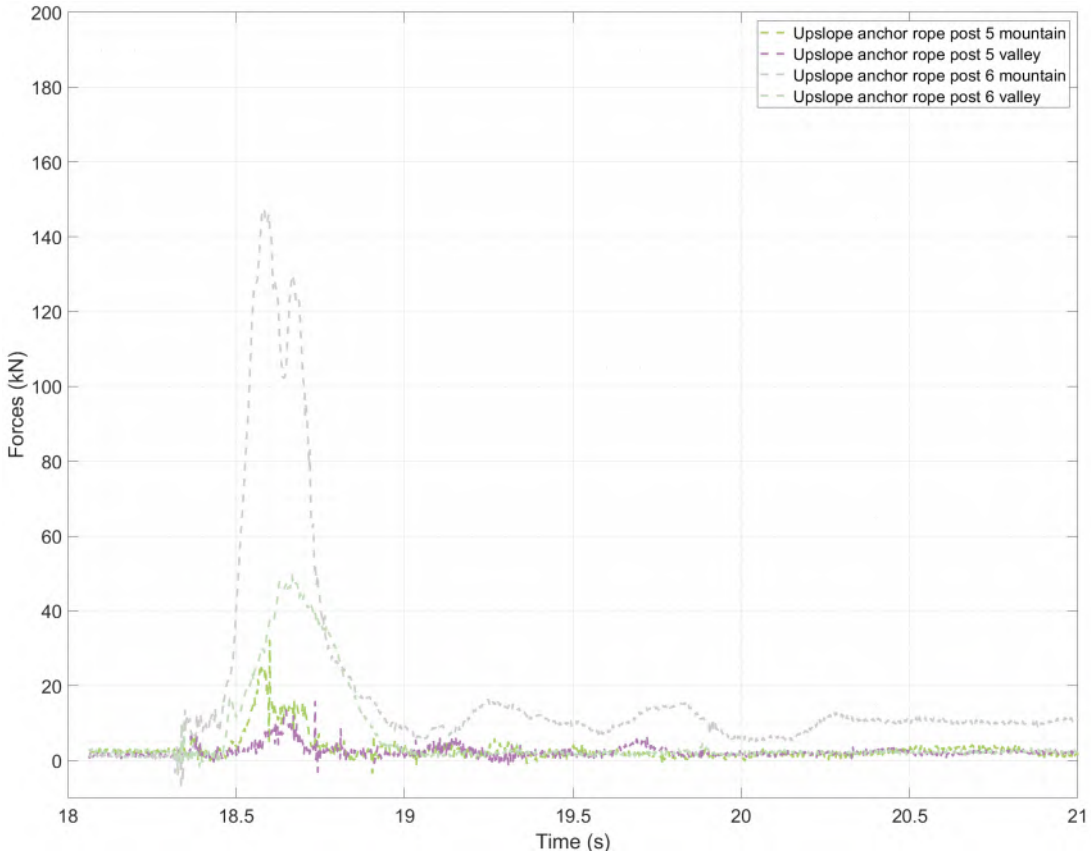
Upslope anchor rope post 5 mountain
Upslope anchor rope post 5 valley
Upslope anchor rope post 6 mountain
Upslope anchor rope post 6 valley
Forces (kN)
Time (s)

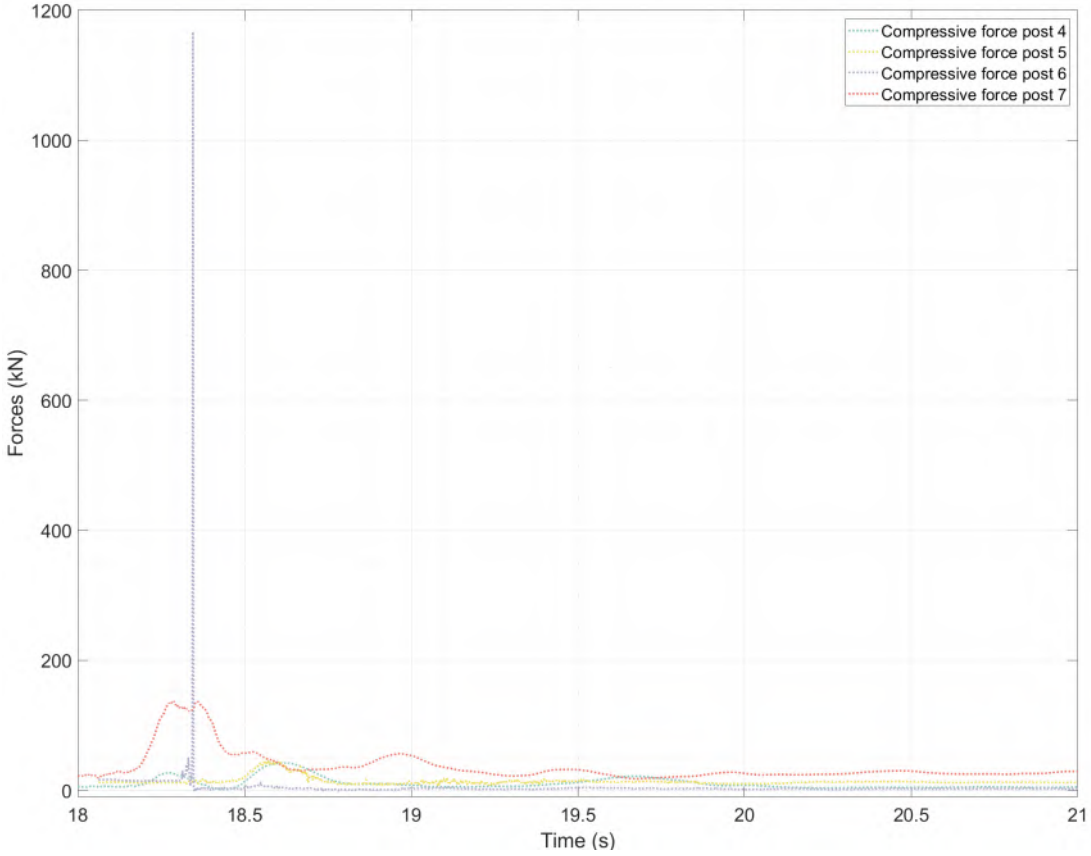
Compressive force post 4
Compressive force post 5
Compressive force post 6
Compressive force post 7
Forces (kN)
Time (s)

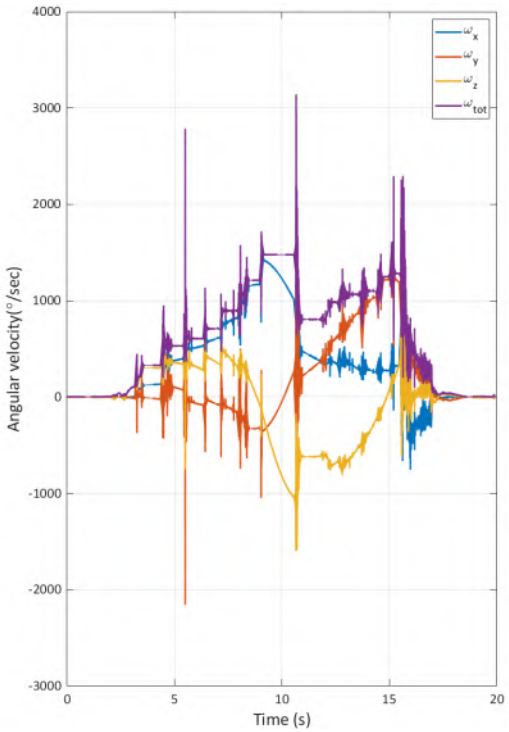
Angular velocity(°/sec)
Time (s)
ω_x
ω_y
ω_z
ω_{tot}

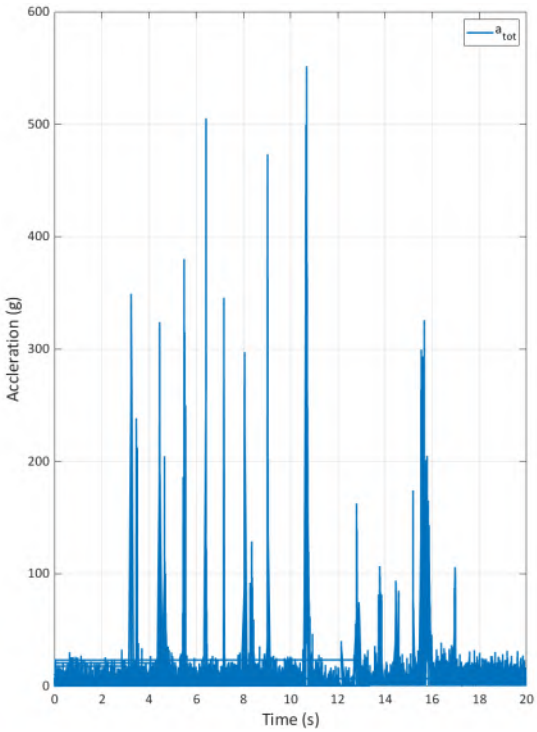
Accleration (g)
Time (s)
a_{tot}

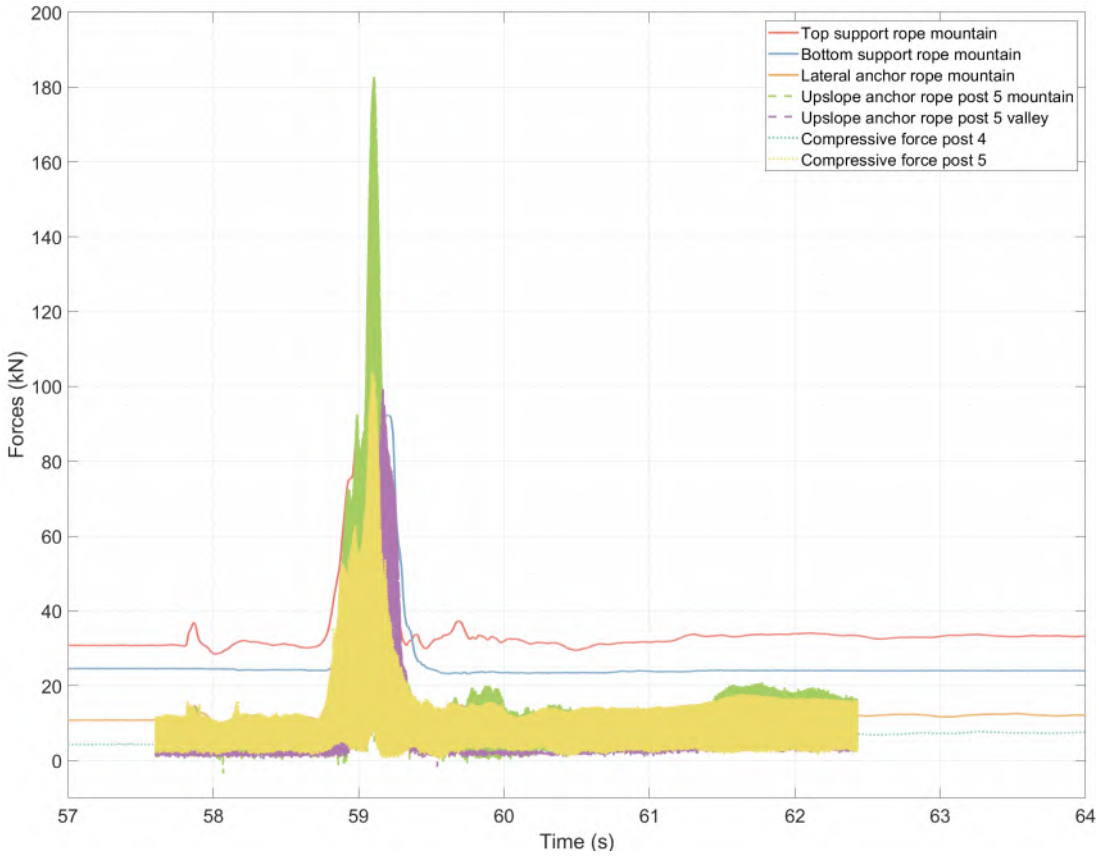
Top support rope mountain
Bottom support rope mountain
Lateral anchor rope mountain
Upslope anchor rope post 5 mountain
Upslope anchor rope post 5 valley
Compressive force post 4
Compressive force post 5
Forces (kN)
Time (s)

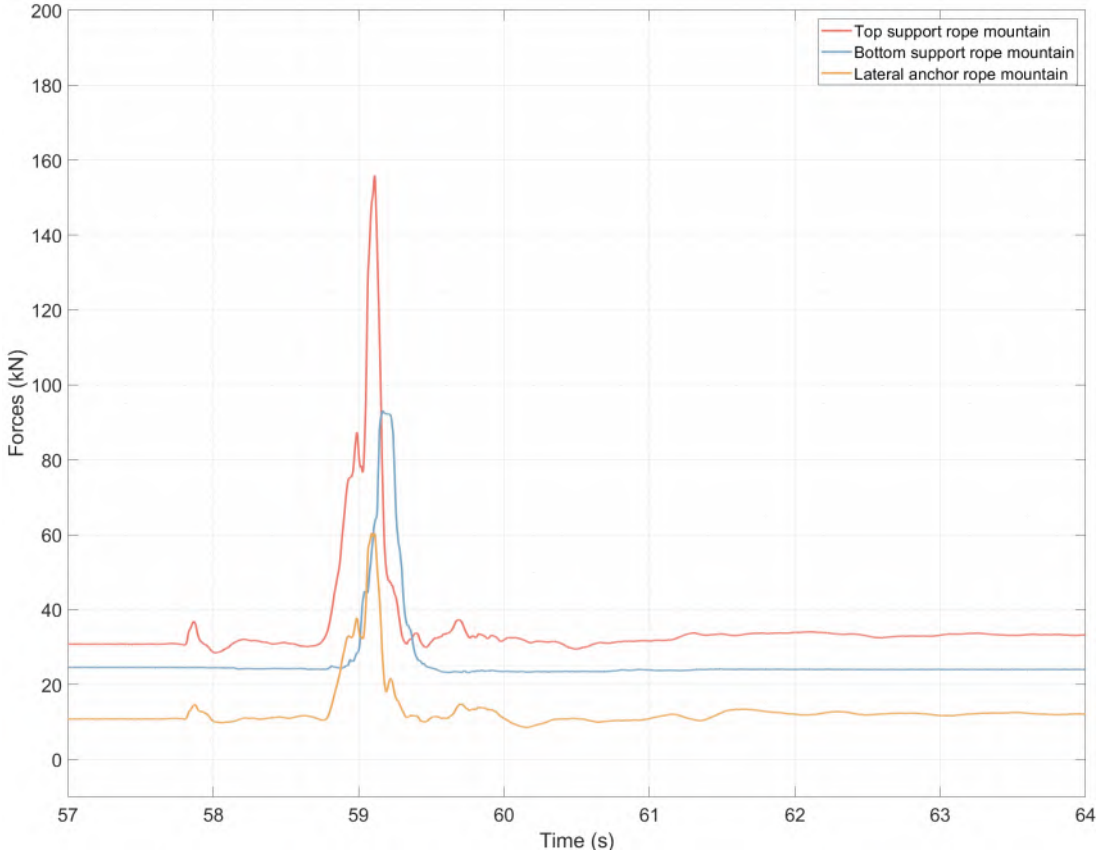
Top support rope mountain
Bottom support rope mountain
Lateral anchor rope mountain
Forces (kN)
Time (s)

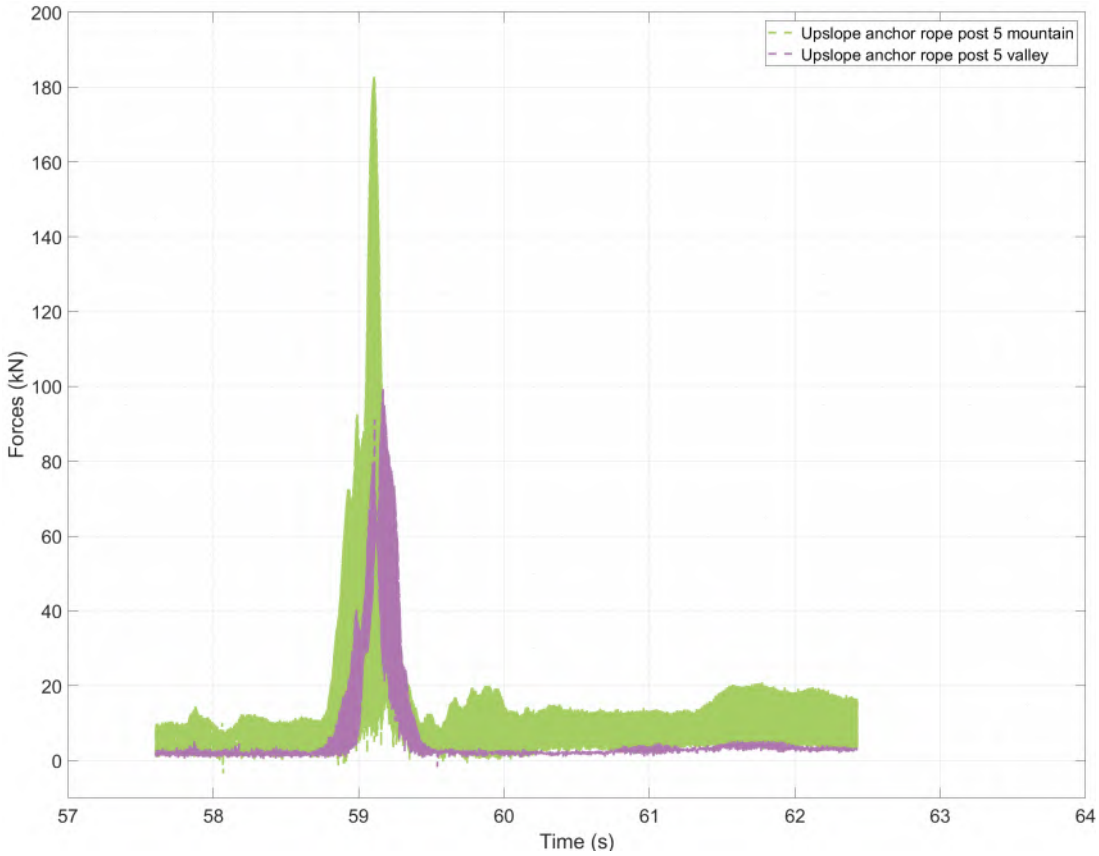
Upslope anchor rope post 5 mountain
Upslope anchor rope post 5 valley
Forces (kN)
Time (s)

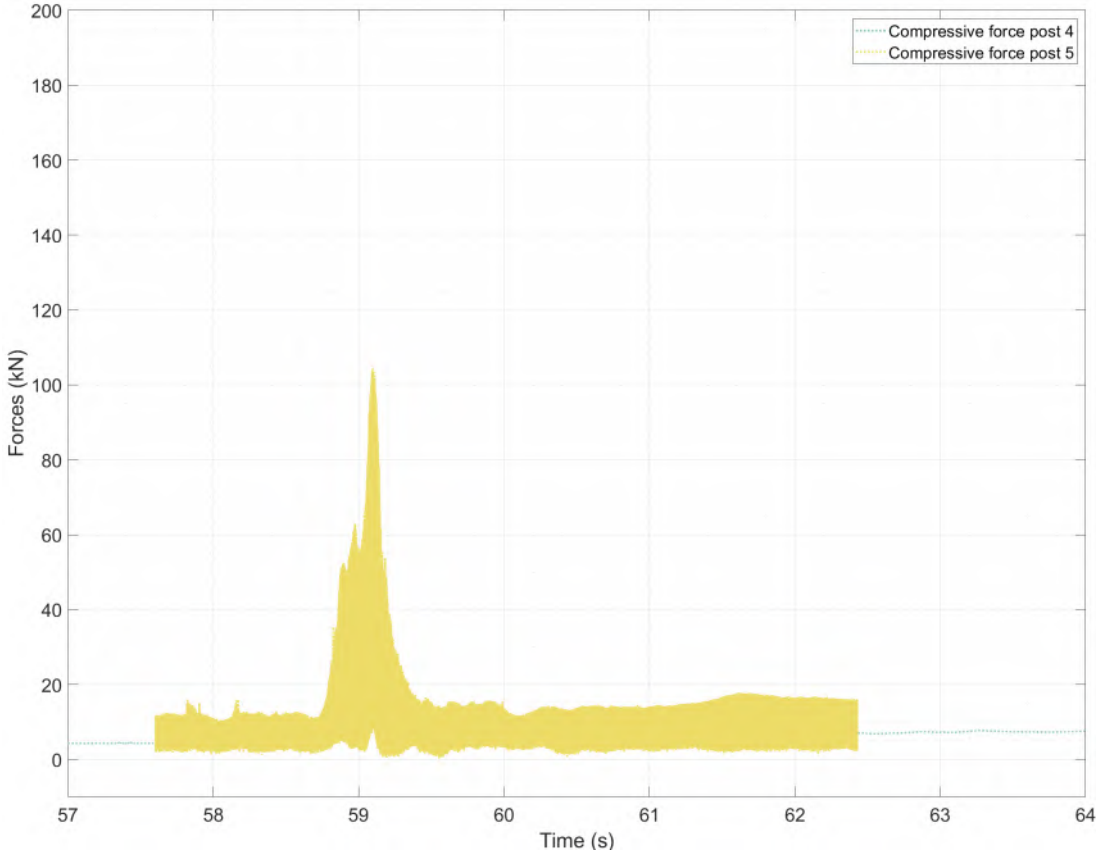
Compressive force post 4
Compressive force post 5
Forces (kN)
Time (s)

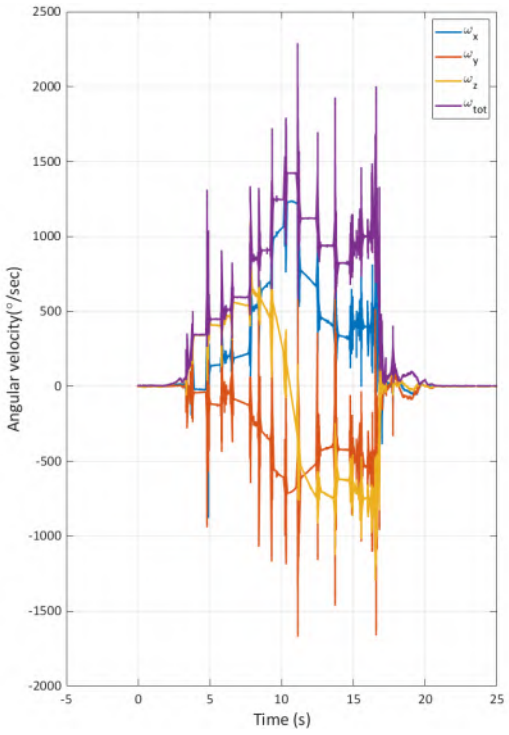
Angular velocity(°/sec)
Time (s)
ω_x
ω_y
ω_z
ω_{tot}

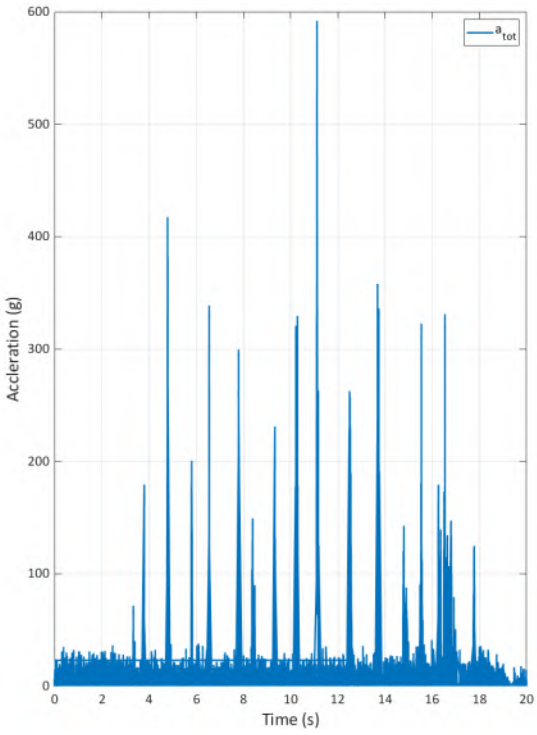
Accleration (g)
Time (s)
a_{tot}

C. Load cells and amplifiers

C.1. Zhendan tensile load cell

MODEL LTR-1 RESISTIVE STRAIN GAGE BASED LOAD CELL

SPECIFICATIONS：

Full Scale Output：	＞1.0mV/V
Non-linearity：	0.5% Full scale
Hysteresis：	0.5% Full scale
Repeatability：	0.3% Full scale
Bridge resistance：	700 ohms
Rated Excitation：	10V DC（15Vmaximum）
Insulation Resistance：	2000megohms
Operating temp：	-10～+55℃
Temp zero variation：	0.4% Full scale/10℃
Overload capability：	20% Full scale
Cable Length：	2m
Protection Level:	IP65
Cable Color Code：	Red ＋Excitation
	White －Excitation
	Yellow ＋Signal
	Blue －Signal

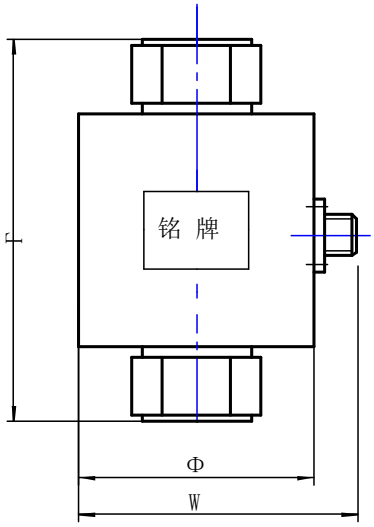

Rated Capacity (kN)	Dimension （Φ×L×W） mm	Thread Dimension （mm）
0.2，0.5，1，1.5，2，3，5，7，10	Φ52×84×68	M 16×1.5
15，20，30，50，70	Φ70×115×90	M 24×1.5）
100，150，200	Φ90×160×110	M 36×3
300，500	Φ117×210×132	M 45×4.5
700，1000	Φ130×224×145	M 56×4

SHANGHAI ZHEN-DAN SENSOR INSTRUMENT FACTORY

Address：No.33 Lane 65，Chenxiang Road，Jiading district, Shanghai，China

Tel：0086-021- 69174338 69174337 Fax：0086-021-56433966

E-mail：zhen_dan@163.com Website：//www.shzhendan.com

Post Code：201802

C.2. GTM pressure load cell

Technische Daten 25 kN – 630 kN

	Nennkraft Druck/Zug	$\pm F_{nom}$	kN	25	50	63	100	200	250	300	400	500	630
Messtechnische Daten	Genauigkeitsklasse			0,05									
	Kraftmessbereich		%	1 - 100									
	Linearitätsabweichung	d_{lin}	%	0,05									
	Interpolationsabweichung	f_c	%	0,4									
	Hysterese	h	%	0,1									
	Umkehrspanne	v	%	0,5									
	Reproduzierbarkeit		%	0,005									
	Kriechen		%	0,025									
	Temperatureinfluss auf den Kennwert pro 10 K	TK_C	%/10K	0,05									
	Temperatureinfluss auf das Nullsignal pro 10 K	TK_0	%/10K	0,05									
	Exzentrizitätseinfluss		%/mm	0,02									
	Querkrafteinfluss		$\%/0,1 \cdot F_{nom}$	0,2									
	Drehmomenteinfluss		$\%/mm \cdot F_{nom}$	0,005									
	Zug-/Druckkraft-Kennwertunterschied	d_{ZD}	%	1									
Elektrische Daten	Nennkennwert[3)]	C_{nom}	mV/V	1			2						
	Kennwerttoleranz	d_c	%	0,4			0,2						
	Nullsignaltoleranz	$d_{S,0}$	%	1			0,5						
	Eingangswiderstand	R_e	Ω	ca. 750									
	Ausgangswiderstand	R_a	Ω	ca. 500			ca. 750						
	Isolationswiderstand	R_{is}	Ω	$>10^9$									
	Nennbereich der Versorgungsspannung	$B_{U,G}$	V	5 - 12									
	IP-Schutzart (DIN EN 60529)			IP 67[2)]			IP 54[1)]						

Mechanische Daten	Nennkraft Druck/Zug	$\pm F_{nom}$	kN	25	50	63	100	200	250	300	400	500	630
	Nennmessweg	s_{nom}	mm	0,07			0,1			0,2			
	Federsteifigkeit	c_{ax}	kN/mm	350	700	900	1000	2000	2500	1500	2000	2500	3000
	Masse	m	kg	0,5			3			9			
	Anteilige bewegte Masse	m_{mess}	kg	0,25			1,5			4,5			
	Grundresonanzfrequenz	f_G	kHz	›9			›5			›4			
	Zulässige Schwingbeanspruchung[3]		%	± 80									
Grenzwerte	Statische Grenzkraft		%	150									
	Statische Bruchkraft		%	300									
	Statische Grenzquerkraft		%	80									
	Zulässige Exzentrizität statisch	e_G	mm	30			40			50			
	Statisches Grenzbiegemoment	$M_{b\,zul}$	kN·m	1	2	4	6	11	14	24	33	40	49
	Nenntemperaturbereich	$B_{T,\,nom}$	°C	+10 – +60									
	Gebrauchstemperaturbereich	$B_{T,\,G}$	°C	- 10 – +80									

1) Steckverbindung

2) Fester Kabelanschluss

3) Nennkennwert 1 mV/V mit einer zul. Schwingbeanspruchung ± 100% auf Anfrage möglich.

C.3. Qantum X MX840A amplifier

Technische Daten MX840A

Allgemeine Technische Daten		
Eingänge	Anzahl	8, untereinander und zur Versorgung[1] galvanisch getrennt
Aufnehmertechnologien pro Anschluss		DMS-Voll- und Halbbrücke, Induktive Voll- und Halbbrücke, Piezoresistive Vollbrücke, Potentiometrische Aufnehmer, Elektrische Spannung (100 mV, 10 V, 60 V, bis 300 V CAT II mit 1-SCM-HV), Strom, Widerstand (z. B. PTC, NTC, KTY), Widerstandsthermometer (PT100, PT1000), Thermoelemente (K, N, E, T, S, ...) mit Vergleichsmessstelle im Stecker (1-THERMO-MXBOARD). Frequenz, Impulszählung, SSI, Inkrementalgeber (nur Anschlüsse 5–8). CAN-Signale empfangen oder Messsignale auf CAN senden (ISO 11898, nur Anschluss 1).
A/D-Wandlung pro Kanal		24 Bit Delta Sigma Wandler
Messrate	Hz	0,1 ... 19200, pro Kanal individuell einstellbar
Aktives Tiefpassfilter (Bessel/Butterworth, abschaltbar)	Hz	0,01 ... 3200 (–3 dB)
Aufnehmeridentifikation (TEDS, IEEE 1451.4)		
max. Abstand des TEDS-Moduls	m	100
Aufnehmeranschluss		D-SUB-15HD
Versorgungsspannungsbereich (DC)	V	10 ... 30 (Nennspannung 24 V)
Versorgungsspannungsunterbrechung		max. für 5 ms bei 24 V
Leistungsaufnahme		
ohne einstellbare Aufnehmerspeisung	W	< 9
mit einstellbarer Aufnehmerspeisung	W	< 12
Aufnehmerspeisung (aktive Aufnehmer)		
Einstellbare Versorgungsspannung (DC)	V	5 ... 24; kanalweise einstellbar
Maximale Ausgangsleistung	W	0,7 je Kanal / 2 insgesamt
Ethernet (Datenverbindung)		10Base-T / 100Base-TX
Protokoll/Adressierung	–	TCP/IP (Direkte IP-Adresse oder DHCP)
Steckverbindung	–	8P8C-Stecker (RJ-45) mit Twisted-Pair-Kabel (CAT-5)
Max. Kabellänge zum Modul	m	100
Synchronisationsmöglichkeiten		FireWire (nur QuantumX, automatisch, empfohlen)
EtherCAT®[5]		über CX27
NTP		über Ethernet
IRIG-B (B000 bis B007; B120 bis B127)		über MX440A- oder MX840A-Eingangskanal
FireWire (Modulsynchronisation, Datenverbindung, optionale Spannungsversorgung)		IEEE 1394b (nur HBM-Module)
Baudrate	MBaud	400 (ca. 50 MByte/s)
Max. Strom von Modul zu Modul	A	1,5
Max. Kabellänge zwischen den Teilnehmern	m	5
Max. Anzahl in Reihe verbundener Module (daisy chain)	–	12 (=11 Hops)
Max. Anzahl der Module in einem FireWire-System (inkl. Hubs[2], Backplane)	–	24
Max. Anzahl von Hops[3]	–	14
Nenntemperaturbereich	°C	–20 .. +60
Gebrauchstemperaturbereich	°C	–20 ... +65
Lagerungstemperaturbereich	°C	–40 ... +75
Relative Luftfeuchte	%	5 ... 95 (nicht kondensierend)
Schutzklasse		III
Schutzart		IP20 nach EN60529 (IP67-Variante verfügbar)
Mechanische Prüfungen[4]		
Schwingen (30 min)	m/s^2	50
Schock (6 ms)	m/s^2	350
EMV-Anforderungen		nach EN 61326
Maximale Eingangsspannung an Aufnehmerbuchse gegen Masse (PIN 6)		
PIN 1, 2, 3, 4, 5, 7, 8, 10, 13, 15	V	5,5 (transientenfrei)
PIN 14 (Spannung)	V	60 (transientenfrei)/typ. 500
Abmessungen, liegend (H x B x T)	mm	52,5 x 200 x 124 (mit Schutzelement)
	mm	44 x 174 x 124 (ohne Schutzelement)
Gewicht, ca.	g	980

1) Beim Verwenden der variablen Aufnehmerspeisung wird die galvanische Trennung zur Versorgung aufgehoben.
2) Hub: FireWire-Knotenpunkt bzw. Verteiler
3) Hop: Übergang von Modul zu Modul oder Signalaufbereitung/Verteilung über FireWire (Hub, Modulträger)
4) Die mechanische Beanspruchung wird gemäß den Europäischen Normen EN60068-2-6 für Schwingungen und EN60068-2-27 für Schocken geprüft. Die Geräte werden einer Beschleunigung von 50 m/s^2 innerhalb des Frequenzbereichs von 5...65 Hz in allen 3 Achsen ausgesetzt. Dauer dieser Schwingungsprüfung: 30 Minuten pro Achse. Die Schockprüfung wird durchgeführt mit einer Nennbeschleunigung von 350 m/s^2 von 6 ms Dauer, halbsinusförmig und mit Schocken in jede der sechs möglichen Richtungen.
5) EtherCAT® ist eine eingetragene Marke und patentierte Technologie, lizensiert durch die Beckhoff Automation GmbH, Deutschland

C.4. Lord Sensing Wireless amplifier

SG-Link-200 Wireless Analog Input Node

Analog Input Channels		
Sensor input channels	3 differential	
Sensor excitation output*	Configurable 1.5 or 2.5 V (100 mA)	
Measurement range	0 to Excitation voltage (1.5 or 2.5 V)	
Adjustable gain	1 to 128	
ADC resolution	24-bit	
Noise (Gain = 128)	1 µVp-p to 20 µVp-p (filter selection dependent)	
Noise (Gain = 1)	15 to 250 µVp-p (filter selection dependent)	
Temperature stability	0.172 µV/°C (typical)	
Digital filter**	Configurable SINC4 low pass filter for reducing noise	
Strain calibration	Onboard shunt resistor used for deriving linear strain calibration coefficients	
Shunt calibration resistor	499k Ohm (± 0.1%)	
Integrated Temperature Channel		
Measurement range	- 40°C to 85°C	
Accuracy	±0.25°C	
Sampling		
Sampling modes	Continuous, periodic burst, event triggered	
Output options	Analog: Calibrated engineering units, adc counts and derived channels (mean, RMS and peak-peak)	
Sampling rates	1 S/hr to 1024 Hz	
Sample rate stability	±5 ppm	
Network capacity	Up to 128 nodes per RF channel (bandwidth calculator:) www.microstrain.com/configure-your-system	
Node synchronization	±50 µsec	
Data storage capacity	16 MB (up to 8,000,000 data points)	
Operating Parameters		
Wireless range	Onboard antenna: 1 km (ideal), 400 m (typical) Indoor/obstructions: 50 m (typical)	
Radio frequency (RF)	License-free 2.405 to 2.480 GHz (16 channels)	
RF transmit power	User-settable 0 dBm to 20 dBm (restricted regionally)	
Power input range	Battery: 3.6 V Lithium D-cell 1.5 V Alkaline D-cell***	External Input Power: 4.0 - 36 VDC
Battery lifetime	TBD	
Operating temperature	-40°C to +85°C	
Mechanical Shock Limit	1000*g*/1.5ms	
ESD	4 kV	
Physical Specifications		
Sensor Interface	AMPSEAL 14-pin connector with 1.3 mm contacts	
Mounting	2 x M8	
Ingress Protection	IP68, 3.0m for 30 mins	
Enclosure Material	PBT base, polycarbonate lid, stainless steel compression limiters	
Dimensions	3" x 5" x 2.2" (76.2 x 127 x 55.9 mm)	
Weight	326 grams (with battery), 235 grams (without battery)	
Integration		
Compatible gateways	All WSDA gateways	
Software	SensorCloud, SensorConnect, Windows 7, 8, & 10 compatible	
Software development kit	http://www.microstrain.com/software/mscl	
Regulatory compliance	FCC (USA), IC (Canada), CE (European Union), JET (Japan)	

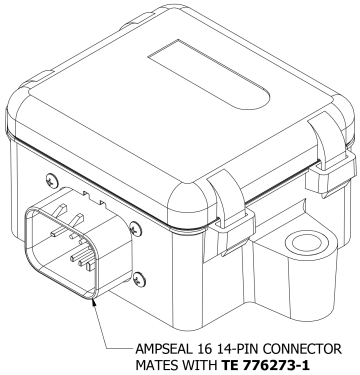

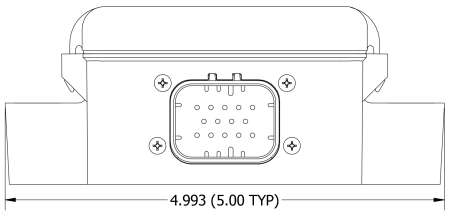

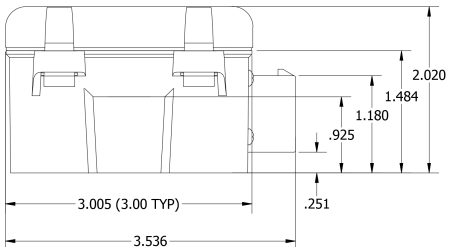

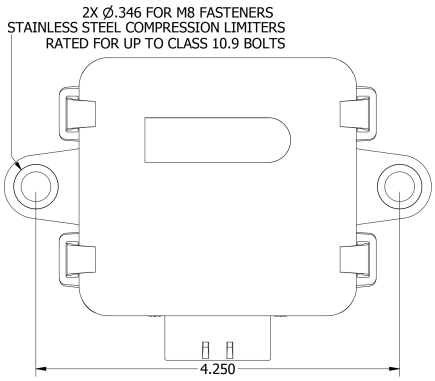

* Sensor excitation may be duty cycled to conserve power for sampling rates less than 1024 Hz.

** Extend battery life by using a faster filtering setting.

*** Limited temperature range and transmit power (10 dBm)

LORD SENSING
MicroStrain

ZSE ELECTRONIC MESS-SYSTEME & SENSORTECHNIK GmbH
Postfach 1830 ■ 74308 Bietigheim-Bissingen
Telefon: 07142 6845 ■ Fax: 07142 6997
e-mail: info@zse.de ■ www.zse.de